TECHNICAL UNIVERSITY OF LIBEREC

FACULTY OF TEXTILES

YARN STRENGTH AS A STOCHASTIC PROCESS

PH.D. DISSERTATION

LIBEREC 2005

DIPAYAN DAS

TECHNICKÁ UNIVERZITA V LIBERCI
TECHNICAL UNIVERSITY OF LIBEREC

Fakulta textilní
Faculty of Textiles

Katedra textilní technologie
Department of Textile Technology

Disertační práce
Ph.D. Dissertation

Pevnost příze jako stochastický proces
Yarn Strength as a Stochastic Process

2005

Vypracoval: Dipayan Das, M.Tech.
Worked out by: Dipayan Das, M.Tech.

Školitel: Prof. Ing. Bohuslav Neckář, DrSc.
Supervisor: Prof. Ing. Bohuslav Neckář, DrSc.

KTT

[illegible]

ABSTRACT

In this research work, strength of thirty-one cotton yarns with different fineness and twist characteristics produced by four different spinning technologies was studied under the model of yarn strength as a summation of two independent stationary, ergodic, Markovian, and Gaussian (SEMG) stochastic processes. A special methodology was applied to measure the strength of every alternate short section – each of 50 mm length – along a yarn and the strength autocorrelation characteristics were determined. Those characteristics were found different in different yarns. Using those characteristics, computer simulations were performed to obtain the frequency distribution as well as basic statistical parameters (mean value and standard deviation) of strength of yarn specimens with different lengths (50 mm – 5000 mm). It was found that depending on the degree of strength autocorrelation, the empirical strength versus gauge length relations were different in different yarns and those relations were in a better correspondence with the actual ones as compared to those derived traditionally on the basis of strength independency. It was revealed that probably two highly different and mutually independent phenomena are acting together so as to cause yarn strength variability and those phenomena are partially related to yarn mass irregularity.

ABSTRAKT

Disertační práce zkoumá pevnost jedenatřiceti bavlněných přízí o různých jemnostech a zákrutech, vyrobených čtyřmi různými technologiemi. Modelová pevnost byla uvažována jako součet dvou nezávislých stacionárních, ergodických, Markovských a Gausovských (SEMG) stochastických procesů. Speciální experimentální přístup umožňoval měřit pevnost 50mm úseků příze, jdoucích za sebou vždy ob jeden. Experimentální data byla vyhodnocena a nalezeny autokorelační charakteristiky pevnosti příze, odlišné pro různé příze. Výsledky byly využity k výpočtu hustoty pravděpodobnosti pevnosti příze na různých upínacích délkách příze (50mm – 5000mm) a k výpočtu standardních pravděpodobnostních charakteristik (střední hodnoty, směrodatné odchylky) na těchto délkách. Bylo zjištěno, že metoda predikce pevnosti příze pro různé upínací délky, užitá v této práci, je v lepší shodě s experimentálními výsledky, než tradiční výpočet, založený na předpokladu statistické nezávislosti pevnosti. Bylo odhaleno, že variabilitu pevnosti příze pravděpodobně způsobují dva velmi odlišné a vzájemně nezávislé jevy, působí současně. Ukazuje se, že tyto dva jevy částečně souvisí s hmotnou nestejnoměrností příze.

Dedicated

to

my beloved parents

ACKNOWLEDGEMENTS

I experience great pleasure to convey my profound sense of respect and gratitude to my supervisor, Prof. Ing. Bohuslav Neckář DrSc., for his excellent supervision, encouraging discussion, inspiring suggestions, and also for his sympathy to me. It was indeed a wonderful event in my life to work with a great theoretician like him in our branch of science.

I would like to appreciate the comments and suggestions I received from Prof. Ing. Jiri Militky CSc. and Prof. Ing. Sayed Ibrahim CSc. on my research work.

I wish to extend my appreciation to Prof. Dr.–Ing. Thomas Gries of Institute for Textile Technology of RWTH Aachen, Germany for granting me permissions to carry out a few experiments on the Statimat M tensile tester and also to access the institute library for searching literature.

My sincere appreciation should also to be extended to the technical staffs of my department for their cooperation during the experimental work carried out in this research work.

I would like to thank my colleagues for their help and ready assistances, especially to Ing. Monika Vyšanskà for translating the English abstract into Czech language.

I thank also the Seba Tanvald and the Cotton Research Institute (VUB) of Czech Republic for providing samples for my research work.

Every wheel needs an axis to keep on rotating. In my case, my axis is my parents – source of my all inspirations. There are also my brother, sister, and my friend – Archana, who played very significant roles on different aspects of my life throughout my stay away from my home. Any attempt to thank them would defy the greatness of their contributions.

Dipayan Das

TABLE OF CONTENTS

LIST OF TABLES

LIST OF FIGURES

PREFACE

This dissertation is submitted to the Faculty of Textiles in partial fulfillment of the requirements for the degree of Doctor of Philosophy at the Technical University of Liberec, Czech Republic. It is divided into seven chapters.

Chapter 1 introduces the topic of the dissertation. It discusses the importance and background of the topic. The objectives of this study are also briefly given.

Chapter 2 is based on a thorough review of literature relevant to this research work. It summarizes our existing knowledge on this particular topic. It discusses the approaches of other researchers to solve the problem issued in this research work. The critical assessments of their works are also reported.

The theory of yarn strength as a stochastic process is presented in Chapter 3. The concept of a general stochastic process of yarn strength is introduced. Some special types of stochastic processes together with their characteristics are discussed. How to realize the stochastic process is also demonstrated.

Chapter 4 tells about the materials used in this research work. It discusses some non-standard methods of measurements followed in this research work for special evaluations of some yarn properties. Also the standard methods of those measurements are highlighted.

Chapter 5 demonstrates the theory with one practical example. Proper attention has been paid to see whether the experimental results are consistent with the theoretical knowledge. Also it covers the results obtained on different yarns used in this research work with relevant discussions on them.

The final chapter, Chapter 6, is devoted to present the overall conclusion of this research work. It summarizes the results, highlights the implications of the work, and proposes a new research direction for the future.

The Appendixes mainly contain the essential experimental results that, for the brevity, were not mentioned in the main text. These are equally important as those presented in the main text.

The Bibliography of this dissertation follows the Harvard style of citations.

1 INTRODUCTION

1.1 Prediction of Yarn Strength Behavior at Different Gauge Lengths

Usually, yarn strength measurement is carried out at 500 mm gauge length. However, in practice, yarns are stressed at different lengths. For example, in the weaving preparatory processes, say warping, yarns of much longer than 500 mm are stressed. On the other hand, it is known that the strength of yarns evaluated at shorter gauge length is a better predictor of fabric strength in opposite to the yarn strength measured at long gauge length, say 500 mm (Realff *et al.* 1991). Moreover, the importance of understanding the yarn strength response at different gauge lengths can be further appreciated with an eye to the ever-increasing non-traditional end-uses of our yarns.

In order to know yarn strength behavior at different gauge lengths, we have a few alternatives:

1) To carry out strength measurements using a tensile tester at different gauge lengths,
2) To use the existing empirical equations relating yarn strength and gauge length for prediction of actual yarn strength behavior corresponding to different gauge lengths,
3) To develop a new scientific way for predicting actual yarn strength behavior at different gauge lengths.

Among the three alternatives, it can be easily understood that the first one is not at all a realistic idea. As far as the second alternative is concerned, Peirce's equations (1926) of strength and strength variability between long and short specimens can be used. However, those are not enough precise, as reported by Meredith (1946), Morton & Hearle (1992), to name a few. Therefore, a new scientific way should be developed for predicting actual yarn strength behavior at different gauge lengths. In order to have sufficient information on this behavior, it is necessary to know not only the basic statistical parameters of yarn strength, say the mean value and the coefficient of variation, but also the frequency distribution of yarn strength.

1.2 Understanding Yarn Strength Variability

It is well known that yarn strength variability is one of those very critical factors that determine the performances of the subsequent technological processes as well as of the textile products during their various end-uses. Many attempts were made in the past to investigate the causes of yarn strength variability, but most of them were confined only to establish empirical equations relating yarn strength variability to yarn mass irregularity and to the variations in fiber properties. However, it was observed that the variation in fiber properties influences a little on the total yarn strength variation, whereas the variations induced at different stages of spun yarn manufacturing process play the most significant role on the total yarn strength variation (Suh *et al.* 2001). Nevertheless, no attempt has been made till date to investigate the nature of those variations. Moreover, the physical bases of yarn strength variability are still not enough clear. It is therefore of extreme importance to gain new knowledge leading to improved understanding of yarn strength variability.

2 REVIEW OF LITERATURE

2.1 Theory of Weakest-Link

The mostly quoted theory while studying yarn strength behavior at different gauge lengths is the weakest link theory, which was first used by Peirce (1926). This theory can be understood with a view to Figure 2.1. It is shown that a tensile force S is applied on a yarn ("chain") of length l which is divided into n short sections ("links") of equal length l_0 such that $l = nl_0$; or, $n = l/l_0$, where n is a positive integer. The weakest-link theory tells that the strength of the whole specimen of length l is that of its weakest section. In other words, a single breakage among these short sections causes to break the whole specimen. The effect of this theory, as discussed by Booth (1968) and Morton & Hearle (1992), is illustrated in Figure 2.2. The graph shown in Figure 2.2 indicates the strength of a yarn at infinitely small increments of length along the complete length l. If the yarn is tested for its strength at a gauge length l, then its strength will be equal to the strength of its weakest point and this value is S_1. If the yarn is equally divided into two halves and these two halves each of length $l/2$ are individually tested, then two breaking loads S_1 and S_2 are obtained and the mean of which is higher than S_1. Hence, by testing a yarn at a shorter gauge length the apparent yarn strength has increased. Therefore, the order of ranking of yarns on the basis of their strength values may alter if the gauge length is altered. Moreover, it is believed that this effect is more rapid in case of more irregular yarn.

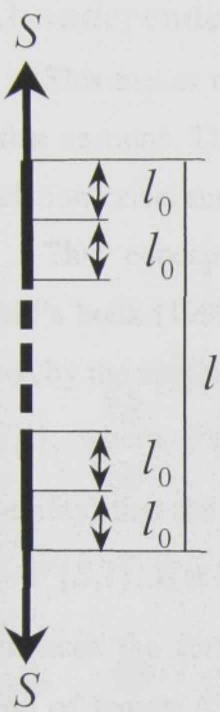

Figure 2.1

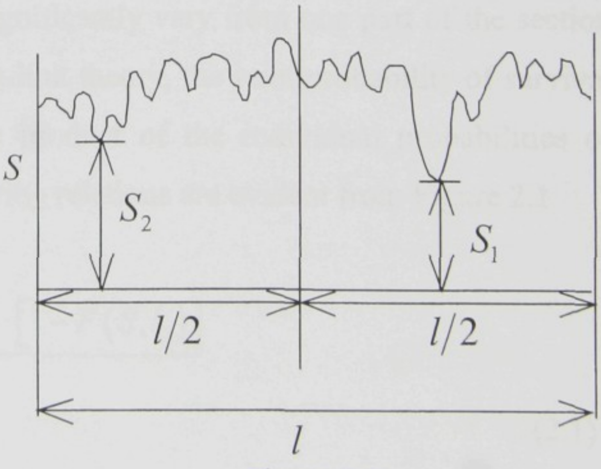

Figure 2.2

2.2 Distributions of Strengths along Yarns

There exits a debate among the textile researchers whether the strength of successive short sections of equal length along the yarns is independent or dependent. These two concepts are presented here.

2.2.1 Independent Strengths

This means the breakage of one small section does not influence the breakage of other sections. This was first imagined by Peirce (1926). Under this hypothesis, no correlation exists among the strength of successive short sections along a yarn.

This concept along with its consequences is very lucidly introduced in Neckář's book (1998). The probability of failure that a yarn specimen of length l is broken by the application of the force S can be described by the distribution function $F(S,l)$, where $F(S,l) \in \langle 0,1 \rangle$. Then the probability of survival (complementary probability) that the yarn specimen of length l is not broken by the force S is given by $1-F(S,l)$. If it is assumed that every small section of the whole yarn of length l experiences the force S equally, then the probability of failure that every small section of length l_0 is broken by the force S is given by the distribution function $F(S,l_0)$. The probability of survival (complementary probability) that the section of length l_0 is not broken by the force S is given by $1-F(S,l_0)$. If it is further assumed that the distribution function does not significantly vary from one part of the section to another, then according to the weakest-link theory, the joint probability of survival of the whole specimen is equal to the product of the individual probabilities of survival for each section. Then the following relations are evident from Figure 2.1

$$1-F(S,l)$$

$$=\underbrace{\left[1-F(S,l_0)\right]\left[1-F(S,l_0)\right]\cdots\cdots\cdots\left[1-F(S,l_0)\right]}_{n \text{ times}}$$

$$=\left[1-F(S,l_0)\right]^n \qquad (2.1)$$

$$=\left[1-F(S,l_0)\right]^{\frac{l}{l_0}}. \qquad (2.2)$$

Rearranging the above expressions, the following equations are obtained

$$F(S,l)$$

$$=1-\left[1-F(S,l_0)\right]^n \tag{2.3}$$

$$=1-\left[1-F(S,l_0)\right]^{\frac{l}{l_0}}. \tag{2.4}$$

The last equation tells the relation between the two distribution functions of strength corresponding to the shorter and longer gauge lengths. Equation (2.2) can also be written in another form as shown below

$$\left[1-F(S,l)\right]^{\frac{1}{l}}=\left[1-F(S,l_0)\right]^{\frac{1}{l_0}}. \tag{2.5}$$

The probability distribution of strength S corresponding to the gauge length l is defined by the probability density function $f(S,l)$. This is related to the distribution function $F(S,l)$ by the following expression

$$f(S,l)=\frac{\partial F(S,l)}{\partial S}. \tag{2.6}$$

Substituting Equation (2.4) into the last equation, the following expression is obtained

$$f(S,l)$$

$$=\frac{l}{l_0}\left[1-F(S,l_0)\right]^{\frac{l}{l_0}-1}\frac{\mathrm{d}F(S,l_0)}{\mathrm{d}S}$$

$$=\frac{l}{l_0}f(S,l_0)\left[1-F(S,l_0)\right]^{\frac{l}{l_0}-1}. \tag{2.7}$$

The above equation tells the relation between the probability density functions of strength corresponding to the shorter and longer gauge lengths.

2.2.2 Dependent Strengths

This means the breakage of one small section influences the breakage of other neighboring sections. Spencer-Smith (1947) introduced this concept with an imagination that the strength of the neighboring fracture zones in yarns is related to each other partly because the same long fibers will occur in a number of fracture zones and partly because of the non-random irregularities introduced into the thickness of the yarn by the preparing and spinning machineries. The fracture zone is that small region where actual fracture takes place while testing the strength of a long length of yarn, as reported by Turner (1928).

2.3 Frequency Distributions of Strengths

Another great controversy exists among the textile researchers on the assumption whether yarn strength follows Gaussian (normal) distribution or Weibullian distribution or different types of Pearsonian distribution. (The "zero" type Pearsonian distribution is called the normal distribution.)

2.3.1 Gaussian Distribution

Peirce (1926) hypothesized that the strength S of short specimens each of length l_0 follows Gaussian probability distribution with mean value $\bar{S}_0$ and standard deviation σ_0, as shown below

$$f(S,l_0)=\frac{1}{\sqrt{2\pi}\sigma_0}\exp\left[-\left(S-\bar{S}_0\right)^2/2\sigma_0^2\right]. \tag{2.8}$$

But he did not make any attempt to verify it. Later on, applying the so-called skewness and kurtosis test on the experimental yarn strength data corresponding to a short gauge length (50 mm), Neckář (1998) concluded that the assumption of Gaussian distribution was true at 95% significance level. Furthermore, he derived that if one assumes Gaussian distribution of yarn strength corresponding to a particular gauge length; then the distribution of the strength at other gauge lengths is not Gaussian. Truevtsev *et al.* (1997) conducted 500 strength measurements on ring and rotor yarns with different counts each at 500 mm gauge length, and based on the χ^2 criterion, they found that the experimental dataset did not differ significantly from Gaussian distribution at 95% significance level. A similar observation was earlier reported by Pozdniakov (1978) and Perepelkin (1991).

2.3.2 Weibullian Distribution

Realff *et al.* (1991) attempted to fit the experimental strength datasets of polyester-cotton (65/35) blended ring and air-jet spun yarns corresponding to different gauge lengths with Weibullian distribution. A three-parameter Weibullian distribution of the strength S of short specimens each of length l_0 has the following distribution function

$$F(S,l_0)=1-\exp\left[-\left(S-S_{\min}\right)^c/Q^c\right], \tag{2.9}$$

where $S \in \langle S_{\min}, \infty \rangle$, $S_{\min}$ is the location parameter, Q is the scale parameter, and c is the shape parameter. These three parameters $S_{\min} \geq 0$, $Q \geq 0$, and $c \neq 0$ characterize the above distribution. A two-parameter Weibullian distribution is obtained by putting $S_{\min} = 0$ in the above equation. Applying the Kolmogorov-Smirnov goodness-of-fit test, Realff *et al.* (1991) found that both of the two and three-parameter Weibullian distributions were in a good agreement with the experimental datasets and the three-parameter Weibullian distribution did not bring any significant increase in the goodness of fit as compared to the two-parameter Weibullian distribution.

2.3.3 Pearsonian Distribution

Kapadia (1934) conducted 80000 strength tests at a gauge length of 12 inches on a tensile tester working on the principle of constant rate of loading and used Pearsonian statistics to verify the experimental results with different types of Pearsonian distribution. According to his observation, the experimental distributions of the strength of cotton carded ring yarns with different counts were not adequately fitted by the Pearsonian curves. He found a high correlation between yarn strength and yarn count; and when these two variables were considered together as one variable, namely count-strength product, the distributions were adequately represented by the Pearsonian types of curves, namely types I, III, and IV. He thus concluded that the heterogeneity of yarn strength was due to the heterogeneity of yarn count.

2.4 Equations Relating Strength and Gauge Length

Several attempts were made by the textile researchers to establish equations describing the relations between strength and gauge length in spun yarns. Those equations and their validity are discussed in the following sections.

2.4.1 Peirce's Equations

Peirce (1926) assumed that 1) the weakest-link theory holds on yarns, 2) strengths of successive short sections of length l_0, forming a long specimen of length l, are independent, 3) strengths of those short sections follow Gaussian distribution. Under these assumptions, he obtained the following approximated relations of strength and strength variability between the short and long specimens

$$\overline{S^*} = \overline{S} + 4.2\sigma_S\left[\left(l/l_0\right)^{-1/5} - 1\right], \tag{2.10}$$

$$\sigma_{S^*} = \sigma_S\left(l/l_0\right)^{-1/5}; \tag{2.11}$$

where $\overline{S^*}$ and $\overline{S}$ are the mean strength of yarn specimens with lengths l and l_0, respectively; σ_{S^*} and σ_S are the standard deviations of strength corresponding to lengths l and l_0, respectively.

From time to time, many attempts were made to verify the validity of Peirce's equations. It was reported by Morton & Hearle (1992), Hussain *et al.* (1990), Knox & Whitwell (1971), Spencer-Smith (1947), Meredith (1946), Kapadia (1935), to name a few, that Peirce's equations did not correspond well to the reality. As a reason for this discrepancy, Spencer-Smith (1947) imagined that Peirce's assumption of independent strengths was not real. According to Spencer-Smith, strengths are dependent (cf. Section 2.2.2). Peirce's assumption of independent weakest link was questionable also to Knox & Whitwell (1971). They reported a sensitive test for validity of any model based on the assumption of the independent weakest link theory. According to this test, the independent weakest link theory holds good if the values of hazard functions corresponding to two different gauge lengths are in the ratio of the two gauge lengths for a sample of constant diameter. They estimated the hazard functions from the strength of 10 inch and 30 inch lengths of cotton yarn, reported by Peirce (1926), and found that although the hazard functions for the two lengths were parallel, as would be predicted if the independent weakest link theory held, over part of the range of breaking force, but the expected ratio of 3/1 did not exist, even in those regions. This forced them to conclude that the cotton yarn could not be represented as systems of simple links connected in series, although they did not deny the existence of some weakest link in the yarn. Later on, a similar conclusion was drawn by Realff *et al.* (1991). They observed that the Weibullian shape and scale parameters changed in a manner not coincident with the independent weakest-link principle. Regarding this behavior they hypothesized that the presence of same sort of flaw at all gauge lengths might not be true in yarns, and on the basis of scanning electron microscopic photographs, they proved that there exist different mechanisms of yarn breakage at different gauge lengths. A very interesting point with respect to Peirce's theory was issued by Zurek (1975). According to his experimental experiences, yarn breakages occur depending on yarn twist and this consideration was neglected in Peirce's theory.

Figure 2.3 discusses this issue. A yarn is schematically outlined as a chain consisting of three links of equal length l_0 in Figure 2.3a. A real yarn is schematically presented in Figure 2.3c. Imaginatively, when these links had been separated from the chain and

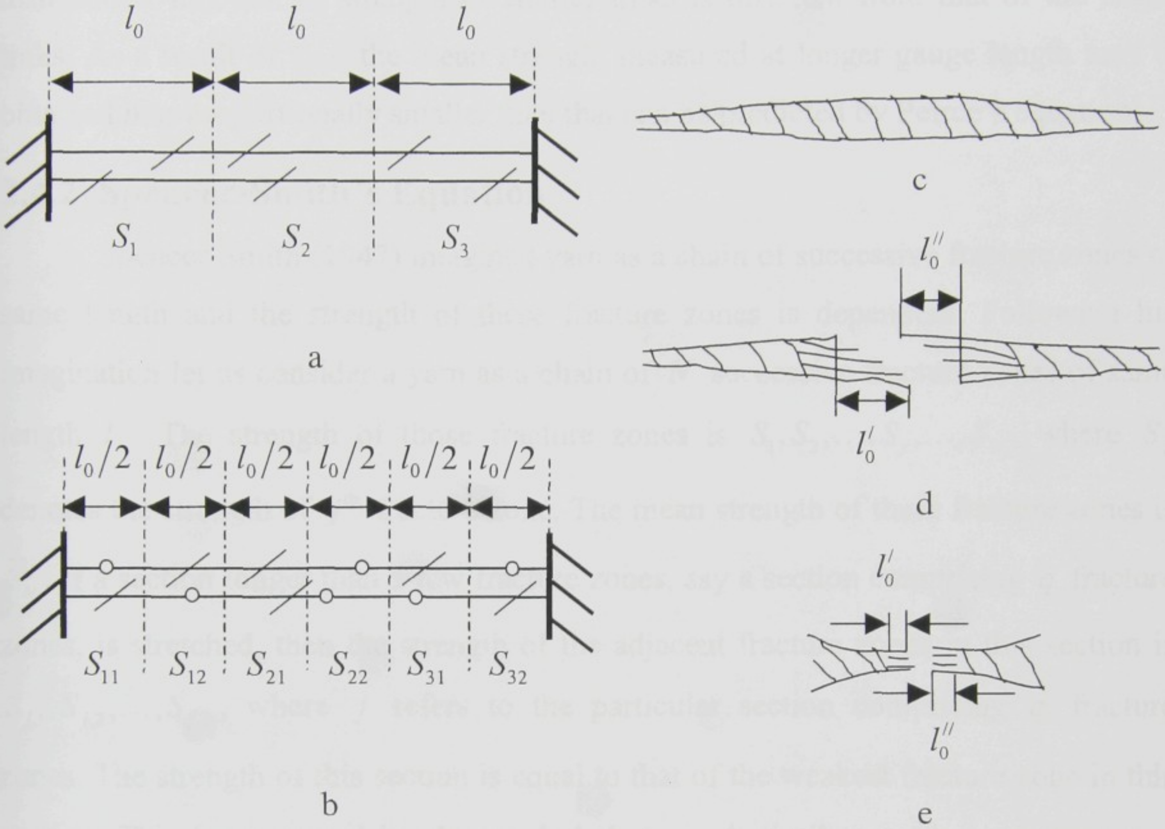

Figure 2.3

individually tested in a tensile tester, the strength was observed as S_1, S_2, and S_3, respectively. The individual breaking places of these links are marked by the symbols / in Figure 2.3a. In this case, the real broken parts were looked like as shown schematically in Figure 2.3d. Hypothetically, when each of these links had been equally divided, six shorter links each of length $l_0/2$ were obtained (Figure 2.3b). Then those shorter links had been individually tested, the strength was found as $S_{11}, S_{12}, S_{21}, S_{22}, S_{31}$, and S_{32}, respectively. As shown here, the breakages of shorter links (length $l_0/2$) occurred at other places than those with longer links (length l_0) and their arrangement was significant: there were links with identical breaking places (*e.g.*, the second link from the left-hand side), or links with new breaking places (*e.g.*, the first and the third links from the left-hand side). The new breaking places are schematically shown by the symbols o in Figure 2.3b. The real broken parts due to breakage of a shorter link were looked like as shown schematically in Figure 2.3e.

According to the weakest link theory, out of the three pairs of strength $(S_{11}$ and $S_{12}), (S_{21}$ and $S_{22})$, and $(S_{31}$ and $S_{32})$, only S_{21} coincides with S_2, while the other ones $(S_{11}$ and $S_{12}) > S_1$ as well as $(S_{31}$ and $S_{32}) > S_3$. In both the cases, the distribution function of strength of shorter links is different from that of the longer links. As a result of this, the mean strength measured at longer gauge length may be obtained non-proportionally smaller than that can be predicted by Peirce's equation.

2.4.2 Spencer-Smith's Equation

Spencer-Smith (1947) imagined yarn as a chain of successive fracture zones of same length and the strength of these fracture zones is dependent. Following his imagination let us consider a yarn as a chain of N successive fracture zones of same length l_f. The strength of those fracture zones is $S_1, S_2, \ldots, S_j, \ldots, S_N$, where S_j denotes the strength of j^{th} fracture zone. The mean strength of these fracture zones is $\overline{S}_N$. If a section longer than a few fracture zones, say a section comprising q fracture zones, is stretched, then the strength of the adjacent fracture zones in this section is $S_{j,1}, S_{j,2}, \ldots, S_{j,q}$, where j refers to the particular section comprising q fracture zones. The strength of this section is equal to that of the weakest fracture zone in this section. This is expressed by the symbol $S_{j(q)\min}$. A similar section comprising q fracture zones is considered, this section is referred by m, and strength of this section is expressed by the symbol $S_{m(q)\min}$. The mean of those minimum strength values, if n sections are broken, is $\overline{S}_{n(q)\min}$. Certainly, $\overline{S}_{n(q)\min}$ is smaller than $\overline{S}_N$. This difference, as worked out theoretically by Spencer-Smith, can be expressed as follows

$$\overline{S}_N - \overline{S}_{n(q)\min} = w(q)\sigma_f R(q), \tag{2.12}$$

where $w(q)$ is a statistical function defined by the mean difference between the mean and the minimum value of q individuals selected at random from the appropriate normalized frequency distribution, σ_f is the variance of the strength of all fracture zones in the yarn, and $R(q)$ is the serial correlation function. A close resemble of the above expression with Peirce's strength equation reveals that both expressions are comparable: $w(q)R(q)$ in Spencer-Smith's equation takes $4.2\left[1-(l/l_0)^{-1/5}\right]$ in Peirce's equation.

Several researchers discussed some salient points on the parameters, mentioned in Equation (2.12), influencing the mean strength of the weakest of q fracture zones. These are reported below.

Length l_f of Fracture Zone: There is no doubt that accurate estimation of the fracture zone length is very difficult. However, as Spencer-Smith (1947) suggested, the fracture length can be indirectly estimated from the best fit of Equation (2.12) to the strength of yarns measured at different gauge lengths, whilst independent confirmation may also be obtained from a purely theoretical approach. Spencer-Smith observed that the fracture zone length varied with the twist factor approximately logarithmically and was independent of yarn count at normal twist factor. Besides the indirect estimation of fracture zone length, it is also possible to make a direct but rough estimation. One such method was reported by Realff *et al.* (1991). From the scanning electron microscopic pictures of partially and completely broken samples, they observed that the cross-sectional shape of the fracture zones was considerably different from that of the unbroken yarn, and the length of the fracture zone was equal to the length of the region of reduced cross-section of one of the failed ends. Interestingly, this length was different in different technological yarns, and it was also changing with the change in gauge length. Table 2.1 shows the range of fracture zone lengths depending on the strength measurements carried out at different gauge lengths with 23 tex blended (35% cotton and 65% polyester) ring and air-jet yarns (31.8 mm average staple length). Another method of rough estimation of the fracture zone length was given by Nanjundayya (1966). He adopted the following procedure to reconstruct the profile of the unbroken cotton yarn from the two broken pieces of the same yarn (Figure 2.4). Here $a, b, c, \ldots$ are the fields of view from the broken pieces, $X_a, X_b, X_c, \ldots$ and $Y_a, Y_b, Y_c, \ldots$ are the corresponding numbers of broken fiber ends in piece I and piece II, respectively. For example, if X_d and Y_g were the maximum

Table 2.1

Spinning technology	Gauge length [mm]	Fracture zone length [mm]
Ring	127	<3
Ring	76.2	2-4
Ring	<2	0.5-2
Air-jet	76.2	3.5-10.5
Air-jet	12.7	3-8
Air-jet	<2	0.5-2

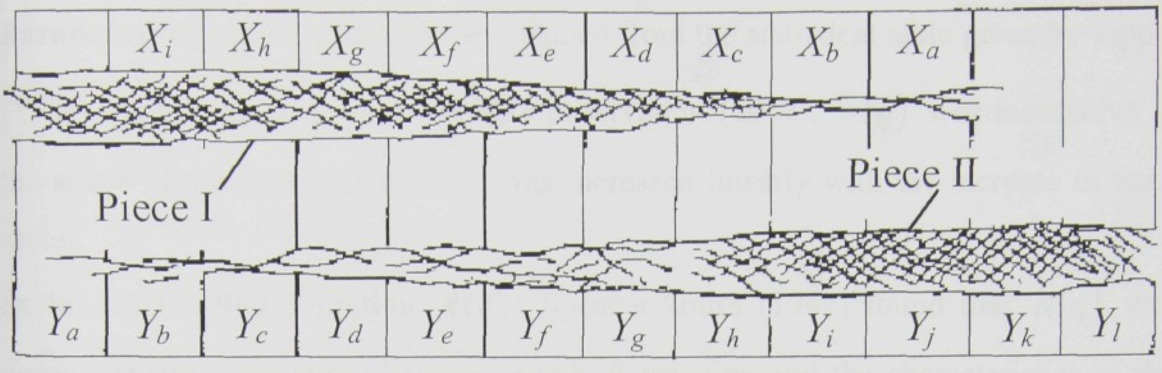

Figure 2.4

number of broken fiber ends in the respective pieces, it is highly probable that the fields d and g should have been coincident in the yarn just prior to break. By coalescing the two broken pieces in such a way that section d in piece I is joined with section g in piece II, it is possible to reconstruct the profile of the yarn before break. In order to determine the number of broken fiber ends, two broken pieces were colored, as suggested by Bright (1926), and then mounted in 18% caustic soda solution on a glass microscopic slide under a microscope.

Incidentally, a new concept of effective gauge length was theoretically introduced by Koo *et al.* (2001). According to them, a spun yarn is considered to be a continuous chain of twisted parallel fiber bundles with a known average number of fibers of which only some are continuous within a given segment of size L, as shown in Figure 2.5. The test gauge length L' is related to the effective gauge length L by the expression: $L' = rL$, where r is the number of bundles. Using computer simulation, Suh *et al.* (2001) determined the optimum effective gauge length (L_0) such that the theoretical strength properties under this gauge length corresponded to the actual strength properties at 95% significance level. The value of L_0 was found smaller for finer yarns and it was decreasing with the increase in the number of turns per meter of yarn. It was mentioned that L_0 was probably related to the short fiber content in the cotton bale, but the exact relation was not reported.

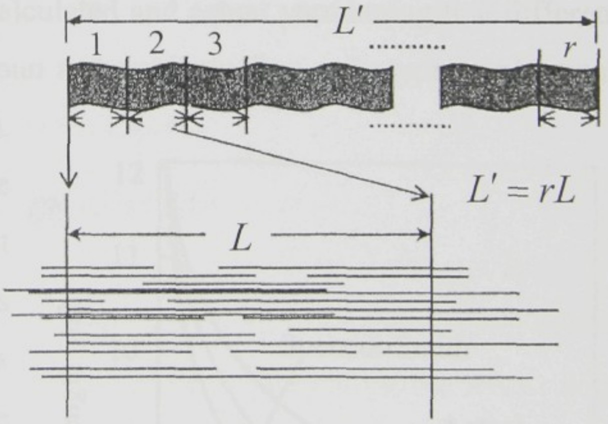

Figure 2.5

Parameter $w(q)$: Its value can be obtained from the statistical table given by Tippet (1925). According to Spencer-Smith's observation (1947), $w(q)$ was insensitive to the shape of the distribution and it was increased linearly with the increase in twist factor.

Serial Correlation Function $R(q)$: Spencer-Smith (1947) found that $R(q)$ was dependent primarily upon the fiber length distribution and the characteristics of the system on which the yarn was spun, and it was practically independent of the yarn count and twist factor for normal flax yarns produced on a standard system with constant drafts.

Strength of Fracture Zones: Spencer-Smith (1947) observed that the strength of the fracture zone was increased to a maximum and then decreased again as the twist factor was increased. He found that the optimum twist factor of a particular material was dependent on the fiber properties. It was also observed that the strength of the fracture zone was independent of the yarn count at normal twist factors.

Standard Deviation σ_f of Strength of Fracture Zones: According to Spencer-Smith's observation (1947), the standard deviation of strength of fracture zones was decided mainly by the mass irregularity along the yarn, but it was also affected by the local fluctuations in the mean size of the fibers and their elastic properties.

A good agreement between the calculated and actual yarn strength at different gauge lengths for several types of wet-spun and dry-spun flax and rayon staple yarns was found by Spencer-Smith (1947), however, according to Morton & Hearle (1992), this agreement is still not perfect (Figure 2.6) Though Spencer-Smith's imagination of dependent strength results in a better correspondence with the experimental results as compared to Peirce's equation, however, Spencer-Smith's relation is open to criticism on the ground that the actual measurement of the fracture zone length is ill defined. Apart from this, it is very likely that the

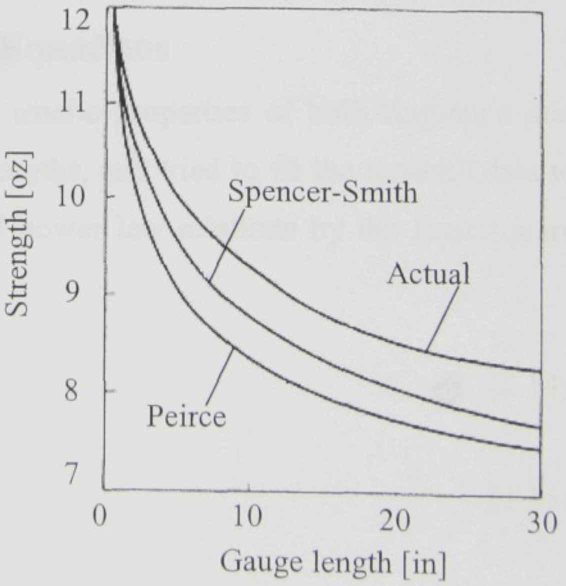

Figure 2.6

mechanism of yarn breakages at all gauge lengths are not the same and turns in the yarns are redistributed during the measurement of yarn strength (Morton & Hearle 1992).

2.4.3 Zurek & His Coworkers' Equation

Zurek and his coworkers (1976, 1987) also worked on the problem of yarn strength-gauge length relation and proposed the following empirical relation

$$S^* = S_f\left[1-3.64\nu\left\{1-\left(l/l_f\right)^{-1/7}\right\}\right], \tag{2.13}$$

where S^* is the yarn strength measured at gauge length l, S_f is the strength of the fracture zone of length l_f, ν is the coefficient of variation of yarn linear density. Using some approximated relations for the theoretical evaluations of S_f, ν, and l_f, they determined the theoretical strength values corresponding to 500 mm gauge length from the above equation, which were moderately correlated (correlation coefficient – 0.79) with the actual strength values of cotton carded and combed ring-spun yarns measured at 500 mm gauge length. Later on, Frydrych (1992), one of the coworkers, replaced ν in the above equation by the coefficient of variation of strength of fracture zones and approximated this coefficient by considering the length of the fracture zone as 5 mm, and then found a high correlation coefficient (0.94) between the theoretical and the actual strength of cotton yarns corresponding to 500 mm gauge length. However, in most of the cases, the theoretically obtained strength values were higher than those obtained experimentally.

2.4.4 Hussain and His Coworkers' Equations

Hussain *et al.* (1990) measured the tensile properties of both ring-spun and rotor-spun cotton yarns at different gauge lengths, and tried to fit the tenacity data to the following logarithmic, exponential, and power law relations by the least square method

$$\frac{S^*}{T} = A + B\log_e l, \tag{2.14}$$

$$\frac{S^*}{T} = Ae^{Bl}, \tag{2.15}$$

$$\frac{S^*}{T} = Al^B, \tag{2.16}$$

where S^* is strength at gauge length l, T is yarn count, A and B are two constants. They found very high and almost same values of the correlation coefficient for the logarithmic and power law expressions, but relatively lower value of the correlation coefficient for the exponential expression. They further analyzed the power law expression and found that the above power law expression gives rise to singularities at extreme values of l, *i.e.*, the tenacity value becomes infinite when $l = 0$ and the tenacity value becomes zero when $l = \infty$, neither of which is feasible. To avoid these, they modified the above power law expression as follows

$$\frac{S^*}{T} = C + \frac{A}{(l+D)^B} \quad \text{or, } \log_e\left(\frac{S^*}{T} - C\right) = \log_e A - B\log_e(l+D), \tag{2.17}$$

where C and D are two additional constants. The constant C is evidently the limiting value of tenacity, and the value of A is the difference between the value of tenacity at gauge length $(1-D)\text{cm}$ and the limiting value of tenacity. The values of C and D were evaluated using a suitable program on a computer. It was observed that the tenacity of both ring and rotor yarns decreased with the increase in gauge length, but the rate of decrease was more in case of ring yarn than rotor yarn. According to Hussain *et al.*, this was due to fact that the rotor yarns are more uniform along their length than their ring counterparts.

2.4.5 Kapadia's Equation

Based on experimental results, Kapadia (1935) suggested the following power law expression

$$S_M = EM^F, \tag{2.18}$$

where M denotes the order of multiple lengths (multiples of 1 foot long) forming various test specimens, S_M is the corresponding strength, E and F are two constants.

2.4.6 Mark's Equation

Mark (1932) proposed the following logarithmic equation

$$\frac{S^*}{T} = \frac{S}{T} - G\log_e\left(\frac{l}{l_0}\right), \tag{2.19}$$

where S^* and S are strengths measured at gauge lengths l and l_0, respectively, T is yarn count, and G is the degree of imperfection indicating the rate of decrease in strength with increasing gauge length.

2.4.7 Sippel's Equation

On the basis of experimental observations, Sippel (1958) proposed the following empirical relation

$$\frac{1}{S^* - S_\infty} = \frac{1}{S_0 - S_\infty} + Hl, \qquad (2.20)$$

where S_0 is the strength at zero gauge length, S^* is the strength of a sample of length l, S_∞ is the strength of an infinity long sample, and H is a factor characteristic to the material.

2.5 Types of Yarn Breakages at Different Gauge Lengths

Hearle & Thakur (1961) classified the yarn breakages into two types: catastrophic and non-catastrophic. The catastrophic yarn breakage occurs when all fibers break or slip completely at the same load. The load-extension curve of a yarn that undergoes catastrophic breakage is shown in Figure 2.7a. A yarn is said to have broken non-catastrophically when all fibers do not completely break or slip at the same load. When a few fibers break, the remaining fibers continue to take up the load, with different sets of fiber breaking at different loads. The load-extension curve for a yarn that breaks non-catastrophically is shown in Figure 2.7b.

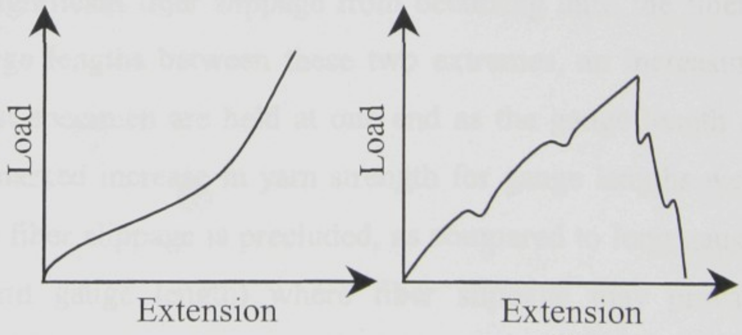

a b

Figure 2.7

Radhakrisnaiah & Huang (1997) studied the influence of gauge length on the load-extension behavior of single (cotton) and blended (polyester 50%-cotton 50%) spun yarns produced by different spinning technologies. They found all yarns showed the catastrophic breakage at 500 mm gauge length testing, and at 45 mm gauge length testing only the ring spun yarns showed mostly catastrophic breakage, while the rotor, air-jet, and friction spun yarns showed mostly non-catastrophic breakage. Thus they concluded that the manner of yarn breakage at short gauge length (45 mm) is different than that at long gauge length (500 mm).

2.6 Physical Mechanisms of Yarn Breakages at Different Gauge Lengths

There are two primary mechanisms of yarn breakages: fiber breakage and fiber slippage (Hearle 1989). In general, if two similar yarns break by different mechanisms, the one breaking due to fiber slippage, as opposed to fiber breakage, should result in lower strength. Yarn twist plays an important role in deciding the mechanism of yarn breakages. It is known that increasing yarn twist causes the breaking mechanism to change from one dominated by fiber slippage at low twist multiplier to one dominated by fiber breakage at higher twist multiplier.

Based on the scanning electron microscopic photographs of unbroken, partially broken, and completely broken samples, Realff *et al.* (1991) concluded that the mechanism of breakage might also change due to a decrease in the gauge length. According to them, at a gauge length well above the staple length of fiber, only a few percent of the fiber population of the specimen are held in either test jaw. Conversely, at a gauge length well below the staple length, nearly all fibers are held at both ends by the test jaws, preventing significant fiber slippage from occurring until the fibers first break in tension. At gauge lengths between these two extremes, an increasing percentage of fibers in the test specimen are held at one end as the gauge length is decreased. Hence, there is a marked increase in yarn strength for gauge lengths well below the staple length where fiber slippage is precluded, as compared to long gauge lengths (for example, standard gauge length) where fiber slippage may prevail depending on yarn structure and fiber properties.

Influence of Yarn Structure: The structural influence on yarn breakages at different gauge lengths is a little known from the study of Realff *et al.* (1991). They conducted strength measurements of polyester-cotton (65/35) blended ring and air-jet spun yarns of same count (23 tex) at different gauge lengths (12.7 mm, 25.4 mm, 54 mm, 76.2 mm, 127 mm, and 254 mm). It was observed that at 95% significance level, the ring yarn was statistically stronger than the corresponding air-jet spun yarn at all gauge lengths more than 12.7 mm, but this difference was not statistically significant at a gauge length of 12.7 mm. They explained this behavior on the basis of their structural differences. The air-jet spun yarn consists of a core of almost parallel fibers encased in wrapper fibers whereas the ring spun yarn is characterized by its concentric migrating helical structures. The core fibers in the air-jet spun yarn is less constrained by their neighbors than their ring spun counterparts, which enables more slippage to occur in case of air-jet spun yarn during tensile testing at long gauge lengths and a dominant breakage mechanism is expected once the constraint of the wrapper fibers is lost.

Influence of Fiber properties: Besides the yarn structural influence, fiber properties are also playing significant roles in determining the strength of yarns at different gauge lengths (Perepelkin *et al.* 1987). It was observed that at short gauge length, say 50 mm, the role of fiber strength in determining yarn tensile characteristics was very dominant; while, at higher gauge length (for example 500 mm) the role of inter-fiber friction was more significant than the role of fiber strength.

2.7 Causes of Yarn Strength Variability

Suh *et al.* (2001) developed a procedure for quantifying variability in strength of spun yarns by introducing a new variance tolerancing and decomposition method. According to them, the total variance of yarn strength $\left(\sigma_T^2\right)$ decomposes into two components: the between-package variance $\left(\sigma_{bp}^2\right)$ and the within-package variance $\left(\sigma_{wp}^2\right)$, as shown below

$$\sigma_T^2 = \sigma_{bp}^2 + \sigma_{wp}^2 . \qquad (2.21)$$

The between-package variance $\left(\sigma_{bp}^2\right)$ is entirely due to variations in processing machines accrued at different stages of spinning. The within-package variance $\left(\sigma_{wp}^2\right)$, on the other hand, further decomposes into two subcomponents: random variance $\left(\sigma_r^2\right)$ and nonrandom variance $\left(\sigma_{nr}^2\right)$, as follows

$$\sigma_{wp}^2 = \sigma_r^2 + \sigma_{nr}^2 . \qquad (2.22)$$

The random component $\left(\sigma_r^2\right)$ is due to variances in raw material properties and those resulting from random errors associated with fiber arrangement within the yarn. The variance from the nonrandom component $\left(\sigma_{nr}^2\right)$ reflects the variations caused by systematic fluctuations of the fiber mass due to process-induced drafting waves, operator effects, environmental effects, etc. The total amount of process-induced variance $\left(\sigma_p^2\right)$ can be obtained by adding the two nonrandom components $\left(\sigma_{nr}^2 \text{ and } \sigma_{bp}^2\right)$, as shown below

$$\sigma_p^2 = \sigma_{nr}^2 + \sigma_{bp}^2 . \tag{2.23}$$

Then the total variance of yarn strength can be expressed as a summation of two variances: the total process-induced variance $\left(\sigma_p^2\right)$ and the variance due to the random components $\left(\sigma_r^2\right)$, as follows

$$\sigma_T^2 = \sigma_p^2 + \sigma_r^2 . \tag{2.24}$$

It was found that the process-induced variations accounted for 69-82% of the total observed variation in yarn strength and the rest (18-31%) was due to the variations in fiber properties and the random arrangement of fibers within the yarn. Clearly, the relatively large proportion of process-induced variation is most significant and needs to be controlled and reduced.

The following sections are dealt with the effect of variation of fiber properties and the influence of yarn mass irregularity on yarn strength variability.

2.7.1 Variation in Fiber Properties

Suh *et al.* (2001) observed that the coefficient of variation of fiber strength was translated into a higher coefficient of variation of yarn strength, but the effect of fiber length coefficient of variation was small and less consistent.

2.7.2 Yarn Mass Irregularity

Solovev (1938) found from the experimental analysis of several cotton yarns including both carded and combed cotton yarns that the variability in yarn strength can be expressed by the following formula

$$P = P_0 + \sqrt{\frac{1000}{\overline{T}}} , \tag{2.25}$$

where P is the yarn strength variability, $\overline{T}$ is the average yarn count expressed in tex, and P_0 is a constant responsible for the component of variance resulting from the spinning system depending on the correctness of the process. The boundary values for P_0, as reported by him, are: $3.5 \le P_0 \le 4.0$ for combed material and $4.5 \le P_0 \le 6.0$ for carded material. Based on the experimental results, Vinter & Drokhanova (1977) found yarn strength variability was directly proportional to yarn mass irregularity. In another research, based on the consideration that the variability in strength of fracture zones of 5 mm length is directly proportional to the mass variation of the same length, Frydrych (1992) obtained a very high correlation coefficient (0.94) between the theoretical and experimental yarn strength measured at 500 mm gauge length. Yang & Lamb (1998) found a linear dependence of the strength on the unevenness in case of worsted yarn and observed that the amount of reduction of yarn strength at higher gauge length from the strength of the fracture zone could be accounted for yarn unevenness. Hamby *et al.* (1960) observed the following empirical power law relation between mass irregularity and strength variations of American combed cotton yarns with different counts

$$\nu(S) = JK^{\nu(T)}, \tag{2.26}$$

where $\nu(T)$ and $\nu(S)$ are coefficients of variation of mass and strength, respectively, J and K are two constants. Based on their experimental data, the correlation coefficient between these two was found as 0.83. A similar relation was found by El-Behery & Mansoor (1970) in case of the Egyptian carded and combed cotton yarns with different counts. According to their observation, the correlation coefficients between mass and strength variations of carded and combed cotton yarn were 0.93 and 0.71, respectively, and the appearance of greater number of thick and thin places in carded yarn than combed yarn of same count resulted the former to be more sensitive for mass and strength variations than the latter. Mandl (1981) observed the following relations between yarn mass irregularity and strength

$$\overline{S^*} = \frac{S^*}{T}\overline{T}\left\{1 - 0.80\frac{\mathrm{CV_w}(l)}{100}\right\}, \tag{2.27}$$

$$\mathrm{CV}_S(l) = \frac{1}{1 - 0.80\dfrac{\mathrm{CV_w}(l)}{100}\cdot\mathrm{CV_B}(l)}, \tag{2.28}$$

where S^* is the strength at gauge length l, $\overline{S^*}$ is the mean strength at gauge length l, T is the yarn count (tex), $\overline{T}$ is the mean yarn count (tex), $\mathrm{CV_w}(l)$ is the coefficient of variation of mass within the yarn section, $\mathrm{CV_B}(l)$ is the coefficient of variation of mass between yarn sections, and $\mathrm{CV_S}(l)$ is the coefficient of variation of strength. It is clear from the above expressions that, for a fixed length, improvement in yarn evenness has the same effect on strength. It is also evident that, when the gauge length is increased, both $\overline{S^*}$ and $\mathrm{CV_S}(l)$ are reduced.

3 THEORY

3.1 Concept of Stochastic Process

Let us take a long length of yarn and successively divide into several short sections of equal length l_0, as shown in Figure 3.1. These successive sections are designated by the serial numbers $i = 1, 2, 3, \ldots, k, \ldots$. Each i^{th} section possesses some value of strength S_i. These strength values are found depending on the serial number of the section i. The whole procedure can be independently repeated many times from the other places of the same yarn. In this way, strength of the same-numbered sections can be found many times. Therefore, S_i, where $i = 1, 2, \ldots$, are stochastic variables. Now S_i can be understood as a function assigning strength values to each serial number i denoting sections of equal length l_0. Because each S_i is a stochastic quantity, this function can be called as stochastic function having a discrete argument i or stochastic process with discrete argument i. In this case, those repetitions are called as realizations of the stochastic process. It is also possible to describe a general section of length l_0 in terms of its distance x from the first section (Section No. 1 in Figure 3.1) by the following expression

$$x = l_o(i-1). \tag{3.1}$$

Then the discrete parameter x is another argument of the stochastic process.

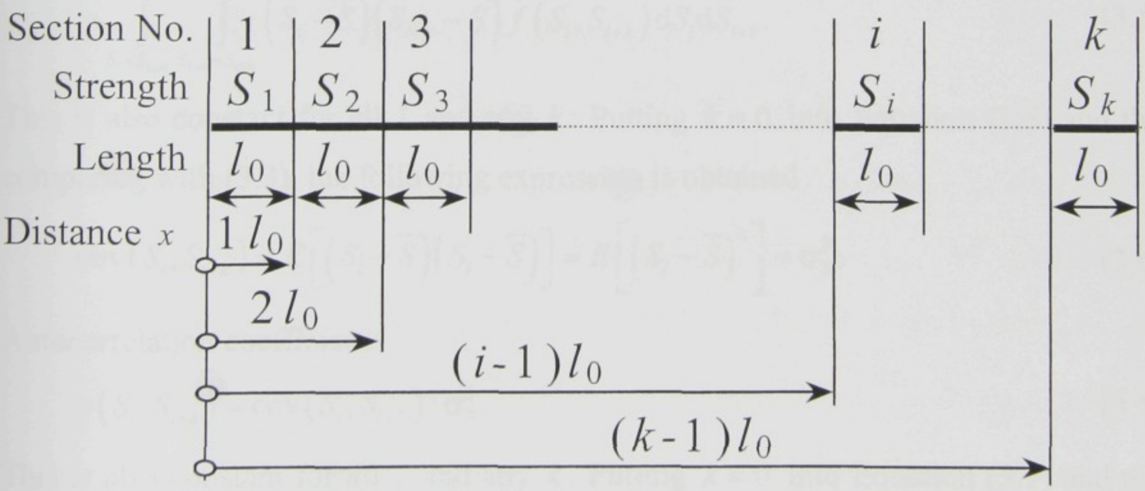

Figure 3.1

3.2 Stationary Stochastic Process

A stationary stochastic process has a behavior that does not depend on where the time origin is placed. It means that the distribution of the stochastic variables

$S_i, S_{i+a_1}, S_{i+a_2}, \ldots, S_{i+a_n}$ (parameters $a_1 \langle a_2 \langle \cdots \langle a_n$ are same for all values of *i*) depends on the value of $a_1, a_2, \ldots, a_n$, but does not depend on the value of *i*. Hence the probability density function $f(S_i), S_i \in (S_{\min}, S_{\max})$ is same for all values of *i*. The statistical characteristics of this process are given below.

Mean:

$$E(S_i) = \int_{S_{\min}}^{S_{\max}} S_i f(S_i)\,\mathrm{d}S_i = \overline{S}. \tag{3.2}$$

This is constant for all values of $i = 1, 2, \ldots$.

Variance:

$$\operatorname{var}(S_i) = E\left[\left(S_i - \overline{S}\right)^2\right] = \int_{S_{\min}}^{S_{\max}} \left(S_i - \overline{S}\right)^2 f(S_i)\,\mathrm{d}S_i = \sigma_S^2. \tag{3.3}$$

This is also constant for all values of $i = 1, 2, \ldots$.

Standard deviation:

$$\sigma_S = \sqrt{\sigma_S^2}. \tag{3.4}$$

This is also constant for all values of $i = 1, 2, \ldots$.

Autocovaraince:

$$\operatorname{cov}(S_i, S_{i+k}) = E\left[\left(S_i - \overline{S}\right)\left(S_{i+k} - \overline{S}\right)\right] =$$

$$= \int_{S_i = S_{\min}}^{S_{\max}} \int_{S_{i+k} = S_{\min}}^{S_{\max}} \left(S_i - \overline{S}\right)\left(S_{i+k} - \overline{S}\right) f(S_i, S_{i+k})\,\mathrm{d}S_i \mathrm{d}S_{i+k}. \tag{3.5}$$

This is also constant for all i and any k. Putting $k = 0$ into Equation (3.5) and then comparing with (3.3), the following expression is obtained

$$\operatorname{cov}(S_i, S_{i+k}) = E\left[\left(S_i - \overline{S}\right)\left(S_i - \overline{S}\right)\right] = E\left[\left(S_i - \overline{S}\right)^2\right] = \sigma_S^2. \tag{3.6}$$

Autocorrelation coefficient:

$$\rho(S_i, S_{i+k}) = \operatorname{cov}(S_i, S_{i+k}) / \sigma_S^2. \tag{3.7}$$

This is also constant for all i and any k. Putting $k = 0$ into Equation (3.7) and then using (3.6), the following expression for the autocorrelation coefficient is obtained

$$\rho(S_i, S_{i+k}) = \operatorname{cov}(S_i, S_{i+k}) / \sigma_S^2 = \sigma_S^2 / \sigma_S^2 = 1. \tag{3.8}$$

3.3 Ergodic Stochastic Process

In this stochastic process, the probability and the statistical characteristics related to one single realization do not change from those corresponding to other realizations. The statistical characteristics of this stochastic process are given below.

Mean:

$$\overline{S} = \lim_{k \to \infty} \frac{1}{k} \sum_{i=1}^{k} S_i \,. \tag{3.9}$$

Variance:

$$\sigma_S^2 = \lim_{k \to \infty} \frac{1}{k} \sum_{i=1}^{k} \left(S_i - \overline{S} \right)^2 . \tag{3.10}$$

Standard deviation:

$$\sigma_S = \lim_{k \to \infty} \sqrt{\frac{1}{k} \sum_{i=1}^{k} \left(S_i - \overline{S} \right)^2} \,. \tag{3.11}$$

Autocovaraince:

$$\operatorname{cov}\left(S_i, S_{i+k}\right) = \lim_{k \to \infty} \frac{1}{k} \sum_{i=1}^{k} \left[\left(S_i - \overline{S} \right) \left(S_{i+k} - \overline{S} \right) \right]. \tag{3.12}$$

Autocorrelation coefficient:

$$\rho\left(S_i, S_{i+k}\right) = \lim_{k \to \infty} \frac{1}{k} \sum_{i=1}^{k} \left[\left(S_i - \overline{S} \right) \left(S_{i+k} - \overline{S} \right) \right] \Big/ \lim_{k \to \infty} \frac{1}{k} \sum_{i=1}^{k} \left(S_i - \overline{S} \right)^2 . \tag{3.13}$$

3.4 Markovian Stochastic Process

Usually, by the event “strength is S_i” or “strength has a value S_i”, it is imagined that the strength value of the i^{th} section lies somewhere in the interval $\left(S_i, S_i + \mathrm{d}S_i\right)$. Analogously, by the event “strength is $S_i, S_{i+1}, \ldots, S_{i+k}$” or “strength has different values $S_i, S_{i+1}, \ldots, S_{i+k}$”, we imagine that the strength values of the $i^{\text{th}}, i+1^{\text{th}}, \ldots, i+k^{\text{th}}$ sections lie somewhere in the intervals $\left(S_i, S_i + \mathrm{d}S_i\right), \left(S_{i+1}, S_{i+1} + \mathrm{d}S_{i+1}\right), \ldots, \left(S_{i+k}, S_{i+k} + \mathrm{d}S_{i+k}\right)$. The probability that the strength of any section lying between S and $\left(S + \mathrm{d}S\right)$ is $f\left(S\right)\mathrm{d}S$. The probability of strength S_{i+1} of $i+1^{\text{th}}$ section can be obtained from the already known strength $S_1, S_2, \ldots, S_i$ of first i sections. If the strength of $i+1^{\text{th}}$ section is independent of the strength of the preceding i sections, then the probability that the strength of $i+1^{\text{th}}$ section lying between S_{i+1} and $(S_{i+1}+\mathrm{d}S_{i+1})$ is $f(S_{i+1})\mathrm{d}S_{i+1}$. Generally, the probability of strength S_{i+1} depends on the strength $S_1, S_2, ..., S_i$ of all previous sections. (It is usually considered that if the strength values of all previous sections are higher, then the strength value of the following section is also higher and vice-versa.) Under the Markovian stochastic process, it is assumed that the knowledge of only the "present" strength value S_i is necessary to determine the "future" strength value S_{i+1}, where information on the "past" strength values $S_1, S_2, ..., S_{i-1}$ is already considered in the "present" strength value. This is known as Markovian property of the Markovian stochastic process.

3.5 SEM-Stochastic Process

Sometimes the above three stochastic processes are combined together and then the stochastic process is called as stationary, ergodic, and Markovian stochastic process, or in short SEM-stochastic process.

3.5.1 Probability Characteristics

The SEM-stochastic process is usually described by the probability density function $f(S_i)$ and the conditional probability density function $\varphi(S_{i+k}|S_i)$. The former function tells about the distribution of S_i and the latter describes the distribution of S_{i+1}, when the strength S_i of the previous section is known.

According to the theory of probability, the probability that i^{th} section has the strength S_i and simultaneously $i+1^{\text{th}}$ section has the strength S_{i+1} is $f(S_i, S_{i+1})\mathrm{d}S_i\mathrm{d}S_{i+1}$, where $f(S_i, S_{i+1})$ is the joint probability density function of the strength of two consecutive sections. This probability can be written as follows

$$f(S_i, S_{i+1})\mathrm{d}S_i\mathrm{d}S_{i+1} = f(S_i)\mathrm{d}S_i \cdot \varphi(S_{i+1}|S_i)\mathrm{d}S_{i+1}. \tag{3.14}$$

The above expression can be written in another form

$$f(S_i, S_{i+1}) = f(S_i)\varphi(S_{i+1}|S_i). \tag{3.15}$$

Now the following expression is evident from the above equation

$$\varphi(S_{i+1}|S_i) = \frac{f(S_i, S_{i+1})}{f(S_i)}. \tag{3.16}$$

Under the assumption of the stationary process, both of the functions at the right-hand side of Equation (3.16) are same for all values of *i*; hence, $\varphi\left(S_{i+1}\middle|S_i\right)$ is also same for all values of *i*.

Similarly, using the multiplication rule of probability, the joint probability of the strength of three consecutive sections can be written as follows

$$\begin{aligned}&f\left(S_i,S_{i+1},S_{i+2}\right)\mathrm{d}S_i\mathrm{d}S_{i+1}\mathrm{d}S_{i+2}=\\&=\left[f\left(S_i\right)\mathrm{d}S_i\cdot\varphi\left(S_{i+1}\middle|S_i\right)\mathrm{d}S_{i+1}\right]\cdot\left[\varphi\left(S_{i+2}\middle|S_{i+1}\right)\mathrm{d}S_{i+2}\right]=\\&=f\left(S_i\right)\varphi\left(S_{i+1}\middle|S_i\right)\varphi\left(S_{i+2}\middle|S_{i+1}\right)\mathrm{d}S_i\mathrm{d}S_{i+1}\mathrm{d}S_{i+2}.\end{aligned}\tag{3.17}$$

Then the following expression is evident from the above equation

$$f\left(S_i,S_{i+1},S_{i+2}\right)=f\left(S_i\right)\varphi\left(S_{i+1}\middle|S_i\right)\varphi\left(S_{i+2}\middle|S_{i+1}\right).\tag{3.18}$$

The last expression tells the joint probability density function $f\left(S_i,S_{i+1},S_{i+2}\right)$ of the strength of three consecutive sections.

Analogously, it is possible to obtain the joint probability of the strength of $k=3$ consecutive sections, then $k=4$, and so on till the last repeat. Thus the following expression is found

$$\begin{aligned}&f\left(S_i,S_{i+1},S_{i+2},...,S_{i+k}\right)\mathrm{d}S_i\mathrm{d}S_{i+1}\mathrm{d}S_{i+2}\cdots\mathrm{d}S_{i+k}=\\&=\left[f\left(S_i\right)\mathrm{d}S_i\cdot\varphi\left(S_{i+1}\middle|S_i\right)\mathrm{d}S_{i+1}\cdot\varphi\left(S_{i+2}\middle|S_{i+1}\right)\mathrm{d}S_{i+2}\cdots\varphi\left(S_{i+k-1}\middle|S_{i+k-2}\right)\mathrm{d}S_{i+k-1}\right]\cdot\\&\cdot\left[\varphi\left(S_{i+k}\middle|S_{i+k-1}\right)\mathrm{d}S_{i+k}\right]\\&=f\left(S_i\right)\varphi\left(S_{i+1}\middle|S_i\right)\varphi\left(S_{i+2}\middle|S_{i+1}\right)\cdots\varphi\left(S_{i+k}\middle|S_{i+k-1}\right)\mathrm{d}S_i\mathrm{d}S_{i+1}\mathrm{d}S_{i+2}\cdots\mathrm{d}S_{i+k}.\end{aligned}\tag{3.19}$$

From the above equation, the following relation is evident

$$f\left(S_i,S_{i+1},S_{i+2},...,S_{i+k}\right)=f\left(S_i\right)\prod_{j=1}^{k}\varphi\left(S_{i+j}\middle|S_{i+j-1}\right),\tag{3.20}$$

where $k=1,2,\ldots$. The last expression tells the joint probability density function $f\left(S_i,S_{i+1},S_{i+2},\ldots S_{i+k}\right)$ of the strength of k consecutive sections. Under the assumption of the stationary process, both of the functions at the right-hand side of Equation (3.20) are same for all values of *i*; accordingly, $f\left(S_i,S_{i+1},S_{i+2},...,S_{i+k}\right)$ is also same for all *i*.

Now the joint probability of the strength of any two sections i^{th} and $i+k^{\text{th}}$ can be written as follows

$$f\left(S_i,S_{i+k}\right)\mathrm{d}S_i\mathrm{d}S_{i+k}=f\left(S_i\right)\mathrm{d}S_i\cdot\varphi\left(S_{i+k}\middle|S_i\right)\mathrm{d}S_{i+k}.\tag{3.21}$$

From the above equation, the following expression is evident

$$f\left(S_i, S_{i+k}\right) = f\left(S_i\right) \cdot \varphi\left(S_{i+k} \middle| S_i\right), \tag{3.22}$$

where $k = 1, 2, \ldots$. The last expression tells the joint probability density function $f\left(S_i, S_{i+k}\right)$ of the strength any two sections. In accordance with the theory of probability and using Equation (3.20), we obtain another form of the above distribution function as shown below

$$\begin{aligned}
f\left(S_i, S_{i+k}\right) &= \\
&= \int\limits_{S_{i+1}=S_{\min}}^{S_{\max}} \int\limits_{S_{i+2}=S_{\min}}^{S_{\max}} \cdots \int\limits_{S_{i+k-1}=S_{\min}}^{S_{\max}} f(S_i, S_{i+1}, S_{i+2}, \ldots, S_{i+k-1} S_{i+k}) \mathrm{d}S_{i+1} \mathrm{d}S_{i+2} \cdots \mathrm{d}S_{i+k-1} \\
&= \int\limits_{S_{i+1}=S_{\min}}^{S_{\max}} \int\limits_{S_{i+2}=S_{\min}}^{S_{\max}} \cdots \int\limits_{S_{i+k-1}=S_{\min}}^{S_{\max}} f(S_i) \left[\prod_{j=1}^{k} \varphi\left(S_{i+j} \middle| S_{i+j-1}\right) \right] \mathrm{d}S_{i+1} \mathrm{d}S_{i+2} \cdots \mathrm{d}S_{i+k-1} \\
&= f(S_i) \int\limits_{S_{i+1}=S_{\min}}^{S_{\max}} \int\limits_{S_{i+2}=S_{\min}}^{S_{\max}} \cdots \int\limits_{S_{i+k-1}=S_{\min}}^{S_{\max}} \left[\prod_{j=1}^{k} \varphi\left(S_{i+j} \middle| S_{i+j-1}\right) \right] \mathrm{d}S_{i+1} \mathrm{d}S_{i+2} \cdots \mathrm{d}S_{i+k-1},
\end{aligned} \tag{3.23}$$

where $k = 2, 3, \ldots$. Comparing Equation (3.23) with (3.22), the following expression for the conditional probability density function $\varphi\left(S_{i+k} \middle| S_i\right)$ is obtained

$$\varphi\left(S_{i+k} \middle| S_i\right) = \int\limits_{S_{i+1}=S_{\min}}^{S_{\max}} \int\limits_{S_{i+2}=S_{\min}}^{S_{\max}} \cdots \int\limits_{S_{i+k-1}=S_{\min}}^{S_{\max}} \left[\prod_{j=1}^{k} \varphi\left(S_{i+j} \middle| S_{i+j-1}\right) \right] \mathrm{d}S_{i+1} \mathrm{d}S_{i+2} \cdots \mathrm{d}S_{i+k-1}, \tag{3.24}$$

where $k = 2, 3, \ldots$. The above integral function is same for all values of *i* in the case of stationary process; accordingly, $\varphi\left(S_{i+k} \middle| S_i\right)$ is also same for all values of *i*.

3.5.2 Statistical Characteristics

The statistical characteristics of the SEM-stochastic process are usually described by the mean, variance or standard deviation, autocovariance, and autocorrelation coefficient. Certainly, the expressions for the statistical characteristics of the SEM-stochastic process are identical to those of the stationary stochastic process.

3.6 Summation of Two Independent SEM-Stochastic Processes

Sometimes the stochastic process S_i is considered as a summation of two independent SEM-stochastic processes ${}^{(1)}S_i$ and ${}^{(2)}S_i$ as defined below

$$S_i = {}^{(1)}S_i + {}^{(2)}S_i , \tag{3.25}$$

where ${}^{(1)}S_i$ and ${}^{(2)}S_i$ represent the first and second stochastic process of the above type, respectively.

The statistical characteristics of this process are given below.

Mean:

$$\overline{S} = \overline{{}^{(1)}S} + \overline{{}^{(2)}S} . \tag{3.26}$$

Since the two SEM-stochastic processes are mutually independent, then the following expression is valid for $i = 1, 2, \ldots$ and $k = 0, 1, 2, \ldots$,

$$E\left({}^{(1)}S_i \, {}^{(2)}S_{i+k}\right) = E\left({}^{(2)}S_i \, {}^{(2)}S_{i+k}\right) = \overline{{}^{(1)}S} \; \overline{{}^{(2)}S} . \tag{3.27}$$

Using this expression, the following expressions for the other statistical characteristics of this process are obtained.

Variance:

$$\sigma_S^2 = {}^{(1)}\sigma_S^2 + {}^{(2)}\sigma_S^2 . \tag{3.28}$$

Standard deviation:

$$\sigma_S = \sqrt{{}^{(1)}\sigma_S^2 + {}^{(2)}\sigma_S^2} . \tag{3.29}$$

Autocovariance:

$$\operatorname{cov}\left(S_i, S_{i+k}\right) = \operatorname{cov}\left({}^{(1)}S_i, {}^{(1)}S_{i+k}\right) + \operatorname{cov}\left({}^{(2)}S_i, {}^{(2)}S_{i+k}\right) . \tag{3.30}$$

Autocorrelation coefficient:

$$\rho\left(S_i, S_{i+k}\right) = \frac{{}^{(1)}\sigma_S^2}{\sigma_S^2} \rho\left({}^{(1)}S_i, {}^{(1)}S_{i+k}\right) + \frac{{}^{(2)}\sigma_S^2}{\sigma_S^2} \rho\left({}^{(2)}S_i, {}^{(2)}S_{i+k}\right) . \tag{3.31}$$

The expressions at the right-hand side of Equations (3.25) to (3.31) are independent of *i*; therefore, the left-hand side of those expressions are also independent of *i*. Consequently, the summation of two independent SEM-stochastic processes ${}^{(1)}S_i$ and ${}^{(2)}S_i$ is also a similar type of stochastic process S_i.

3.7 Gaussian Stochastic Process

Sometimes the probability density function of the strength S_i is given by

$$f\left(S_i\right) = \frac{1}{\sqrt{2\pi}\sigma_S} \exp\left\{ -\frac{\left(S_i - \overline{S}\right)^2}{2\sigma_S^2} \right\} . \tag{3.32}$$

The above function follows Gaussian distribution with mean value $\overline{S}$ (parameter) and variance σ_S^2 (parameter). Then the stochastic process is called Gaussian stochastic process. The conditional probability density function can be written as follows

$$\varphi\left(S_{i+1}, S_i\right) = \frac{1}{\sqrt{2\pi}\sigma_S\sqrt{1-r^2}} \exp\left\{-\frac{\left(S_{i+1} - \left[\overline{S} + r\left(S_i - \overline{S}\right)\right]\right)^2}{2\sigma_S^2\left(1-r^2\right)}\right\}, \tag{3.33}$$

where the parameter $r = \rho\left(S_i, S_{i+1}\right)$ is the autocorrelation coefficient between S_i and S_{i+1}. The conditional probability density function also follows Gaussian distribution with two parameters: mean value $\left[\overline{S} + r\left(S_i - \overline{S}\right)\right]$ and variance $\sigma_S^2\left(1-r^2\right)$.

3.8 SEMG-Stochastic Process

When the SEM-stochastic process follows Gaussian distribution, then the stochastic process is called SEMG-stochastic process. In that case, all equations mentioned under Sections 3.5 to 3.7 are also valid in the case of SEMG-stochastic process.

3.9 Standardized SEMG-Stochastic Process

The SEMG-stochastic process S_i can be further considered as standardized SEMG-stochastic process U_i as defined below

$$U_i = \frac{S_i - \overline{S}}{\sigma_S} \quad \text{or, } S_i = \overline{S} + \sigma_S U_i. \tag{3.34}$$

Differentiation of the above expression with respect to U_i yields the following expression

$$\frac{\mathrm{d}S_i}{\mathrm{d}U_i} = \sigma_S. \tag{3.35}$$

3.9.1 Probability Characteristics

The probability density function $f\left(U_i\right)$ of the standardized SEMG-stochastic process U_i is obtained using Equations (3.32), (3.34), and (3.35) in the following manner

$$\begin{aligned} & f(U_i) = \\ & = f(S_i)\frac{\mathrm{d}S_i}{\mathrm{d}U_i} = \\ & = \frac{1}{\sqrt{2\pi}\sigma_S}\exp\left\{-\frac{U_i^2}{2}\right\}\cdot\sigma_S = \\ & = \frac{1}{\sqrt{2\pi}}\exp\left\{-\frac{U_i^2}{2}\right\}. \end{aligned} \tag{3.36}$$

Now the following expression is considered

$$U_{i+1} = \frac{S_{i+1} - \overline{S}}{\sigma_S} \quad \text{or, } S_{i+1} = \overline{S} + \sigma_S U_{i+1}. \tag{3.37}$$

Differentiation of the above expression with respect to results in the following expression

$$\frac{\mathrm{d}S_{i+1}}{\mathrm{d}U_{i+1}} = \sigma_S. \tag{3.38}$$

Using Equations (3.33), (3.37), and (3.38), the following expression for the conditional probability density function $\varphi(U_{i+1}|U_i)$ is obtained

$$\begin{aligned} & \varphi(U_{i+1}|U_i) = \\ & = \varphi(S_{i+1}|S_i)\frac{\mathrm{d}S_{i+1}}{\mathrm{d}U_{i+1}} = \\ & = \frac{1}{\sqrt{2\pi}\sqrt{1-r^2}}\exp\left\{-\frac{(U_{i+1} - rU_i)^2}{2(1-r^2)}\right\}. \end{aligned} \tag{3.39}$$

Using Equations (3.36) and (3.39), the following expression for the probability density function $f(U_i, U_{i+1})$ is obtained

$$\begin{aligned} & f(U_i, U_{i+1}) = \\ & = f(U_i)\varphi(U_{i+1}|U_i) = \\ & = \frac{1}{\sqrt{2\pi}}\exp\left\{-\frac{U_i^2}{2}\right\}.\frac{1}{\sqrt{2\pi}\sqrt{1-r^2}}\exp\left\{-\frac{(U_{i+1} - rU_i)^2}{2(1-r^2)}\right\} = \\ & = \frac{1}{2\pi\sqrt{1-r^2}}\exp\left\{-\frac{U_i^2 - 2rU_iU_{i+1} + U_{i+1}^2}{2(1-r^2)}\right\}. \end{aligned} \tag{3.40}$$

From the theory of probability and using Equation (3.39), the following expression for the conditional probability density function $\varphi(U_{i+k}|U_i)$ is obtained

$$\varphi\left(U_{i+k}\left|U_i\right.\right)=$$
$$=\int\limits_{U_{i+1}=-\infty}^{\infty}\int\limits_{U_{i+2}=-\infty}^{\infty}\cdots\int\limits_{U_{i+k-1}=-\infty}^{\infty}\left[\prod_{j=1}^{k}\varphi\left(U_{i+j}\left|U_{i+j-1}\right.\right)\right]\mathrm{d}U_{i+1}\mathrm{d}U_{i+2}\cdots\mathrm{d}U_{i+k-1}=$$
$$=\int\limits_{U_{i+1}=-\infty}^{\infty}\int\limits_{U_{i+2}=-\infty}^{\infty}\cdots\int\limits_{U_{i+k-1}=-\infty}^{\infty}$$
$$\left[\prod_{j=1}^{k}\frac{1}{\sqrt{2\pi}\sqrt{1-r^2}}\exp\left\{-\frac{\left(U_{i+j}-rU_{i+j-1}\right)^2}{2\left(1-r^2\right)}\right\}\right]\mathrm{d}U_{i+1}\mathrm{d}U_{i+2}\cdots\mathrm{d}U_{i+k-1}. \tag{3.41}$$

This is valid for $k=2,3,\ldots$. Using some mathematical relations, derived in Neckář's book (1998), the above expression can be expressed as

$$\varphi\left(U_{i+k}\left|U_i\right.\right)=\frac{1}{\sqrt{2\pi}\sqrt{1-r^{2k}}}\exp\left[-\frac{\left(U_{i+k}-r^kU_i\right)^2}{2\left(1-r^{2k}\right)}\right]. \tag{3.42}$$

Using Equations (3.36) and (3.42), the probability density function $f\left(U_i,U_{i+k}\right)$ can be expressed as follows

$$f\left(U_i,U_{i+k}\right)=f\left(U_i\right)\varphi\left(U_{i+k}\left|U_i\right.\right)=$$
$$=\frac{1}{\sqrt{2\pi}}\exp\left[-\frac{U_i^2}{2}\right]\frac{1}{\sqrt{2\pi}\sqrt{1-r^{2k}}}\exp\left[-\frac{\left(U_{i+k}-r^kU_i\right)^2}{2\left(1-r^{2k}\right)}\right]$$
$$=\frac{1}{2\pi\sqrt{1-r^{2k}}}\exp\left[-\frac{U_i^2-2r^kU_iU_{i+k}+U_{i+k}^2}{2\left(1-r^{2k}\right)}\right]. \tag{3.43}$$

3.9.2 Statistical Characteristics

The statistical characteristics of this process U_i are given below.

Mean:

$$\overline{U}=E\left(U_i\right)=\int\limits_{-\infty}^{\infty}U_if\left(U_i\right)\mathrm{d}U_i=0. \tag{3.44}$$

Variance:

$$\sigma_U^2=E\left(U_i^2\right)-\overline{U}^2=\int\limits_{-\infty}^{\infty}\left(U_i-\overline{U}\right)^2f\left(U_i\right)\mathrm{d}U_i=1-0=1. \tag{3.45}$$

Standard deviation:

$$\sigma_U=\sqrt{\sigma_U^2}=1. \tag{3.46}$$

Autocovariance:

$$\operatorname{cov}(U_i,U_{i+k}) = E(U_i U_{i+k}) - \overline{U}^2 =$$

$$= \int\limits_{U_i=-\infty}^{\infty} \int\limits_{U_{i+k}=-\infty}^{\infty} U_i U_{i+k} f(U_i,U_{i+k})\,\mathrm{d}U_i \mathrm{d}U_{i+k} - \overline{U}^2 =$$

$$= \int\limits_{-\infty}^{\infty} U_i \frac{1}{\sqrt{2\pi}} \exp\left[-\frac{U_i^2}{2}\right] \cdot$$

$$\cdot \left\{ \int\limits_{-\infty}^{\infty} U_{i+k} \frac{1}{\sqrt{2\pi}\sqrt{1-r^{2k}}} \exp\left[-\frac{\left(U_{i+k}-r^k U_i\right)^2}{2\left(1-r^{2k}\right)}\right] \mathrm{d}U_{i+k} \right\} \mathrm{d}U_i =$$

$$V = \frac{U_{i+k}-r^k U_i}{\sqrt{1-r^{2k}}} \qquad U_{i+k} = V\sqrt{1-r^{2k}} \qquad \mathrm{d}U_{i+k} = \mathrm{d}V\sqrt{1-r^{2k}}$$

$$= \int\limits_{-\infty}^{\infty} U_i \frac{1}{\sqrt{2\pi}} \exp\left[-\frac{U_i^2}{2}\right] \cdot$$

$$\cdot \left\{ \frac{\sqrt{1-r^{2k}}}{\sqrt{1-r^{2k}}} \int\limits_{-\infty}^{\infty} \left(V\sqrt{1-r^{2k}} + r^k U_i\right) \frac{1}{\sqrt{2\pi}} \exp\left[-\frac{V^2}{2}\right] \mathrm{d}V \right\} \mathrm{d}U_i =$$

$$= \int\limits_{-\infty}^{\infty} U_i \frac{1}{\sqrt{2\pi}} \exp\left[-\frac{U_i^2}{2}\right] \cdot$$

$$\cdot \left\{ \sqrt{1-r^{2k}} \int\limits_{-\infty}^{\infty} V \frac{1}{\sqrt{2\pi}} \exp\left[-\frac{V^2}{2}\right] dV + r^k U_i \int\limits_{-\infty}^{\infty} \frac{1}{\sqrt{2\pi}} \exp\left[-\frac{V^2}{2}\right] \mathrm{d}V \right\} \mathrm{d}U_i =$$

$$= \int\limits_{-\infty}^{\infty} U_i \frac{1}{\sqrt{2\pi}} \exp\left[-\frac{U_i^2}{2}\right] \left\{ \sqrt{1-r^{2k}}.0 + r^k U_i.1 \right\} \mathrm{d}U_i =$$

$$= r^k \int\limits_{-\infty}^{\infty} U_i^2 \frac{1}{\sqrt{2\pi}} \exp\left[-\frac{U_i^2}{2}\right] \mathrm{d}U_i =$$

$$= r^k \int\limits_{-\infty}^{\infty} U_i^2 \frac{1}{\sqrt{2\pi}} \exp\left[-\frac{U_i^2}{2}\right] \mathrm{d}U_i =$$

$$= r^k E\left(U_i^2\right) =$$

$$= r^k.1 =$$

$$= r^k. \tag{3.47}$$

Autocorrelation coefficient:

$$\rho(U_i,U_{i+k}) = \operatorname{cov}(U_i,U_{i+k}) / \sigma_U^2 = \operatorname{cov}(U_i,U_{i+k}) = r^k. \tag{3.48}$$

Evidently, $\rho(U_i,U_{i+k})$ is decreasing exponentially with increasing k.

3.9.3 Simulation

The conditional probability density function $\varphi(U_{i+k}|U_i)$, expressed in Equation (3.42), can be possible to express in another form by considering the following stochastic variable

$$V_{i+1}=\frac{U_{i+1}-rU_i}{\sqrt{1-r^2}}. \tag{3.49}$$

where $\sqrt{1-r^2}, rU_i$ are parameters. The following expression is then evident from the above expression

$$\frac{\mathrm{d}U_{i+1}}{\mathrm{d}V_{i+1}}=\sqrt{1-r^2}. \tag{3.50}$$

Using Equations (3.42), (3.49), and (3.50), the probability density function $f(V_{i+1})$ of the stochastic variable V_{i+1} can be obtained as follows

$$f(V_{i+1})=\varphi(U_{i+1}|U_i)\frac{\mathrm{d}U_{i+1}}{\mathrm{d}V_{i+1}}=\frac{1}{\sqrt{2\pi}\sqrt{1-r^2}}\exp\left\{-\frac{V_{i+1}^2}{2}\right\}\sqrt{1-r^2}=$$
$$=\frac{1}{\sqrt{2\pi}}\exp\left\{-\frac{V_{i+1}^2}{2}\right\}. \tag{3.51}$$

This is, however, the probability density function of the standardized Gaussian distribution. The value of the stochastic quantity U_{i+1} can be determined from Equation (3.49) by introducing the generated value of V_{i+1} from the standardized Gaussian distribution. If the values of $\overline{S}, \sigma_S, r$ are known for Gaussian distribution of S_i, then the values of S_i can be obtained from the standardized Gaussian distribution by the following manner.

1) The value of S_1 can be obtained from the following expression, which is obtained by putting $i=1$ into Equation (3.34)

   $$S_1=\sigma_S U_1+\overline{S}, \tag{3.52}$$

   the value of U_1 can be generated from the probability density function of the standardized Gaussian distribution as shown in Equation (3.36).

2) Then the value of S_2 can be obtained from the following expression, which is obtained by putting $i=1,2$ into Equation (3.37) and putting $i=1$ into (3.49)

   $$S_2=\sigma_S U_2+\overline{S}=\sigma_S\sqrt{1-r^2}V_2+r\left(S_1-\overline{S}\right)+\overline{S}. \tag{3.53}$$

   The value of S_1 is already known and the value of V_2 can be generated from the probability density function of the standardized Gaussian distribution, as shown in Equation (3.51).

3) Afterwards, the value of S_3 can be obtained from the following expression, which is obtained similarly by putting $i = 2,3$ into Equation (3.37) and putting $i = 2$ into (3.49)

$$S_3 = \sigma_S \sqrt{1-r^2} V_3 + r\left(S_2 - \overline{S}\right) + \overline{S}. \tag{3.54}$$

The value of S_2 is already known and the value of V_3 can be generated from the probability density function of the standardized Gaussian distribution, as shown in Equation (3.51).

⋮

k) The value of S_k can be obtained from the following expression, which is obtained similarly by putting $i = k-1, k$ into Equation (3.37) and putting $i = k-1$ into (3.49)

$$S_k = \sigma_S \sqrt{1-r^2} V_k + r\left(S_{k-1} - \overline{S}\right) + \overline{S}. \tag{3.55}$$

The value of S_{k-1} is already known and the value of V_k can be generated from the probability density function of the standardized Gaussian distribution, as shown in Equation (3.51).

⋮

3.10 Relation Between Standardized and Non-Standardized SEMG-Stochastic Processes

The standardized SEMG-stochastic process U_i is characterized by the mean $\overline{U} = 0$ and the variance $\sigma_U^2 = 1$ or the standard deviation $\sigma_U = 1$. Using Equation (3.47), the autocovariance can be expressed in the following form

$$\operatorname{cov}(U_i, U_{i+k}) = E(U_i U_{i+k}) = \frac{1}{\sigma_S^2} E\left[\left(S_i - \overline{S}\right)\left(S_{i+k} - \overline{S}\right)\right] = \frac{\operatorname{cov}(S_i, S_{i+k})}{\sigma_S^2} = r^k. \tag{3.56}$$

Using Equations (3.56) and (3.7), the autocorrelation coefficient can be expressed as follows

$$\rho(U_i, U_{i+k}) = \operatorname{cov}(U_i, U_{i+k}) / \sigma_U^2 = \operatorname{cov}(S_i, S_{i+k}) / \sigma_S^2 = r^k = \rho(S_i, S_{i+k}). \tag{3.57}$$

3.11 Summation of Two Independent SEMG-Stochastic Processes

Consider the summation of two independent stochastic processes according to Equation (3.25), where ${}^{(1)}S_i$ has parameters ${}^{(1)}\overline{S}, {}^{(1)}\sigma_S, {}^{(1)}r$ and ${}^{(2)}S_i$ has parameters ${}^{(2)}\overline{S}, {}^{(2)}\sigma_S, {}^{(2)}r$. The three statistical characteristics – mean, variance, and standard deviation – of this process can be directly obtained from Equations (3.26), (3.28), and (3.29), respectively. Using Equation (3.56) into (3.30), the following expression for the autocovariance function is obtained

$$\operatorname{cov}\left(S_i, S_{i+k}\right) = {}^{(1)}\sigma_S^2\, {}^{(1)}r^k + {}^{(2)}\sigma_S^2\, {}^{(2)}r^k . \tag{3.58}$$

Using Equation (3.57) into (3.31), the following expression for the autocorrelation coefficient is obtained

$$\rho\left(S_i, S_{i+k}\right) = \frac{1}{\sigma_S^2}\left({}^{(1)}\sigma_S^2\, {}^{(1)}r^k + {}^{(2)}\sigma_S^2\, {}^{(2)}r^k\right). \tag{3.59}$$

These relations are valid for all i; therefore, the autocovariance and the autocorrelation coefficients can be expressed as

$$\operatorname{cov}(k) = \operatorname{cov}\left(S_i, S_{i+k}\right) = {}^{(1)}\sigma_S^2\, {}^{(1)}r^k + {}^{(2)}\sigma_S^2\, {}^{(2)}r^k , \tag{3.60}$$

$$\rho(k) = \rho\left(S_i, S_{i+k}\right) = \frac{1}{\sigma_S^2}\left({}^{(1)}\sigma_S^2\, {}^{(1)}r^k + {}^{(2)}\sigma_S^2\, {}^{(2)}r^k\right). \tag{3.61}$$

3.12 Shorter and Longer Specimens

In analogy to Figure 3.1, if a longer length l is equally divided into $k+1$ sections of shorter length l_0 (each section is designated by serial number $i, i+1, i+2, ..., i+k$), then the lengths of longer and shorter specimen are related by

$$l = l_0\left(k+1\right). \tag{3.62}$$

The above expression can also be written as follows

$$k = l/l_0 - 1 . \tag{3.63}$$

It is evident from Figure 3.1 that the distance of i^{th} section from the first section is given by the value $l_0\left(i-1\right)$; similarly, the distance of $i+k^{\text{th}}$ section from the first section is given by the value $l_0\left(i+k-1\right)$; and hence, the distance between these two sections is given by

$$x = l_0(i+k-1) - l_0(i-1) = l_0 k. \tag{3.64}$$

Substituting Equation (3.64) into (3.62), the following expression is obtained

$$l = x + l_0. \tag{3.65}$$

3.13 Distribution of Strength of Longer Specimens

The distribution of the strength $S_i, S_{i+1}, \ldots, S_{i+k}$ of shorter specimens each of length l_0 is described by the following expression

$$\begin{aligned} & f(S_i, S_{i+1}, S_{i+2}, \ldots, S_{i+k}) = \\ & = f(S_i)\varphi(S_{i+1}|S_i)\varphi(S_{i+2}|S_{i+1})\cdots(S_{i+k}|S_{i+k-1}) = \\ & = f(S_i)\prod_{j=1}^{k}\varphi(S_{i+j}|S_{i+j-1}). \end{aligned} \tag{3.66}$$

where $k = 1, 2, \ldots$. It is considered that the strength of longer specimen of length l is S^*. The probability that the strength of each section is considerably higher than some chosen value S^* is $\left[1 - G(S^*, k)\right]$, then the following expression is valid

$$\begin{aligned} 1 - G(S^*, k) &= \int_{S_i=S^*}^{\infty}\int_{S_{i+1}=S^*}^{\infty}\cdots\int_{S_{i+k}=S^*}^{\infty} f(S_i, S_{i+1}, \ldots, S_{i+k})\,\mathrm{d}S_i\mathrm{d}S_{i+1}\cdots\mathrm{d}S_{i+k} = \\ &= \int_{S_i=S^*}^{\infty}\int_{S_{i+1}=S^*}^{\infty}\cdots\int_{S_{i+k}=S^*}^{\infty} f(S_i)\prod_{j=1}^{k}\varphi(S_{i+j}|S_{i+j-1})\,\mathrm{d}S_i\mathrm{d}S_{i+1}\cdots\mathrm{d}S_{i+k}, \end{aligned} \tag{3.67}$$

where $k = 1, 2, \ldots$. This is known as the probability of survival: the longer specimen will not be broken by the application of a force S^*. Hence, the probability of breakage (complementary probability) states that the longer section will be broken by the application of force S^*. This is expressed as follows

$$\begin{aligned} G(S^*, k) &= 1 - \int_{S_i=S^*}^{\infty}\int_{S_{i+1}=S^*}^{\infty}\cdots\int_{S_{i+k}=S^*}^{\infty} f(S_i, S_{i+1}, \ldots, S_{i+k})\,\mathrm{d}S_i\mathrm{d}S_{i+1}\cdots\mathrm{d}S_{i+k} = \\ &= 1 - \int_{S_i=S^*}^{\infty}\int_{S_{i+1}=S^*}^{\infty}\cdots\int_{S_{i+k}=S^*}^{\infty} f(S_i)\prod_{j=1}^{k}\varphi(S_{i+j}|S_{i+j-1})\,\mathrm{d}S_i\mathrm{d}S_{i+1}\cdots\mathrm{d}S_{i+k}, \end{aligned} \tag{3.68}$$

where $k = 1, 2, \ldots$. In the above distribution function $G(S^*, k)$, S^* is a stochastic variable and k is a parameter. Now the probability density function $g(S^*, k)$ of the strength S^* can be found by differentiation of the above distribution function $G(S^*, k)$ with respect to S^*. This is shown below

$$g\left(S^*,k\right)=\frac{\partial G\left(S^*,k\right)}{\partial S^*}=$$

$$=-\frac{\partial}{\partial S^*}\left\{\int\limits_{S_i=S^*}^{\infty}\int\limits_{S_{i+1}=S^*}^{\infty}\cdots\int\limits_{S_{i+k}=S^*}^{\infty}f(S_i)\prod_{j=1}^{k}\varphi\left(S_{i+j}\left|S_{i+j-1}\right.\right)\mathrm{d}S_i\mathrm{d}S_{i+1}...\mathrm{d}S_{i+k}\right\}, \tag{3.69}$$

where $k=1,2,\ldots$. Now we consider the following expression

$$U^*=\left(S^*-\overline{S}\right)/\sigma_S\,. \tag{3.70}$$

(The above expression has a sense of the transformation of strength, not the standardization of strength.) Using Equation (3.69) and some mathematical relations shown in Neckář's book (1998), it is possible to obtain the following expression for the probability density function of the variable U^*

$$g\left(U^*,k\right)=g\left(S^*,k\right)\frac{\mathrm{d}S^*}{\mathrm{d}U^*}$$

$$=-\frac{1}{\sqrt{2\pi}}\left(\frac{1}{\sqrt{2\pi}\sqrt{1-r^2}}\right)^k\cdot\frac{\partial}{\partial U^*}\left[\int\limits_{U_i=U^*}^{\infty}\int\limits_{U_{i+1}=U^*}^{\infty}\cdots\int\limits_{U_{i+k}=U^*}^{\infty}\left\{\exp\left(-\frac{U_i^2}{2}\right)\right\}.\right.$$

$$\left.\cdot\prod_{j=1}^{k}\exp\left(-\frac{\left(U_{i+j}+rU_{i+j}\right)}{2\left(1-r^2\right)}\right)\right\}\mathrm{d}U_i\mathrm{d}U_{i+1}\cdots\mathrm{d}U_{i+k}\Bigg]. \tag{3.71}$$

This function does not depend on $\overline{S}$ and σ_S, but depends on r only (apart from the parameter k).

3.14 Application

Using the simulation technique, discussed earlier, a huge number of strength values $\left\{S_i,S_{i+1},\cdots,S_{i+k}\right\}\equiv\left\{S_{i+j}\right\}_{j=0}^{j=k}$ of successive sections of shorter gauge length l_0, altogether forming the longer gauge length l, can be generated; then applying the weakest link theory (Peirce 1926), the strength value S^* of the longer gauge length l can be obtained from the minimum of those strength values, as shown below

$$S_i^*=\min\left\{S_{i+j}\right\}_{j=0}^{j=k}. \tag{3.72}$$

Thus, for a particular value of k, it is possible to obtain strength values S_i^* corresponding to the gauge length l; hence, the probability density function $g\left(S^*,k\right)$ as well as statistical parameters corresponding to the gauge length l. The same technique can be repeated for different values of $k \in \{0,1,2,\ldots\}$, and the probability density functions $g\left(S^{*},k\right)$ can be evaluated for different values of *k*, *i.e.*, for different gauge lengths $l = l_0, 2l_0, \ldots$. (The strength value of any gauge length, which is not a whole number multiple of l_0, can also be found by the interpolation technique.)

4 MATERIALS AND METHODS

4.1 Materials

In order to illustrate the theory of yarn strength as a stochastic process, discussed in Chapter 3, 100% cotton carded and combed yarns with different fineness and twist characteristics produced by ring, rotor, compact, and "new"[1] spinning technologies were examined. The distinguishing features of these yarns are shown in the tables in Appendix A. All the new yarns were produced from the same variety of cotton fiber (Egyptian Giza 70 – MII), but the rest of the yarns were produced from different varieties of cotton fibers.

4.2 Methods

In this research work, different standard and nonstandard methods were used to measure different characteristics – strength, mass, and twist – of yarns. These are discussed in the following sections.

4.2.1 Yarn Strength

Yarn strength was measured at short gauge length (50 mm) and also at higher gauge lengths (100, 200, 350, 500, and 700 mm).

4.2.1.1 Measurements at Short Gauge Length

In order to realize the yarn strength measurements, discussed in Section 3.1, a special attachment was devised for feeding equal length of yarn specimens in-between the jaws of the tensile tester (INSTRON-4411) one after another semi-automatically. The gauge length was so selected as 50 mm that no single fiber could be clamped by both of the jaws at the same time, and the testing speeds were selected for different yarns in such a manner that almost all yarn specimens were broken within 20±3 seconds. The measurement procedure can be understood from the following discussion in connection with Figure 4.1. Let us imagine that the successive sections ($l_0 = 50\,\text{mm}$) along a yarn were marked by the serial numbers $1, 2, 3, 4 \ldots, 59, 60$. Then

---

[1] The Cotton Research Institute (VUB) of Czech Republic invented a new spinning technology, which, at the time of writing of this dissertation, was not commercialized, and no specific name was given to that technology. Throughout this dissertation, that technology is called "New Spinning Technology" and the yarns made from that technology are called "New Yarns."

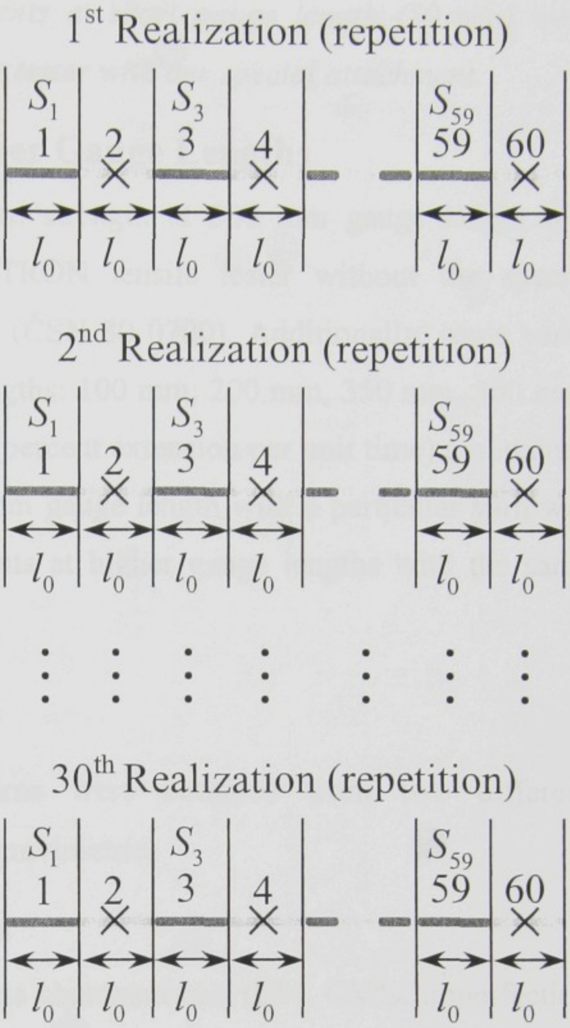

Figure 4.1

the strengths of the sections marked by the numbers $1, 3, \ldots, 59$ were measured one after another; the remaining sections (shown by the symbol '×') were used for clamping. Thus strengths $S_1, S_3, \ldots, S_{59}$ of 30 alternate sections were obtained. This procedure was repeated 30 times at different places of the yarn randomly chosen from different cops or bobbins. As a result, a time series of 900 strength values was obtained with one yarn. In this way, yarn strength measurements at 50 mm gauge length were performed with all yarns. Sometimes a few ($\approx 1\%$) out of those 900 consecutive measurements were found faulty due to improper gripping of the yarn specimens by the jaws. Those erroneous values were simply discarded while obtaining the descriptive statistical parameters and the frequency distribution of yarn strength at short gauge length. But, while estimating yarn strength autocorrelation characteristics, those erroneous values were, however, replaced numerically by zero.

Note: It is possible to perform the strength measurements automatically following the above methodology using some of the commercially available tensile testers. One such tester is STATIMAT M tensile tester. During the strength measurements using this instrument available at the Institute for Textile Technology of RWTH Aachen, Germany, it was observed that the length of the yarn wasted in-between two successive measurements was approximately 120 m, whereas this length was about 50 mm using our special attachment. It is understandable that the wastage of more length of yarn in-between two successive measurements has its significance (loss of more information) on the stochastic assessment of yarn strength. Therefore, in this *research work, yarn strength measurements at short gauge length (50 mm) were performed only using the INSTRON tensile tester with our special attachment.*

4.2.1.2 Measurements at Higher Gauge Lengths

The standard measurement of yarn strength at 500 mm gauge length was performed on all yarns using the INSTRON tensile tester without the special attachment following the Czech Standard (ČSN 80 0700). Additionally, some yarns were tested for strength at other gauge lengths: 100 mm, 200 mm, 350 mm, 500 mm, and 700 mm. Customarily, the strain rate (percent extension per unit time) maintained during the strength measurements at 50 mm gauge length with a particular yarn was the same during the strength measurements at higher gauge lengths with the same yarn.

4.2.2 Yarn Mass

The mass characteristics of yarns were obtained from two different measurement techniques – capacitive and gravimetric.

4.2.2.1 Capacitive Measurements

In order to obtain the common mass characteristics (U%, CV%, imperfection counts, mass diagram, mass spectrogram, mass variance-length curve, etc.), all yarns were tested using the USTER TESTER 4 instrument following the Czech Standard (ČSN 80 0706).

Besides the common mass characteristics, the USTER TESTER 4 instrument also displays a huge number of mass readings (18458 readings corresponding to 100 meter length of yarn) as a special output. (In order to see those readings, one has to collect them from the hard disk of the computer attached with the instrument.) A typical format containing a few among those readings, as appeared on the monitor attached with the instrument, is shown in Figure B1 of Appendix B. It was understood that those readings are usually used by the Uster instrument in order to construct the mass diagram. In this research work, those were used to estimate the mass correlograms of yarns.

4.2.2.2 Gravimetric Measurements

In this research work, 900 consecutive mass measurements were carried out manually by using an electronic weighing balance (SARTORIUS R200D with a precision of 0.01 mg) with 20 tex and 35.5 tex carded rotor yarns. The method of measurements can be understood from the following discussion in connection with Figure 4.2. Let us imagine that the successive sections, each of 50 mm length, along a yarn were marked by the serial numbers $1,2,3,\ldots,30$. Then the mass of those sections was measured individually one after another. Thus mass of 30 successive sections along the yarn was obtained. This procedure was repeated 30 times at different places of the yarns randomly chosen from different bobbins. As a result, a time series of 900 mass values, each corresponding to 50 mm length, was obtained with one yarn. The time series data was used in order to construct the yarn mass correlogram.

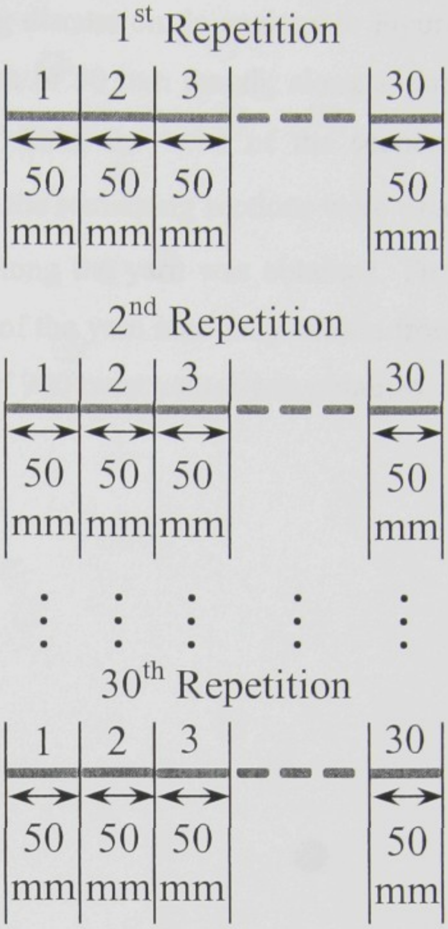

Figure 4.2

In order to obtain the descriptive statistical characteristics of yarn count, each yarn was also tested gravimetrically following the Czech Standard (ČSN 80 0702).

4.2.3 Yarn Twist

The twist measurements of yarns were carried out manually by using the SDL-SHIRLEY ELECTRIC TWIST TESTER-Y220B, working on the principle of twisting and untwisting of yarns.

4.2.3.1 Measurements with Longer Specimens

With each yarn, 50 twist measurements were performed each at 250 mm length following the Czech Standard (ČSN 80 0701), and then the common descriptive statistical parameters (mean value, standard deviation, and coefficient of variation) were estimated.

4.2.3.2 Measurements with Shorter Specimens

In order to estimate yarn twist correlogram, 900 consecutive twist measurements were carried out on 35.5 tex cotton carded rotor yarn. The method of measurements can be understood from the following discussion. In analogy to Figure 4.1, let us imagine that the successive sections, each of 50 mm length, along a yarn were marked by the serial numbers $1,2,3,\ldots,60$. Then the twist of the sections marked by the numbers $1,3,5,\ldots,59$ was measured; the remaining sections were used for clamping. Thus twist of 30 alternate sections along the yarn was obtained. This procedure was repeated 30 times at different places of the yarn randomly chosen from different cops or bobbins. As a result, a time series of 900 twist values was obtained.

5 RESULTS AND DISCUSSION

5.1 Basic Statistical Parameters of Actual Yarn Strength

The basic statistical parameters of strength of 7.4 tex and 20 tex combed ring yarns measured at different gauge lengths are presented in Table 5.1. Similar results for the other yarns are reported in Tables C1-C6 in Appendix C.

Table 5.1

Count [tex]	Gauge length [mm]	Mean [cN/tex]	Standard deviation [cN/tex]	Coefficient of Variation [%]	Number of measurements
7.4	50	21.8135	2.6730	12.2548	885
	100	20.2230	2.3730	11.7553	300
	200	20.4351	2.2284	10.9012	300
	350	19.6149	2.3446	11.9563	300
	500	18.7365	1.8554	9.9056	300
	700	17.1782	1.6420	9.5587	300
20	50	13.6290	1.3780	10.1108	897
	100	13.2590	1.3245	9.9907	300
	200	13.2015	1.2345	9.3502	300
	350	13.1950	1.0705	8.1129	300
	500	12.7985	1.1045	8.6280	300

5.1.1 Effect of Gauge Length

It can be easily understood from the table that the mean yarn tenacity decreases with increasing gauge length. This phenomenon, as explained by Peirce (1926), Kapadia (1935), Kaushik *et al.* (1989), Hussain *et al.* (1990), to name a few, is due to the result of the weakest-link effect. At the same time, the variability in yarn tenacity also decreases with the increase in gauge length.

5.1.2 Effect of Twist Multiplier

The effect of twist multiplier on mean tenacity of yarns with different mean counts is shown in Figure 5.1. Here $\overline{S}$ represents the mean strength of yarn measured at 50 mm gauge length, $\overline{T}$ denotes mean count of yarn, and α is twist multiplier

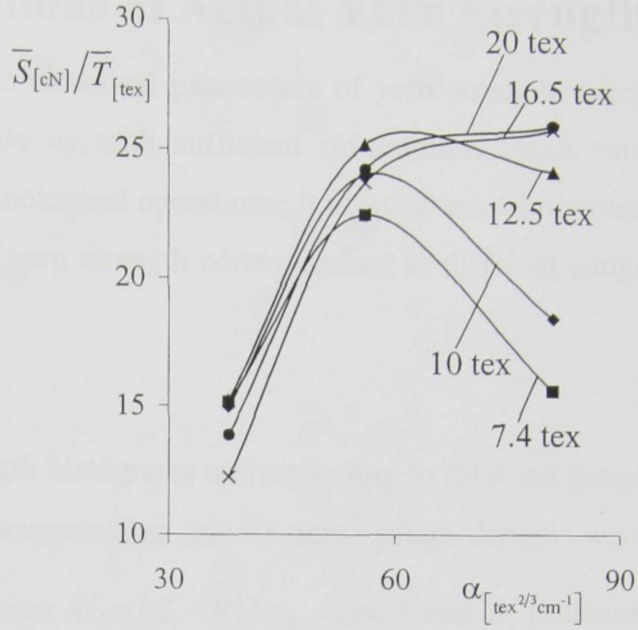

Figure 5.1

(Phrix type). Similar trend was found with the strength results corresponding to other gauge lengths. This behavior is to some extent known to us. Gegauff (1907), Platt (1950), and Neckář (2004) interpreted it as a combination of two effects: one is the resulting effect of fiber path and fiber straining in yarn, and the other is a complex of frictional mechanisms. The former effect results in reduction in yarn tenacity. This was theoretically studied by Gegauff (1907). On the other hand, as a consequence of the latter effect, yarn tenacity increases. However, this effect is still not clear. These individual effects along with the combined effect are schematically shown in Figure 5.2. Also, it is shown that there exists an optimum twist multiplier at which highest tenacity can be obtained.

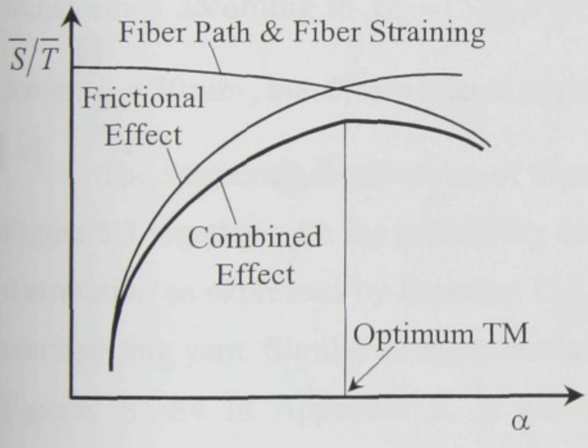

Figure 5.2

5.1.3 Comparison with The Uster Statistics 2001

Yarn tenacity parameters estimated from the actual strength data measured at 500 mm gauge length were compared with the worldwide spinning mill data reported in the Uster Statistics 2001. The comparison is presented in Table D1 in Appendix D. It can be observed that the mean tenacity of the yarns used in this research work corresponded mostly to that achieved by 95% of the spinning mills in the world, while the coefficient of variation of tenacity of the yarns used in this research work corresponded mostly to what was achieved by 50% of the worldwide spinning mills.

5.2 Frequency Distributions of Actual Yarn Strength

It is well known that the basic statistical parameters of yarn strength, taken separately or together, cannot provide us with sufficient information about yarn behavior during the post-spinning technological operations; it is much more important to know the frequency distribution of yarn strength corresponding to different gauge lengths.

5.2.1 Histograms

Prior to obtain the actual strength histograms corresponding to different gauge lengths, the strength values S_i corresponding to 50 mm gauge length were standardized according to the expression $U_i = \left(S_i - \overline{S}\right)/\sigma_S$, mentioned in Equation (3.34), and the strength values S_i^* corresponding to the other gauge lengths were transformed according to $U_i^* = \left(S_i^* - \overline{S}\right)/\sigma_S$. (Here $\overline{S}$ and σ_S are related to gauge length $l_0 = 50\,\text{mm}$, but S_i^* are related to gauge length l.)

The frequency distributions of these quantities are shown by the histograms in Figure 5.3 together with the probability density function of the standardized Gaussian distribution as expressed by Equation (3.32). These histograms correspond to 7.4 tex combed ring yarn. Similar strength histograms for some other yarns are presented in Figures E1-E4 in Appendix E. It can be observed that as the gauge length is increasing, the shape of the histogram is changing: it becomes higher and narrower. This is due to the reduction in strength variability with the increase in gauge length. The relative shifting of the histogram to the left-hand side direction with the increase in gauge length is also noticeable. This is ascribed to the decrease in mean strength value with the increase in gauge length. It is also notable that the strength histogram corresponding to 50 mm gauge length is smoother than the strength histograms corresponding to higher than 50 mm gauge length. This is because of the relatively high number of strength values available for 50 mm yarn section as compared to the longer yarn sections. This is shown in Table 5.1 and the tables presented in Appendix C.

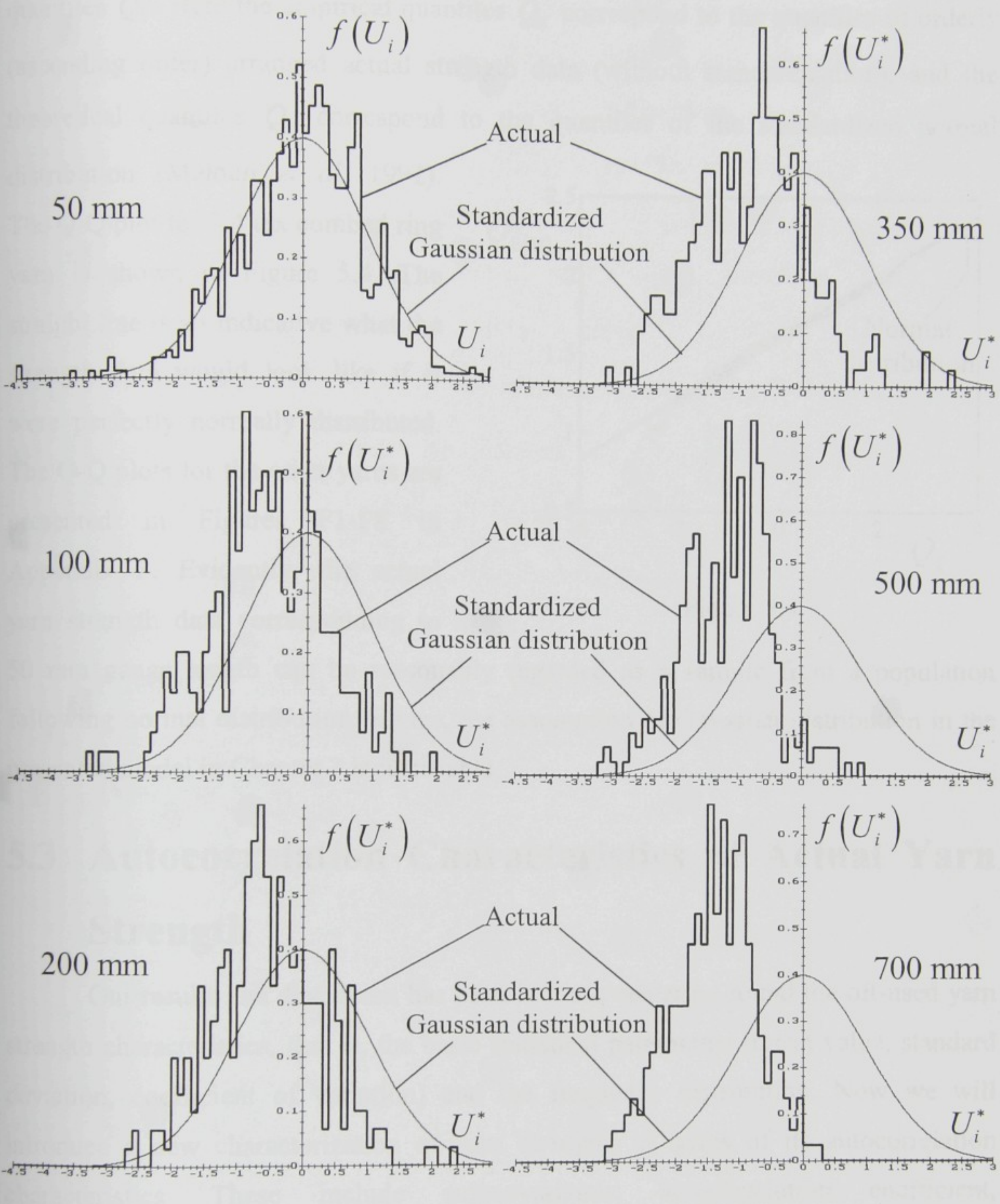

Figure 5.3

5.2.2 Checking for Normality

The mathematical model, presented in Chapter 3, assumes Gaussian (normal) distribution of yarn strength S_i corresponding to gauge length l_0. Here $l_0 = 50\,\text{mm}$. To check the normality of the actual strength distributions corresponding to 50 mm gauge length for different yarns, the quantile-quantile plot (Q-Q plot) was used in this research work. This plot compares the empirical quantiles Q_E with the theoretical quantiles Q_T. Here the empirical quantiles Q_E correspond to the quantiles of orderly (ascending order) arranged actual strength data (without standardization), and the theoretical quantiles Q_T correspond to the quantiles of the standardized normal distribution (Meloun *et al.* 1992).

The Q-Q plot for 7.4 tex combed ring yarn is shown in Figure 5.4. The straight line is an indicative what the strength data would look like if it were perfectly normally distributed. The Q-Q plots for the other yarns are presented in Figures F1-F8 in Appendix F. Evidently, the actual yarn strength data corresponding to 50 mm gauge length can be reasonably regarded as a sample from a population following normal distribution. Hence, the assumption of Gaussian distribution in the presented model in Chapter 3 is justifiable.

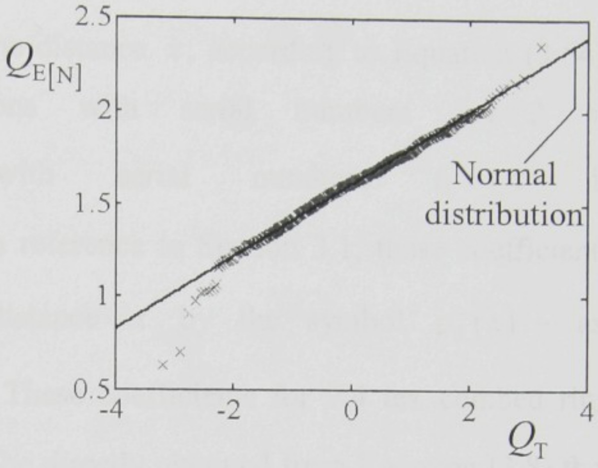

Figure 5.4

5.3 Autocorrelation Characteristics of Actual Yarn Strength

Our results and discussion has been hitherto centering round the oft-used yarn strength characteristics, that is, the basic statistical parameters (mean value, standard deviation, coefficient of variation) and the frequency distribution. Now we will introduce a new characterization of yarn strength, in terms of its autocorrelation characteristics. These include autocovariance, autocorrelation coefficient, correlogram, autocorrelation function, etc.

5.3.1 Double Exponential Strength Autocorrelation Functions

At first the autocovariances and then the autocorrelation coefficients $\rho(U_i,U_{i+2}),\rho(U_i,U_{i+4}),\rho(U_i,U_{i+6}),\ldots$ were calculated from the standardized strength values corresponding to 50 mm gauge length. (It can be easily understood from Section 4.2.1.1 that we had values $U_1,U_3,U_5,\ldots$ corresponding to every alternate sections, each of 50 mm length, along the yarn.) According to Equation (3.57), however, the autocorrelation coefficient between two standardized strength quantities is the same as between the corresponding original strength quantities, so $\rho(U_i,U_{i+2})=\rho(S_i,S_{i+2}),\ \rho(U_i,U_{i+4})=\rho(S_i,S_{i+4})$, and so on. It is also possible to express these coefficients in terms of the distance x, according to Equation (3.64), the distance between two sections with serial numbers $i,\ i+2$ is $2\cdot l_0=2\cdot 50=100\,\text{mm}$, sections with serial numbers $i,\ i+4$ is $4\cdot l_0=4\cdot 50=200\,\text{mm}$, and so on. With reference to Section 3.1, these coefficients can be referred in terms of the distance x by the symbol $\rho_S(x)$:- as, $\rho(U_i,U_{i+2})=\rho(S_i,S_{i+2})=\rho_S(100\,\text{mm})$. These coefficients for 7.4 tex combed ring yarn are presented in Figure 5.5. (It can be directly obtained from Equation (3.8) that $\rho_S(0\,\text{mm})=1$.)

Using the standard statistical regression method, it was observed that those coefficients were satisfactorily expressed by the following double exponential function

$$\rho_S(x)=0.6604e^{-0.014049x}+0.3396e^{-0.000376x}, \tag{5.1}$$

where x is expressed in mm. This function is shown in Figure 5.5. It can be also expressed in terms of lag k as follows

$$\rho_S(k)=0.6604e^{-0.7025k}+0.3396e^{-0.0188k}, \tag{5.2}$$

where $k=x_{[\text{mm}]}/50$. Evidently, the strength autocorrelation function has two highly different components: steeper fall off and gradual fall-off. The behaviors of these components are shown in Figure 5.5. Similar results with the other yarns are presented in Figures G1-G6 in Appendix G.

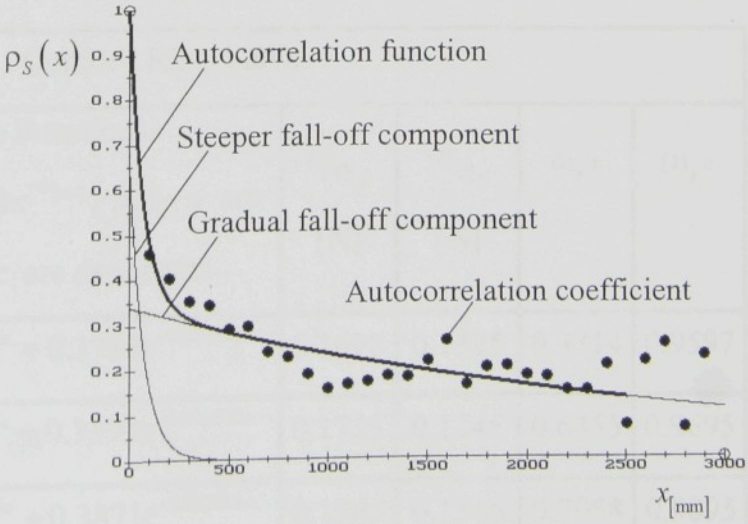

Figure 5.5

Note: Number of strength values available for estimating the autocorrelation coefficients at higher lags (higher distances) was *obviously very low; therefore, those coefficients might not be very representable. Hence, arbitrarily, the autocorrelation coefficients corresponding to higher than 2.5 m distance were discarded while estimating the autocorrelation function.*

Let us now consider Equation (5.2). Because the whole stochastic process is Gaussian and its autocorrelation function is in agreement with Equation (3.61) expressing the summation of two exponential functions, it is presumed that the stochastic process S_i is a summation of two independent stationary, ergodic, and Markovian processes ${}^{(1)}S_i$ and ${}^{(2)}S_i$. Comparing these two equations, we obtain

$$\rho_S(k) = \frac{{}^{(1)}\sigma_S^2}{\sigma_S^2}\,{}^{(1)}r^k + \frac{{}^{(1)}\sigma_S^2}{\sigma_S^2}\,{}^{(1)}r^k = 0.6604e^{-0.7025k} + 0.3396e^{-0.0188k}. \tag{5.3}$$

Then the following characteristics are evident using $\sigma_S = 0.1978$ N in case of 7.4 tex combed ring yarn

$$\frac{{}^{(1)}\sigma_S^2}{\sigma_S^2} = 0.6604; \quad \text{or, } {}^{(1)}\sigma_S = \sqrt{0.6604}\sigma_S = 0.1607 \text{ N}, \tag{5.4}$$

$$\frac{{}^{(2)}\sigma_S^2}{\sigma_S^2} = 0.3396; \quad \text{or, } {}^{(2)}\sigma_S = \sqrt{0.3396}\sigma_S = 0.1153 \text{ N}, \tag{5.5}$$

$${}^{(1)}r^k = e^{-0.7025k}; \quad \text{or, } {}^{(1)}r = e^{-0.7025} = 0.4953, \tag{5.6}$$

$${}^{(2)}r^k = e^{-0.0188k}; \quad \text{or, } {}^{(2)}r = e^{-0.0188} = 0.9814. \tag{5.7}$$

These autocorrelation characteristics together with the autocorrelation functions for the other yarns are presented in Table 5.2.

Table 5.2

Combed Ring Yarns					
$\overline{T}$ [tex]	Autocorrelation Functions: $\rho_S(x) = ae^{-bx_{[mm]}} + (1-a)e^{-cx_{[mm]}}$; $a, 1-a$ are coefficients and b, c are exponents	${}^{(1)}\sigma_S$ [N]	${}^{(2)}\sigma_S$ [N]	${}^{(1)}r^k$	${}^{(2)}r^k$
10	$\rho_S(x) = 0.6214e^{-0.022084x} + 0.3786e^{-0.000822x}$	0.1698	0.1325	0.3314	0.9597
14.5	$\rho_S(x) = 0.6601e^{-0.008756x} + 0.3399e^{-0.000620x}$	0.1735	0.1245	0.6455	0.9695
16.5	$\rho_S(x) = 0.6129e^{-0.006968x} + 0.3871e^{-0.000211x}$	0.1945	0.1546	0.7058	0.9895
20	$\rho_S(x) = 0.7032e^{-0.003868x} + 0.2968e^{-0.000335x}$	0.2311	0.1502	0.8242	0.9834

	Carded Ring Yarns				
$\overline{T}$ [tex]	Autocorrelation Functions $\rho_S(x) = ae^{-bx_{[\mathrm{mm}]}} + (1-a)e^{-cx_{[\mathrm{mm}]}}$; $a, 1-a$ are coefficients and b, c are exponents	${}^{(1)}\sigma_S$ [N]	${}^{(2)}\sigma_S$ [N]	${}^{(1)}r^k$	${}^{(2)}r^k$
20	$\rho_S(x) = 0.6659e^{-0.009063x} + 0.3341e^{-0.000327x}$	0.2363	0.1674	0.6356	0.9837
25	$\rho_S(x) = 0.7048e^{-0.005592x} + 0.2952e^{-0.000364x}$	0.2792	0.1807	0.7561	0.9820
29.5	$\rho_S(x) = 0.7450e^{-0.016243x} + 0.2550e^{-0.000244x}$	0.3956	0.2314	0.4439	0.9879
	Carded Rotor Yarns				
$\overline{T}$ [tex]	Autocorrelation Functions $\rho_S(x) = ae^{-bx_{[\mathrm{mm}]}} + (1-a)e^{-cx_{[\mathrm{mm}]}}$	${}^{(1)}\sigma_S$ [N]	${}^{(2)}\sigma_S$ [N]	${}^{(1)}r^k$	${}^{(2)}r^k$
20	$\rho_S(x) = 0.7830e^{-0.020114x} + 0.2170e^{-0.000069x}$	0.1947	0.3658	0.1025	0.9966
35.5	$\rho_S(x) = 0.5968e^{-0.024083x} + 0.4032e^{-0.000818x}$	0.3754	0.3086	0.3000	0.9599
42	$\rho_S(x) = 0.5507e^{-0.012720x} + 0.4493e^{-0.000045x}$	0.3148	0.2843	0.5294	0.9978
	Combed Compact Yarns				
$\overline{T}$ [tex]	Autocorrelation Functions $\rho_S(x) = ae^{-bx_{[\mathrm{mm}]}} + (1-a)e^{-cx_{[\mathrm{mm}]}}$	${}^{(1)}\sigma_S$ [N]	${}^{(2)}\sigma_S$ [N]	${}^{(1)}r^k$	${}^{(2)}r^k$
7.4	$\rho_S(x) = 0.7624e^{-0.024618x} + 0.2376e^{-0.000371x}$	0.1632	0.0911	0.2920	0.9816
10	$\rho_S(x) = 0.3858e^{-0.010122x} + 0.6142e^{-0.000140x}$	0.1740	0.2196	0.6029	0.9930
11.8	$\rho_S(x) = 0.6719e^{-0.017258x} + 0.3281e^{-0.000358x}$	0.2236	0.1562	0.4219	0.9823
	Carded Compact Yarns				
$\overline{T}$ [tex]	Autocorrelation Functions $\rho_S(x) = ae^{-bx_{[\mathrm{mm}]}} + (1-a)e^{-cx_{[\mathrm{mm}]}}$	${}^{(1)}\sigma_S$ [N]	${}^{(2)}\sigma_S$ [N]	${}^{(1)}r^k$	${}^{(2)}r^k$
20	$\rho_S(x) = 0.7162e^{-0.024023x} + 0.2838e^{-0.000706x}$	0.2937	0.1849	0.3009	0.9653
29.5	$\rho_S(x) = 0.5336e^{-0.017015x} + 0.4664e^{-0.000079x}$	0.3780	0.3535	0.9184	0.9961

Combed New Yarns (Twist Multiplier – 38 $\text{tex}^{2/3}\text{cm}^{-1}$)

$\overline{T}$ [tex]	Autocorrelation Functions $\rho_S(x) = ae^{-bx_{[\text{mm}]}} + (1-a)e^{-cx_{[\text{mm}]}}$; $a, 1-a$ are coefficients and b, c are exponents	${}^{(1)}\sigma_S$ [N]	${}^{(2)}\sigma_S$ [N]	${}^{(1)}r^k$	${}^{(2)}r^k$
7.4	$\rho_S(x) = 0.6160e^{-0.006516x} + 0.3840e^{-0.000212x}$	0.1596	0.1260	0.7220	0.9895
10	$\rho_S(x) = 0.5160e^{-0.011137x} + 0.4840e^{-0.000401x}$	0.1810	0.1753	0.5730	0.9801
12.5	$\rho_S(x) = 0.6140e^{-0.016794x} + 0.3860e^{-0.000225x}$	0.2568	0.2036	0.4318	0.9888
16.5	$\rho_S(x) = 0.6363e^{-0.004231x} + 0.3637e^{-0.000285x}$	0.3674	0.2778	0.8093	0.9859
20	$\rho_S(x) = 0.5394e^{-0.010841x} + 0.4606e^{-0.000580x}$	0.3387	0.3130	0.5816	0.9714

Combed New Yarns (Twist Multiplier – 56 $\text{tex}^{2/3}\text{cm}^{-1}$)

$\overline{T}$ [tex]	Autocorrelation Functions $\rho_S(x) = ae^{-bx_{[\text{mm}]}} + (1-a)e^{-cx_{[\text{mm}]}}$	${}^{(1)}\sigma_S$ [N]	${}^{(2)}\sigma_S$ [N]	${}^{(1)}r^k$	${}^{(2)}r^k$
7.4	$\rho_S(x) = 0.5907e^{-0.024258x} + 0.4093e^{-0.000345x}$	0.2207	0.1837	0.2973	0.9829
10	$\rho_S(x) = 0.7584e^{-0.015810x} + 0.2416e^{-0.000361x}$	0.2317	0.1308	0.4536	0.9821
12.5	$\rho_S(x) = 0.6774e^{-0.016998x} + 0.3226e^{-0.000730x}$	0.2728	0.1883	0.4275	0.9642
16.5	$\rho_S(x) = 0.6038e^{-0.020251x} + 0.3962e^{-0.000418x}$	0.2773	0.2246	0.3633	0.9793
20	$\rho_S(x) = 0.5178e^{-0.010553x} + 0.4822e^{-0.000085x}$	0.3629	0.3502	0.5900	0.9957

Combed New Yarns (Twist Multiplier – 81 $\text{tex}^{2/3}\text{cm}^{-1}$)

$\overline{T}$ [tex]	Autocorrelation Functions $\rho_S(x) = ae^{-bx_{[\text{mm}]}} + (1-a)e^{-cx_{[\text{mm}]}}$	${}^{(1)}\sigma_S$ [N]	${}^{(2)}\sigma_S$ [N]	${}^{(1)}r^k$	${}^{(2)}r^k$
7.4	$\rho_S(x) = 0.8529e^{-0.234263x} + 0.1471e^{-0.000853x}$	0.2269	0.0942	8×10^{-6}	0.9957
10	$\rho_S(x) = 0.7925e^{-0.224813x} + 0.2075e^{-0.002326x}$	0.3031	0.1551	1×10^{-5}	0.8902
12.5	$\rho_S(x) = 0.5802e^{-0.227500x} + 0.4198e^{-0.000092x}$	0.4051	0.3446	1×10^{-5}	0.9954
16.5	$\rho_S(x) = 0.7134e^{-0.230513x} + 0.2866e^{-0.000614x}$	0.4102	0.2600	1×10^{-5}	0.9698
20	$\rho_S(x) = 0.6574e^{-0.021927x} + 0.3426e^{-0.000003x}$	0.5012	0.3619	0.3341	0.9998

Table 5.2 reveals the existence of strength correlation among the neighboring sections along a yarn. In other words, the strengths of neighboring short sections in a yarn are dependent. This contradicts Peirce's assumption of strength independency (1926). It is also noticeable that the degree of strength autocorrelation is different in different yarns. Moreover, this correlation can be satisfactorily characterized by a summation of two exponential functions, where each function possesses very different nature than the other. It issues that two highly different and mutually independent phenomena are acting together on the yarn so as to impart variability to yarn strength. (Here we remark that, hypothetically, if the strengths of successive sections of equal length along a yarn are the same, then the strength autocorrelation function takes the form: $\rho_S(x)=1$, where $x \geq 0$; on the other hand, if those strengths are so variable that no correlation exists among them, then the strength autocorrelation function is represented by the following two expressions: $\rho_S(x)=1$, where $x=0$ and $\rho_S(x)=0$, where $x>0$.) Needless to say, to know those phenomena, it is necessary to understand the physical bases of the individual SEMG-stochastic processes. Attempts made in this research work to understand them will be discussed shortly. But, prior to that, let us know a little more about the nature of those processes.

Table 5.2 highlights a little about the characters of those two processes. In general, independent to yarn count and yarn manufacturing technology, the process indicated by the steeper fall-off component is more dominant than the process characterized by the gradual fall-off component (Please look at the values of the coefficients a and $1-a$.) In addition, our observations do not figure out any characteristic relation between these coefficients and yarn manufacturing technology. Interestingly, the standard deviations $\left({}^{(1)}\sigma_S \text{ and } {}^{(2)}\sigma_S\right)$ of both of those processes are generally increasing when yarn becomes coarser. The autocorrelation coefficient ${}^{(2)}r^k$ of the process corresponding to the gradual fall-off component is significantly higher than that ${}^{(2)}r^k$ of the other process. It is remarkable to observe the "decaying speed" of the quick-fall-off component in case of the highly twisted new yarns (twist multiplier – 81 tex$^{2/3}$cm^{-1}); however, the reason behind it is yet to be known.

5.3.2 Periodicity in Strength Autocorrelation

Sometimes yarn strength autocorrelation may reveal periodicity. In that case, the double exponential function of the form $\rho_S(x) = ae^{-bx} + (1-a)e^{-cx}$ is not sufficient to characterize the strength autocorrelation. (The meaning of a, b, c is already stated in Table 5.2.) It is then more logical to fit the autocorrelation coefficients with a summation of three functions of the form $\rho_S(x) = ae^{-bx} + ce^{-dx} + (1-a-c)\cos(fx)$, where a, c are the coefficients of the individual exponential functions, b, d are the exponents of the individual exponential functions, $(1-a-c)$ is the amplitude of the harmonic function, and f is the frequency of the harmonic function. The harmonic function characterizes the periodicity in the strength data. This periodicity may arise due to some local periodic disturbances at the different stages of the yarn manufacturing process. The value of the amplitude of the harmonic function tells the degree of these disturbances.

To study these disturbances was, however, beyond the scope of this research work; hence, the harmonic function was not deeply analyzed in this work. We treated the harmonic function in the following manners depending on the situations.

Case 1: When we found very low value of the amplitude regardless of its sign (positive or negative), then we simply ignored the summation of three functions and considered the double exponential function as a representative of the strength autocorrelation for further study. Except one, all the yarns studied in this research work followed this case.

Case 2: When we found higher value of the amplitude having positive sign, we accounted that value and distributed it between the two coefficients of the double exponential function, as shown below

$$\rho_S(x) = ae^{-bx} + ce^{-dx} + (1-a-c)\cos(fx) \rightarrow \rho_S(x) = \frac{a}{(a+c)}e^{-bx} + \frac{c}{(a+c)}e^{-dx}. \quad (5.8)$$

This situation was faced with 16.5 tex combed ring yarn. The strength autocorrelation function of this yarn was initially estimated as follows

$$\rho_S(x) = 0.9081e^{-0.00254213x} + 0.0919e^{0.00030441x}, \quad (5.9)$$

where x is expressed in mm. This function together with the individual components and the actual autocorrelation coefficients is shown in Figure 5.6a. Clearly, it had one exponentially increasing component that was very illogical. Similar result was

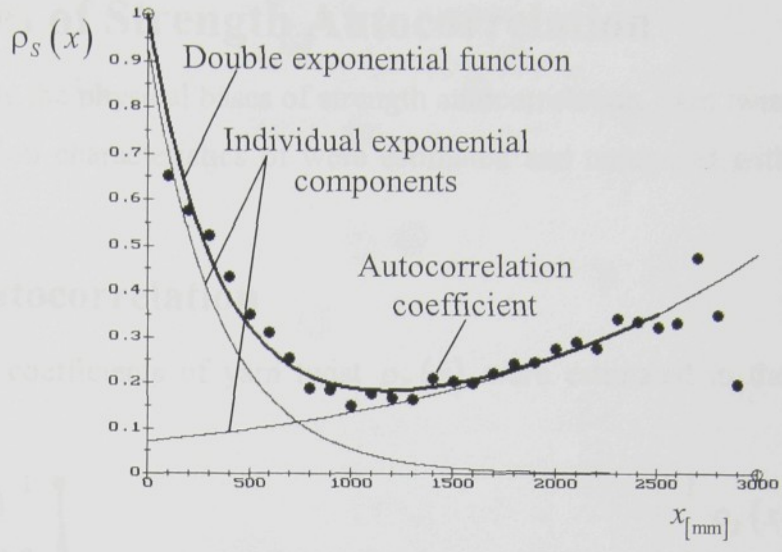

Figure 5.6a

obtained with another trial (a set of 900 measurements) with this yarn. It was then understood that the strength autocorrelation of this yarn had a harmonic component with a high value of the amplitude with positive sign, as shown below

$$\rho_S(x) = 0.5455e^{-0.006968x} + 0.3445e^{-0.000212x} + 0.1100\cos(0.002650x), \tag{5.10}$$

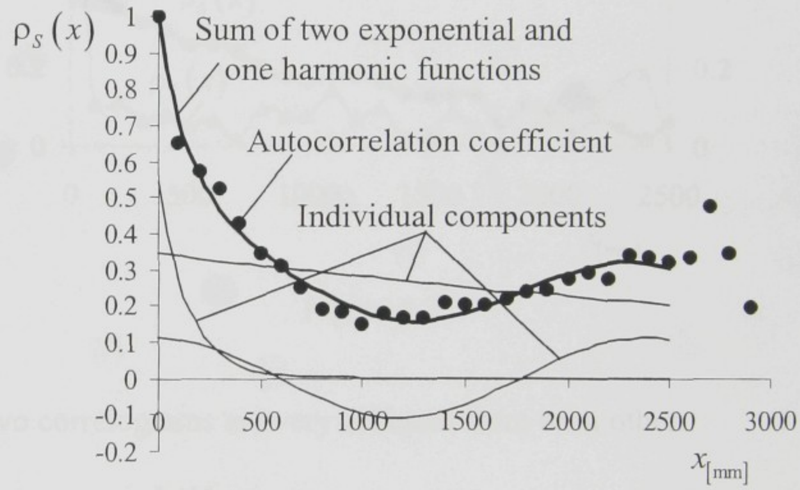

Figure 5.6b

where x is expressed in mm. This function together with the individual components and the actual autocorrelation coefficients is shown in Figure 5.6b. The above function was then recalculated according to Equation (5.8) and as a result, the following function was obtained

$$\rho_S(x) = 0.6129e^{-0.006968x} + 0.3871e^{-0.000212x}, \tag{5.11}$$

here x is expressed in mm. This function was finally considered as the strength autocorrelation function of this yarn and was used for further study.

Case 3: If we were found higher value of the amplitude having negative sign, it would have been necessary to modify the theory. But, no single yarn in this study followed this case.

5.4 Physical Bases of Strength Autocorrelation

In order to investigate the physical bases of strength autocorrelation, yarn twist and yarn mass autocorrelation characteristics of were estimated and compared with those of yarn strength.

5.4.1 Yarn Twist Autocorrelation

The autocorrelation coefficients of yarn twist $\rho_Z(x)$ were estimated in the same manner as the autocorrelation coefficients of yarn strength $\rho_S(x)$ were calculated. The twist correlogram and the strength correlogram of 35.5 tex carded rotor yarn are shown together in Figure 5.7. Clearly, these two correlograms are very different from each other.

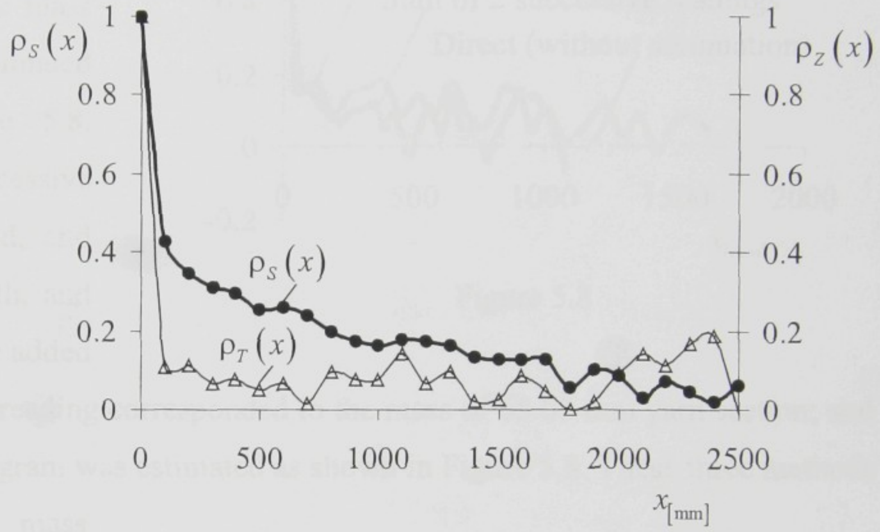

Figure 5.7

5.4.2 Yarn Mass Autocorrelation

Yarn mass autocorrelation was estimated from the data obtained from the capacitive measurements (Uster Tester 4) as well as gravimetric measurements.

5.4.2.1 Capacitive

The primary data file collected from the hard disk of the Uster Tester 4 instrument was used for estimating yarn mass correlograms. It was always observed that the data file contained 18458 readings against the testing of 400 m length of yarn. Assuming no yarn was wasted in-between two successive measurements, it was considered that each reading, as appeared in the primary data file, corresponded to the mass of about 21.67 mm $(400\,\text{m} \div 18458 \approx 0.02167\,\text{m})$ yarn section. Based on this consideration, the mass autocorrelation coefficients $\rho_M(x)$ were estimated directly from those readings. The resulting mass correlogram of 7.4 tex combed ring yarn is presented in Figure 5.8. In addition, the same primary data file was also used in different ways to estimate the mass correlograms. We added every two successive readings (first and second, then third and fourth, and so on) so that each resulting reading corresponded to the mass of 43.34 mm yarn section; and then; the mass correlogram was estimated as shown in Figure 5.8. Also, three successive readings (first, second, and third, then fourth, fifth, and sixth, and so on) were added so that each resulting reading corresponded to the mass of 65.01 mm yarn section; and then, the mass correlogram was estimated as shown in Figure 5.8. These three methods of estimation of mass correlograms were also followed on other yarns. Figure 5.9 shows these mass correlograms in case of 20 tex carded compact yarn.

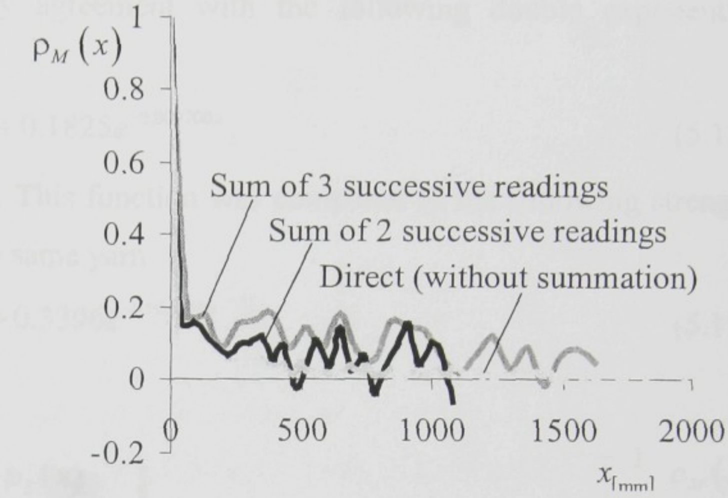

Figure 5.8

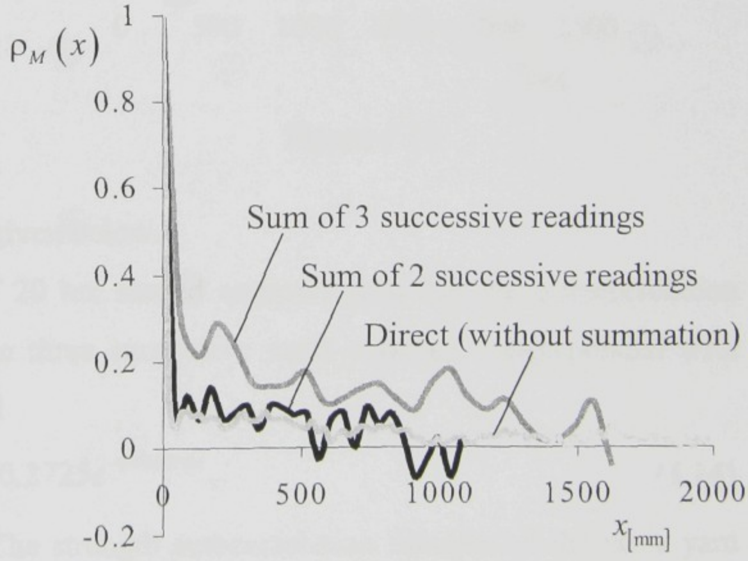

Figure 5.9

In general, it was observed that the mass correlogram based on the summation of three successive readings showed significantly higher correlation than that estimated directly from the primary data file. The reason for this difference is not yet precisely known. At this moment, this difference can be very roughly imagined as a natural consequence of fiber distribution along a yarn caused by the drafting operations at different stages of yarn manufacturing process. This "working" hypothesis needs to be verified in future.

The autocorrelation coefficients, estimated from the mass data corresponding to the summation of three successive readings in case of 7.4 tex combed ring yarn, were found in a satisfactory agreement with the following double exponential function

$$\rho_M(x) = 0.8175e^{-0.091440x} + 0.1825e^{-0.000700x}, \tag{5.12}$$

where x is expressed in mm. This function was compared to the following strength autocorrelation function of the same yarn

$$\rho_S(x) = 0.6604e^{-0.014049x} + 0.3396e^{-0.000376x}, \tag{5.13}$$

where x is expressed in mm. (This strength autocorrelation function is already mentioned in Equation 5.1.) The comparison is shown in Figure 5.10. Clearly, in this yarn, the strength correlation was higher than the mass correlation. However, this was not true with all yarns. One example is given below.

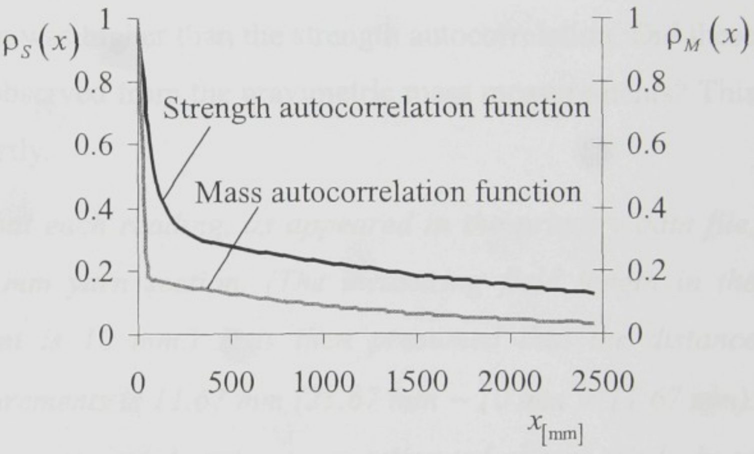

Figure 5.10

It was found in case of 20 tex carded compact yarn that the autocorrelation coefficients, estimated from the three successive mass readings, corresponded with the following function very well

$$\rho_M(x) = 0.7275e^{-0.046590x} + 0.2725e^{-0.001036x}, \tag{5.14}$$

where x is expressed in mm. The strength autocorrelation function of the same yarn was found earlier (Table 5.2) as follows

$$\rho_S(x) = 0.7162e^{-0.024023x} + 0.2838e^{-0.000706x}, \tag{5.15}$$

where x is expressed in mm. Looking at the coefficients and exponents of these two functions, it can be said that the strength autocorrelation in this yarn was highly comparable with the mass autocorrelation. The closeness of these two functions can be visualized from Figure 5.11.

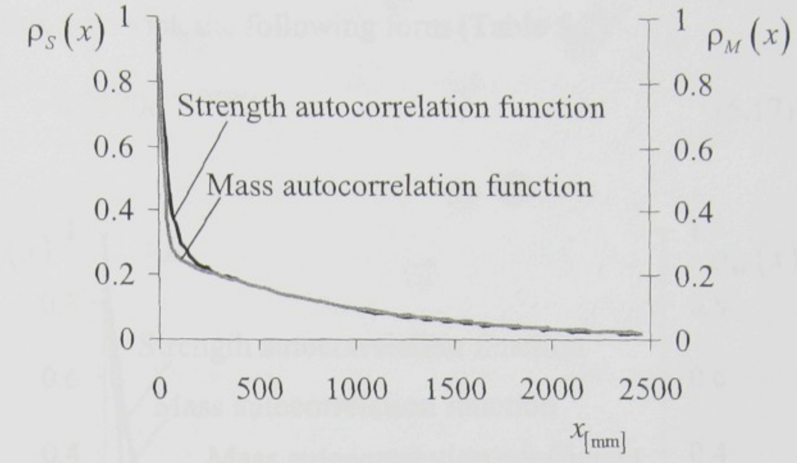

Figure 5.11

In this research work, yarn strength autocorrelation was found sometimes higher than yarn mass autocorrelation and sometimes equal to yarn mass autocorrelation. No yarn was found where the mass autocorrelation was higher than the strength autocorrelation. Did these findings correspond to those observed from the gravimetric mass measurements? This question will be answered shortly.

Note: Sometimes it is said that each reading, as appeared in the primary data file, indicates to the mass of 10 mm yarn section. (The measuring field length in the USTER TESTER 4 instrument is 10 mm.) It is then presumed that the distance between two successive measurements is 11.67 mm (21.67 mm – 10 mm = 11.67 mm). Under this consideration, yarn mass correlograms were estimated almost similarly as described above, and similar results were observed.

5.4.2.2 Gravimetric

Here each mass value corresponds to 50 mm yarn specimen and no yarn was wasted in-between two successive measurements. Keeping this in mind, the mass autocorrelation coefficients $\rho_M(x)$ were estimated almost in the same manner as those $\rho_S(x)$ of the yarn strength.

The estimated mass autocorrelation coefficients in case of 20 tex carded rotor yarn are plotted in Figure 5.12. Using the standard regression technique, it was observed that the following double exponential function satisfactorily represented the mass autocorrelation of this particular yarn

$$\rho_M(x) = 0.7641e^{-0.049940x} + 0.2359e^{-0.000402x}, \tag{5.16}$$

where x is expressed in mm. This function is also shown in Figure 5.12. The strength autocorrelation function of this yarn took the following form (Table 5.2)

$$\rho_S(x) = 0.7830e^{-0.020114x} + 0.2170e^{-0.000069x}, \tag{5.17}$$

where x is expressed in mm. This is also presented in Figure 5.12. The closeness between the strength and mass autocorrelations is very remarkable in this yarn. However, as before, this was not always true.

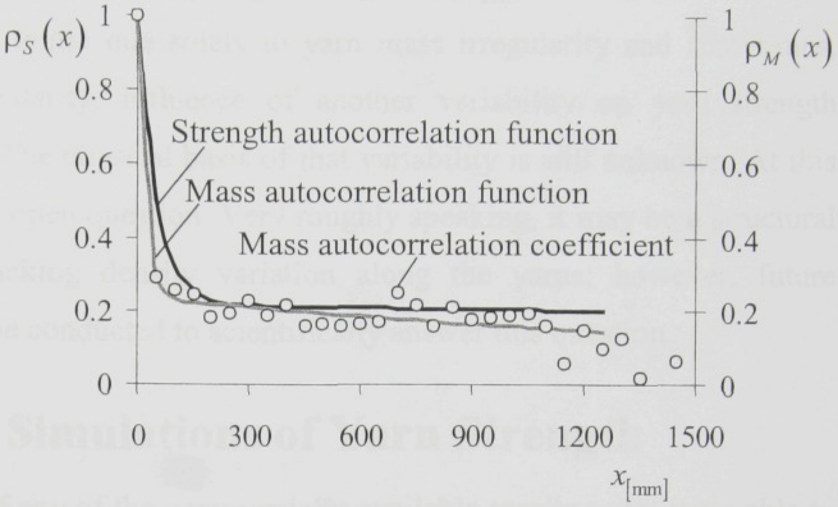

Figure 5.12

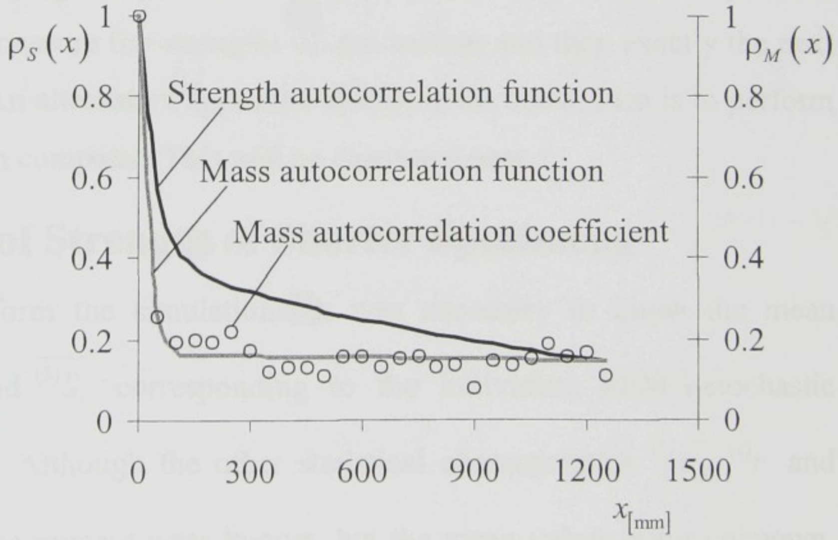

Figure 5.13

Figure 5.13 shows the estimated mass autocorrelation coefficients in case of 35.5 tex carded rotor yarn. Using the standard statistical regression technique, it was observed that those mass autocorrelation coefficients were in a satisfactory agreement with the following double exponential function

$$\rho_M(x) = 0.8360e^{-0.042540x} + 0.1640e^{-0.000099x}, \tag{5.18}$$

where x is expressed in mm. This function is plotted in Figure 5.13. The strength autocorrelation function of the same yarn is already expressed (Table 5.2) as follows

$$\rho_S(x) = 0.5968e^{-0.024082x} + 0.4032e^{-0.000818x}, \tag{5.19}$$

where x is expressed in mm. This is also plotted in Figure 5.13. Evidently, in this yarn, the strength autocorrelation was higher than the mass autocorrelation.

Thus the results obtained from the gravimetric measurements are similar to those found from the capacitive measurements. The influence of yarn mass irregularity on yarn strength variability is generally very significant. Sometimes yarn strength variability was found due solely to yarn mass irregularity and sometimes, besides the mass irregularity, influence of another variability on yarn strength variability was noticed. The physical basis of that variability is still unknown. At this present moment, it is an open question. Very roughly speaking, it may be a structural irregularity, say the packing density variation along the yarns; however, future research works need to be conducted to scientifically answer this question.

5.5 Computer Simulations of Yarn Strength

Hypothetically, if any of the commercially available tensile tester were able to measure the strength of a huge number of successive short sections (50 mm length) along a yarn one after another within a reasonable time; then by applying the weakest link principle on the dataset, we would have calculated the strength values corresponding to higher gauge lengths. But, due to technical reason, it is not possible by any tensile tester to measure the strengths of one section and then exactly the next section along the yarn. An alternative approach to realize the above idea is to perform numerical simulations on computer. This will be discussed now.

5.5.1 Generation of Strength of Shorter Specimens

In order to perform the simulations, it was necessary to know the mean strength values $\overline{{}^{(1)}S_i}$ and $\overline{{}^{(2)}S_i}$ corresponding to the individual SEMG-stochastic processes ${}^{(1)}S_i$ and ${}^{(2)}S_i$. Although the other statistical characteristics ${}^{(1)}\sigma_S, {}^{(1)}r$ and ${}^{(2)}\sigma_S, {}^{(2)}r$ related to those process were known, but the mean values were unknown. Therefore, we generated the centred values ${}^{(1)}S_i^0$ and ${}^{(2)}S_i^0$. These are defined below

$${}^{(1)}S_i^0 = {}^{(1)}S_i - \overline{{}^{(1)}S}, \tag{5.20}$$

$${}^{(2)}S_i^0 = {}^{(2)}S_i - \overline{{}^{(2)}S}. \tag{5.21}$$

Evidently, the mean of the centred quantities is zero $\left(\overline{{}^{(1)}S^0} = \overline{{}^{(2)}S^0} = 0\right)$. The process of generating the centred values ${}^{(1)}S_i^0$ and ${}^{(2)}S_i^0$ is theoretically explained in Equations (3.52) to (3.55). One practical example is given below.

Let us again consider 7.4 tex cotton combed ring yarn. Using the estimated values, mentioned in Equations (5.4) to (5.7), into Equations (3.52) to (3.55), the centred values for the individual processes were generated as follows

$$\left.\begin{array}{l|l}
{}^{(1)}S_1^0 = {}^{(1)}\sigma_S U & {}^{(2)}S_1^0 = {}^{(2)}\sigma_S U \\
{}^{(1)}S_2^0 = {}^{(1)}\sigma_S \sqrt{1-{}^{(1)}r^2}\,U + {}^{(1)}r\,{}^{(1)}S_1^0 = & {}^{(2)}S_2^0 = {}^{(2)}\sigma_S \sqrt{1-{}^{(2)}r^2}\,U + {}^{(2)}r\,{}^{(2)}S_1^0 = \\
\quad = 0.1607\sqrt{1-0.4954^2}\,U + & \quad = 0.1153\sqrt{1-0.9814^2}\,U + \\
\qquad + 0.4954\,{}^{(1)}S_1^0 = & \qquad + 0.9814\,{}^{(2)}S_1^0 = \\
\quad = 0.1396U + 0.4954\,{}^{(1)}S_1^0 & \quad = 0.0221U + 0.9814\,{}^{(2)}S_1^0 \\
\vdots & \vdots \\
{}^{(1)}S_j^0 = 0.1396U + 0.4954\,{}^{(1)}S_{j-1}^0 & {}^{(2)}S_j^0 = 0.0221U + 0.9814\,{}^{(2)}S_{j-1}^0 \\
\vdots & \vdots
\end{array}\right\}, \quad (5.22)$$

where U are the independently generated values for the standardized Gaussian distribution. The generated centred values were then used to calculate the strength values of the whole stochastic process S_i as follows

$$\begin{aligned} S_i &= {}^{(1)}S_i + {}^{(2)}S_i = \left[{}^{(1)}S_i^0 + \overline{{}^{(1)}S}\right] + \left[{}^{(2)}S_i^0 + \overline{{}^{(2)}S}\right] = {}^{(1)}S_i^0 + {}^{(2)}S_i^0 + \overline{S} = \\ &= {}^{(1)}S_i^0 + {}^{(2)}S_i^0 + 1.6142\ \text{N}. \end{aligned} \quad (5.23)$$

In this way, the strengths of a huge number of successive short specimens (each of 50 mm length) were generated on computer within a very short time.

5.5.2 Functionality of Simulation Software

The simulations of strengths were performed arbitrarily with 30000 yarn sections, each of 5000 mm length; hence, $30000 \cdot 100 = 3 \times 10^6$ strength values, each corresponding to 50 mm length, were generated. The autocorrelation function estimated from those simulated strength values is shown in Figure 5.14. The desired autocorrelation function, expressed by Equation (5.1), is also plotted in Figure 5.14. It was remarkable to see the extent to which the simulated autocorrelation function corresponded with the desired autocorrelation function. Similar result was observed with all yarns used in this research work. It therefore means that our original simulation software was right as far as its functionality was concerned

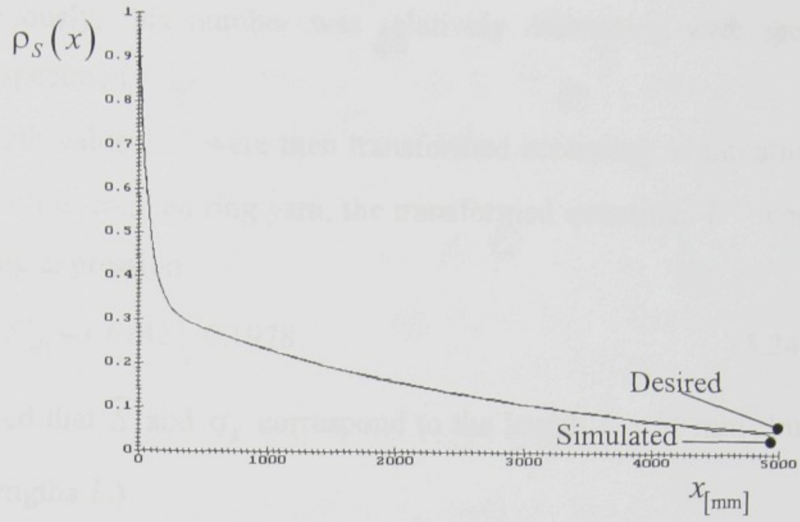

Figure 5.14

Note: In this research work, 3×10^6 *strength values each corresponding to 50 mm length were generated on computer on each yarn. Generation of* 3×10^6 *strength values should be considered as an example only, one can generate more and/or less than this number of strength values.*

5.5.3 Generation of Strength of Longer Specimens

The simulation software also calculated the strength S^* of longer specimens, whose length was a multiple of 50 mm. In this example, this length varied from 50 mm to 5000 mm. Prior to the calculation of strength of longer specimens, different values were given to the parameter k for different lengths in accordance with Equation (3.63). These values are shown in Table 5.3.

Table 5.3

Specimen Length $l_{[\mathrm{mm}]}$	$50\ (l_0)$	100	150	…	5000
Parameter $k=(l/l_0)=\left(l_{[\mathrm{mm}]}/50\right)-1$	0	1	2	…	99

Depending on the value of the parameter k, the strengths S_i^* of yarn specimens of different lengths l were generated according to Equation (3.72). For example, the strength of 150 mm length of yarn specimen was calculated from the expression: $S_i^*=\min\left\{S_{i+j}\right\}_{j=0}^{j=2}=\min\left\{S_i,S_{i+1},S_{i+2}\right\}$, that is, the minimum among the strength of three successive yarn specimens, each of 50 mm length, is the strength of yarn specimen of 150 mm length. To each length, fairly a large number of strength values were generated; and obviously, this number was relatively decreasing with the increase in length of yarn specimen.

The generated strength values S^* were then transformed according to Equation (3.70). In case of 7.4 tex cotton combed ring yarn, the transformed quantities U^* were obtained from the following expression

$$U^* = \left(S^* - \overline{S}\right)/\sigma_S = \left(S^*_{[N]} - 1.6142\right)/0.1978. \tag{5.24}$$

(It should be carefully noted that $\overline{S}$ and σ_S correspond to the length $l_0 = 50\text{ mm}$, but S^* corresponds to other lengths l.)

5.5.4 Frequency Distributions of Simulated Strength

The histograms of the probability density function $g\left(U^*, k\right)$, for different values of k, were estimated by the simulation software. Those corresponding to 7.4 tex combed ring yarn for three values of k are presented here. Figure 5.15a shows the probability density function of the standardized strength quantities corresponding to 50 mm specimen length $(k = 0)$. This accords to the standardized Gaussian distribution. Figure 5.15b and Figure 5.15c illustrate the distribution of the transformed strength quantities related to 500 mm specimen length $(k = 9)$ and 5000 mm specimen length $(k = 99)$, respectively. It can be observed that as the specimen length is

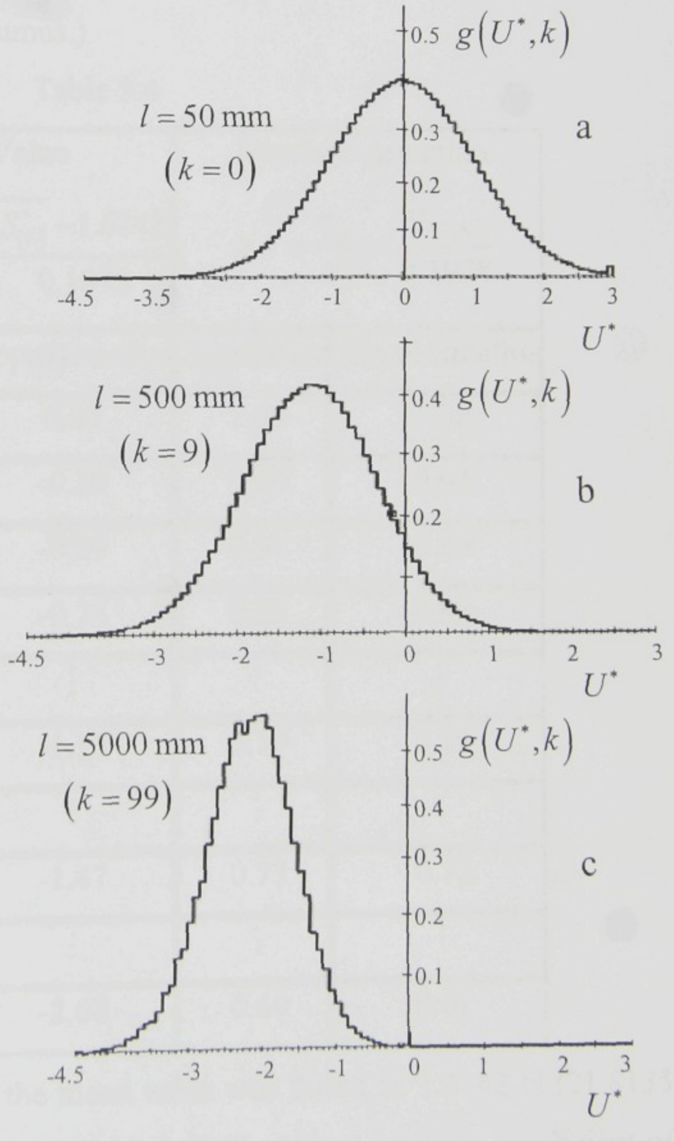

Figure 5.15

increasing, the shape of the histogram is changing: it becomes higher and narrower. This is because of decrease in strength variability with the increase of specimen length. The relative shifting of the histogram to the left-hand side direction with the increase in specimen length is ascribed due to the decrease in mean strength value with the increase in specimen length. A similar trend was found with actual strength data too (Figure 5.3). It is interesting to notice that the smoothness of the histogram reduces with the increase in specimen length. This is because of the relative reduction in the number of simulated strength values available for longer specimens.

5.5.5 Basic Statistical Parameters of Simulated Strength

The mean value and the standard deviation of the simulated strength values were calculated from the generated distributions for different lengths of yarn specimens. These, in case of 7.4 tex cotton combed ring yarn, are presented in Table 5.4. (Please see the “simulation” columns.)

Table 5.4

Specimen Length $l_{[\mathrm{mm}]}$	Mean Value $\overline{U^*} = \dfrac{\overline{S^*} - \overline{S}}{\sigma_S} = \dfrac{\overline{S^*_{[\mathrm{N}]}} - 1.6142}{0.1978}$		Standard deviation $\sigma_{U^*} = \dfrac{\sigma_{S^*}}{\sigma_S} = \dfrac{\sigma_{S^*[\mathrm{N}]}}{0.1978}$	
	Simulation	Approximation	Simulation	Approximation
50	0.00	0.00	1.00	1.00
100	-0.33	-0.38	0.94	0.93
150	-0.53	-0.59	0.91	0.89
200	-0.68	-0.74	0.88	0.86
⋮	⋮	⋮	⋮	⋮
500	-1.13	-1.17	0.79	0.78
⋮	⋮	⋮	⋮	⋮
1000	-1.45	-1.47	0.73	0.72
⋮	⋮	⋮	⋮	⋮
5000	-2.15	-2.08	0.60	0.61

For 50 mm yarn specimens, the mean value was found as 1.6142 N (21.8135 cN/tex), the standard deviation was 0.1978 N (2.6730 cN/tex), and the coefficient of variation was 12.2537 %. In accordance with Equation (5.22), the strength parameters corresponding to 500 mm specimen length were calculated as follows:– mean value: $\overline{S^*} = 0.1978 \cdot (-1.13) + 1.6142\,\mathrm{N} = 1.3907\,\mathrm{N}\,(18.7932\,\mathrm{cN/tex})$, standard deviation: $\sigma_{S^*} = 0.79 \cdot 0.1978\,\mathrm{N} = 0.1563\,\mathrm{N}, (2.1122\,\mathrm{cN/tex})$, and coefficient of variation: 11.2389 %. Analogically, the statistical parameters of strength related to 5000 mm specimen length were determined as follows:– mean value: $\overline{S^*}$ =1.1884 N (16.0595 cN/tex), standard deviation: σ_{S^*} =0.1186 N (1.6027 cN/tex), and coefficient of variation: 9.9798 %. In this way, the statistical parameters for the other lengths were calculated.

The behaviors of the transformed strength quantities with the increase in specimen length are shown in Figure 5.16. The change in $\left(\overline{S^*} - \overline{S}\right)/\sigma_S$ with the increase in length l is evident from Figure 5.16a. The nature of drop in $\left(\sigma_{S^*}/\sigma_S\right)$ with the increase in length l is shown in Figure 5.16b.

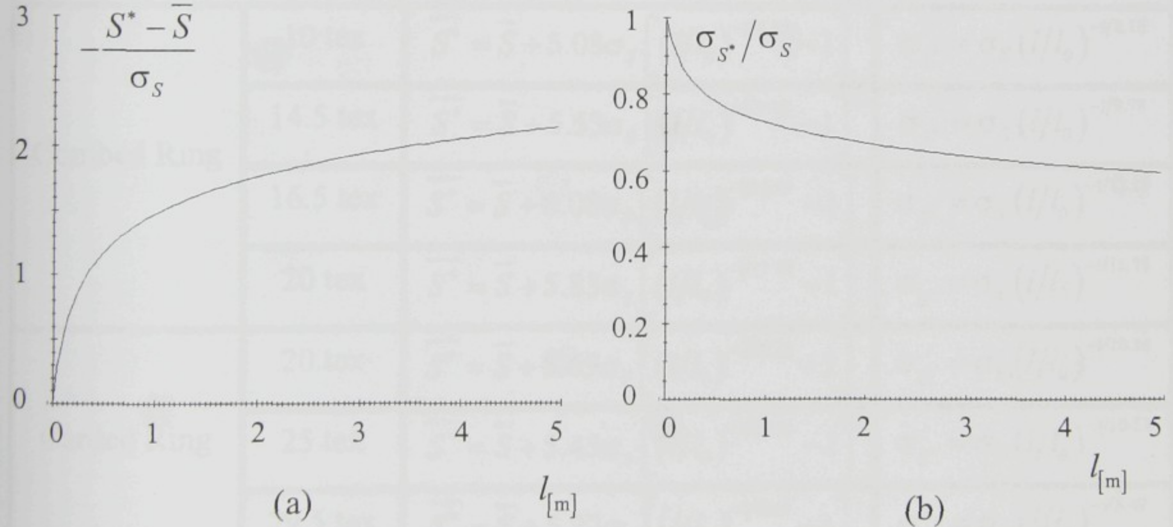

(a) (b)

Figure 5.16

5.5.6 Empirical Relations Between Simulated Strength and Specimen Length

Using the standard statistical regression technique, the simulation results were approximated by suitable empirical relations between yarn strength and specimen length. These relations in case of 7.4 tex cotton combed ring yarn are shown below

$$\sigma_{S^*} = \sigma_S \left(\frac{l}{l_0}\right)^{-\frac{1}{9.3}} \qquad \left(\sigma_{U^*} = \frac{\sigma_{S^*}}{\sigma_S} = \left(\frac{l}{l_0}\right)^{-\frac{1}{9.3}}\right), \tag{5.25}$$

$$\overline{S^*} = \overline{S} + 5.33\sigma_S \left[\left(\frac{l}{l_0}\right)^{-\frac{1}{9.3}} - 1\right] \qquad \left(\overline{U^*} = \frac{\overline{S^*} - \overline{S}}{\sigma_S} = 5.33\left[\left(\frac{l}{l_0}\right)^{-\frac{1}{9.3}} - 1\right]\right). \tag{5.26}$$

The values of the transformed strength quantities $\left(\sigma_{U^*} \text{ and } \overline{U^*}\right)$, obtained from Equations (5.25) and (5.26), are presented in Table 5.4. (Please see the "approximation" columns.) It is evident from the table that those approximated relations characterized the simulation results satisfactorily. The empirical relations between strength and length for the other yarns are presented in Table 5.5.

Table 5.5

Yarns (Technology and Count)		Empirical Relations Between Strength and Length	
Combed Ring	10 tex	$\overline{S^*} = \overline{S} + 5.08\sigma_S\left[(l/l_0)^{-1/8.16} - 1\right]$	$\sigma_{S^*} = \sigma_S (l/l_0)^{-1/8.16}$
	14.5 tex	$\overline{S^*} = \overline{S} + 5.53\sigma_S\left[(l/l_0)^{-1/9.78} - 1\right]$	$\sigma_{S^*} = \sigma_S (l/l_0)^{-1/9.78}$
	16.5 tex	$\overline{S^*} = \overline{S} + 6.08\sigma_S\left[(l/l_0)^{-1/12.19} - 1\right]$	$\sigma_{S^*} = \sigma_S (l/l_0)^{-1/12.19}$
	20 tex	$\overline{S^*} = \overline{S} + 5.83\sigma_S\left[(l/l_0)^{-1/11.75} - 1\right]$	$\sigma_{S^*} = \sigma_S (l/l_0)^{-1/11.75}$
Carded Ring	20 tex	$\overline{S^*} = \overline{S} + 5.69\sigma_S\left[(l/l_0)^{-1/10.38} - 1\right]$	$\sigma_{S^*} = \sigma_S (l/l_0)^{-1/10.38}$
	25 tex	$\overline{S^*} = \overline{S} + 5.45\sigma_S\left[(l/l_0)^{-1/10.55} - 1\right]$	$\sigma_{S^*} = \sigma_S (l/l_0)^{-1/10.55}$
	29.5 tex	$\overline{S^*} = \overline{S} + 5.22\sigma_S\left[(l/l_0)^{-1/8.49} - 1\right]$	$\sigma_{S^*} = \sigma_S (l/l_0)^{-1/8.49}$
Carded Rotor	20 tex	$\overline{S^*} = \overline{S} + 4.69\sigma_S\left[(l/l_0)^{-1/7.29} - 1\right]$	$\sigma_{S^*} = \sigma_S (l/l_0)^{-1/7.29}$
	35.5 tex	$\overline{S^*} = \overline{S} + 5.28\sigma_S\left[(l/l_0)^{-1/8.66} - 1\right]$	$\sigma_{S^*} = \sigma_S (l/l_0)^{-1/8.66}$
	42 tex	$\overline{S^*} = \overline{S} + 6.17\sigma_S\left[(l/l_0)^{-1/12.97} - 1\right]$	$\sigma_{S^*} = \sigma_S (l/l_0)^{-1/12.97}$
Combed Compact	7.4 tex	$\overline{S^*} = \overline{S} + 4.80\sigma_S\left[(l/l_0)^{-1/7.44} - 1\right]$	$\sigma_{S^*} = \sigma_S (l/l_0)^{-1/7.44}$
	10 tex	$\overline{S^*} = \overline{S} + 7.60\sigma_S\left[(l/l_0)^{-1/19.19} - 1\right]$	$\sigma_{S^*} = \sigma_S (l/l_0)^{-1/19.19}$
	11.8 tex	$\overline{S^*} = \overline{S} + 5.29\sigma_S\left[(l/l_0)^{-1/8.89} - 1\right]$	$\sigma_{S^*} = \sigma_S (l/l_0)^{-1/8.89}$

Yarns (Technology and Count)		Empirical Relations Between Strength and Length	
Carded Compact	20 tex	$\overline{S^*} = \overline{S} + 4.87\sigma_S\left[(l/l_0)^{-1/7.40} - 1\right]$	$\sigma_{S^*} = \sigma_S\left(l/l_0\right)^{-1/7.40}$
	29.5 tex	$\overline{S^*} = \overline{S} + 7.69\sigma_S\left[(l/l_0)^{-1/23.92} - 1\right]$	$\sigma_{S^*} = \sigma_S\left(l/l_0\right)^{-1/23.92}$
Combed New (Twist Multiplier: 38 tex$^{2/3}$ cm^{-1})	7.4 tex	$\overline{S^*} = \overline{S} + 5.94\sigma_S\left[(l/l_0)^{-1/12.21} - 1\right]$	$\sigma_{S^*} = \sigma_S\left(l/l_0\right)^{-1/12.21}$
	10 tex	$\overline{S^*} = \overline{S} + 6.04\sigma_S\left[(l/l_0)^{-1/11.91} - 1\right]$	$\sigma_{S^*} = \sigma_S\left(l/l_0\right)^{-1/11.91}$
	12.5 tex	$\overline{S^*} = \overline{S} + 5.72\sigma_S\left[(l/l_0)^{-1/10.46} - 1\right]$	$\sigma_{S^*} = \sigma_S\left(l/l_0\right)^{-1/10.46}$
	16.5 tex	$\overline{S^*} = \overline{S} + 6.06\sigma_S\left[(l/l_0)^{-1/12.77} - 1\right]$	$\sigma_{S^*} = \sigma_S\left(l/l_0\right)^{-1/12.77}$
	20 tex	$\overline{S^*} = \overline{S} + 5.77\sigma_S\left[(l/l_0)^{-1/10.82} - 1\right]$	$\sigma_{S^*} = \sigma_S\left(l/l_0\right)^{-1/10.82}$
Combed New (Twist Multiplier: 56 tex$^{2/3}$ cm^{-1})	7.4 tex	$\overline{S^*} = \overline{S} + 5.60\sigma_S\left[(l/l_0)^{-1/9.89} - 1\right]$	$\sigma_{S^*} = \sigma_S\left(l/l_0\right)^{-1/9.89}$
	10 tex	$\overline{S^*} = \overline{S} + 5.01\sigma_S\left[(l/l_0)^{-1/7.91} - 1\right]$	$\sigma_{S^*} = \sigma_S\left(l/l_0\right)^{-1/7.91}$
	12.5 tex	$\overline{S^*} = \overline{S} + 5.12\sigma_S\left[(l/l_0)^{-1/8.19} - 1\right]$	$\sigma_{S^*} = \sigma_S\left(l/l_0\right)^{-1/8.19}$
	16.5 tex	$\overline{S^*} = \overline{S} + 5.49\sigma_S\left[(l/l_0)^{-1/9.67} - 1\right]$	$\sigma_{S^*} = \sigma_S\left(l/l_0\right)^{-1/9.67}$
	20 tex	$\overline{S^*} = \overline{S} + 6.86\sigma_S\left[(l/l_0)^{-1/15.08} - 1\right]$	$\sigma_{S^*} = \sigma_S\left(l/l_0\right)^{-1/15.08}$
Combed New (Twist Multiplier: 81 tex$^{2/3}$ cm^{-1})	7.4 tex	$\overline{S^*} = \overline{S} + 3.74\sigma_S\left[(l/l_0)^{-1/4.85} - 1\right]$	$\sigma_{S^*} = \sigma_S\left(l/l_0\right)^{-1/4.85}$
	10 tex	$\overline{S^*} = \overline{S} + 4.27\sigma_S\left[(l/l_0)^{-1/5.55} - 1\right]$	$\sigma_{S^*} = \sigma_S\left(l/l_0\right)^{-1/5.55}$
	12.5 tex	$\overline{S^*} = \overline{S} + 3.61\sigma_S\left[(l/l_0)^{-1/5.90} - 1\right]$	$\sigma_{S^*} = \sigma_S\left(l/l_0\right)^{-1/5.90}$
	16.5 tex	$\overline{S^*} = \overline{S} + 4.86\sigma_S\left[(l/l_0)^{-1/7.19} - 1\right]$	$\sigma_{S^*} = \sigma_S\left(l/l_0\right)^{-1/7.19}$
	20 tex	$\overline{S^*} = \overline{S} + 3.87\sigma_S\left[(l/l_0)^{-1/6.35} - 1\right]$	$\sigma_{S^*} = \sigma_S\left(l/l_0\right)^{-1/6.35}$

Evidently different yarns possess different relations between strength and length (different values of the coefficient and the exponent). This is due to different degree of strength autocorrelation in different yarns. On the contrary, under the assumption that no correlation exists among the strength of neighboring sections, Peirce (1926) suggested two unique values (coefficient – 4.2 and exponent – 1/5) for all yarns irrespective of the material and technology used for their manufacturing.

5.5.7 Predictability of Simulation Results

The basic statistical parameters of yarn strength obtained from the simulation results were compared with those corresponding to the actual results as well as Peirce's equations (Equations 2.10 and 2.11). This comparison in case of 7.4 tex combed ring yarn is shown in Figure 5.17. Similar results with a few other yarns are presented in Figures H1-H4 in Appendix H. Evidently, the simulation results are better in terms of predicting the actual results as compared to Peirce's equations. This difference is ascribed to the fact that the simulation results were obtained on the basis of verified assumption of strength dependency; on the contrary Peirce's equations respected the imagination of strength independency, which is not correct as revealed in this research work. It is generally seen that the mean values of actual yarn strength are more closely predicted by the simulation results than the standard deviations of actual yarn strength. The reason of this is not yet known. It is therefore necessary to study the problem of yarn strength variability more deeply in future.

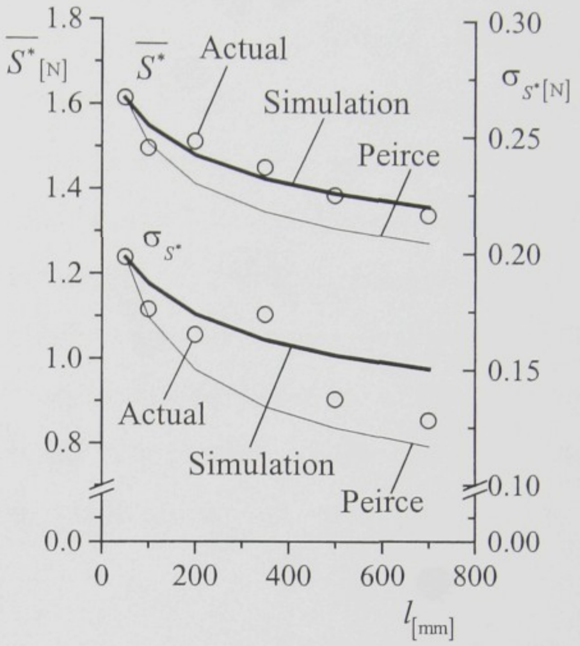

Figure 5.17

Note: In some yarns, the actual strength at longer gauge length was found nearly the same or a little higher than the actual strength at short gauge length (50 mm). Imaginatively, this might happen because the "micro-slippage" of fibers and/or fiber segments was not fully realized in a region near to the jaw gripping line. (Fibers could not slip inside the jaw.) Evidently, this phenomenon was relatively more prominent during tensile testing at short gauge length (50 mm).

6 CONCLUSION

The presented theoretical model of yarn strength as a summation of two mutually independent stationary, ergodic, Markovian, and Gaussian (SEMG) stochastic processes was verified with thirty-one yarns produced from cotton fibers using ring, rotor, compact, and the so-called "new'' spinning technologies. It was observed that the strengths of successive short sections, each of 50 mm length, along the yarns are dependent and the degree of this dependency is different in different yarns. As a result, the empirical relation between strength and gauge length is also different in different yarns. This observation contradicts Peirce's assumption of strength independency (1926) and thus answers why Peirce's strength model is not enough precise. It is remarkable to see the extent to which, in general, the mean values of actual yarn strength measured at different gauge lengths were predicted by the computer simulations; however, that much of closeness was not always obtained with the standard deviation between the actual yarn strength and the simulated yarn strength. It, therefore, evokes a new research direction – to model yarn strength variability.

This research work introduced a new methodology to measure yarn strength at a short gauge length and a special data evaluation technique in order to satisfactorily predict the basic statistical parameters and frequency distributions of actual yarn strength corresponding to different gauge lengths. These non-standard measurement and data evaluation techniques can be easily developed in the textile industries in order to have a new characterization of yarn strength, in terms of its autocorrelation characteristics and strength versus gauge length relation.

Besides the practical application, mentioned above, this research work may also find application for future theoretical work. It was interesting to observe that yarn strength variability is due probably to the additive influence of two highly different and mutually independent phenomena that are partially related to yarn mass irregularity. This knowledge at the empirical level will pave the way for creation of a new theoretical model in order to better understanding of yarn strength variability.

APPENDIX A: DISTINGUISHING FEATURES OF OUR YARNS

Table A1

Yarns	Mean Values of Count $\overline{T}$ [tex]	Mean Values of Twist $\overline{Z}$ [tpm]
Combed Ring	7.4	1080
	10	1013
	14.5	913
	16.5	831
	20	740
Carded Ring	20	944
	25	761
	29.5	871
Carded Rotor	20	887
	35.5	683
	42	568
Combed Compact	7.4	1262
	10	877
	11.8	1059
Carded Compact	20	977
	29.5	842

Table A2

Mean Values of Count $\overline{T}$ [tex]	Mean Values of Twist $\overline{Z}$ [tpm]		
	Twist Multiplier $\alpha = 38$ tex$^{2/3}$ cm^{-1}	Twist Multiplier $\alpha = 56$ tex$^{2/3}$ cm^{-1}	Twist Multiplier $\alpha = 81$ tex$^{2/3}$ cm^{-1}
7.4	1000	1474	2133
10	819	1206	1745
12.5	700	1040	1500
16.5	614	864	1250
20	516	760	1100

APPENDIX B:
A SPECIAL OUTPUT FROM THE USTER TESTER 4 INSTRUMENT

```
MASSDGR

  CrvNo        Points        Average
    1          18458            1

  unitX         xMin          xMax           dX          P1         P2
   35           0.0           400.0       0.021672      0.000      0.000

   unitY        yMin          yMax
    46        -100.000       150.000

x Values      y Values
          -0.8547

          3.907
          21.00
          -1.221
          -8.486
          -14.65
          -1.893
          8.730
          14.59
          -10.81
          -3.602
          -11.72
          2.503
          -14.71
          -22.71
          14.47
          21.67
          -8.059
             ⋮
             ⋮
             ⋮
```

Figure B1

APPENDIX C:
BASIC STATISTICAL PARAMETERS OF ACTUAL YARN STRENGTH

Table C1

Count [tex]	Gauge length [mm]	Mean [cN/tex]	Standard deviation [cN/tex]	Coefficient of variation [%]	Number of measurements
10	50	22.2220	2.1540	9.6950	899
	500	20.1000	1.6500	8.2107	300
14.5	50	14.8821	1.4724	9.8942	900
	500	13.3890	1.2345	9.2218	300
16.5	50	14.1388	1.5061	10.6539	900
	500	13.0612	1.1661	8.9280	300

Table C2

Count [tex]	Gauge length [mm]	Mean [cN/tex]	Standard deviation [cN/tex]	Coefficient of variation [%]	Number of measurements
20	50	17.3970	1.448	8.3220	898
	500	16.4945	0.9635	5.8428	100
25	50	14.3712	1.3300	9.2551	900
	100	13.7196	1.2108	8.8261	300
	200	13.8236	1.2604	9.1188	300
	350	13.1424	1.0528	8.0113	300
	500	13.2492	1.0144	7.6562	300
29.5	50	17.0695	1.5532	9.0990	900
	500	15.7075	1.3119	8.3337	100

Table C3

Count [tex]	Gauge length [mm]	Mean [cN/tex]	Standard deviation [cN/tex]	Coefficient of variation [%]	Number of measurements
20	50	11.1955	1.1005	9.8298	900
	100	10.3955	1.1360	10.9295	500
	200	9.9355	1.0590	10.6692	500
	350	10.0990	0.9725	9.6417	500
	500	9.5980	0.9185	9.5790	500
35.5	50	12.9341	1.3690	10.5839	900
	500	12.3611	0.9017	7.2955	300
42	50	12.0088	1.0100	8.4106	900
	500	11.3729	0.7267	6.3902	300

Table C4

Count [tex]	Gauge length [mm]	Mean [cN/tex]	Standard deviation [cN/tex]	Coefficient of variation [%]	Number of measurements
7.4	50	24.4203	2.5257	10.3419	882
	100	22.9865	2.2676	9.8640	100
	200	23.1932	1.8878	8.1372	300
	350	22.2851	1.9041	8.5459	100
	500	19.9878	2.0419	10.2143	600
10	50	22.1220	2.8020	12.6645	900
	500	18.3700	1.3550	7.3738	100
11.8	50	25.1542	2.3119	9.1905	890
	500	21.8466	1.5856	7.2567	300

Table C5

Count [tex]	Gauge length [mm]	Mean [cN/tex]	Standard deviation [cN/tex]	Coefficient of variation [%]	Number of measurements
20	50	19.8455	1.6040	8.0865	895
	100	19.0675	1.3455	7.0567	300
	200	18.9160	1.3020	6.8820	300
	350	18.0470	1.2210	6.7660	300
	500	17.9365	1.3365	7.3688	300
29.5	50	17.1014	1.7556	10.2661	900
	500	15.6356	1.1383	7.2792	100

Table C6

Count [tex]	TM[1] [tex$^{2/3}$ cm^{-1}]	Gauge length [mm]	Mean [cN/tex]	Standard deviation [cN/tex]	Coefficient of variation [%]	Number of measurements
7.4	38	50	15.1649	2.7473	18.1180	900
		100	13.1500	2.4919	18.9532	100
		200	13.5176	2.0851	15.4480	100
		350	13.3919	2.6622	19.8780	100
		500	12.7189	2.0608	16.1988	100
		700	12.0473	1.9446	16.1469	100
7.4	56	50	22.4851	3.8811	17.2602	900
		100	21.7135	3.3108	15.2491	100
		200	20.9703	3.0770	14.6709	100
		350	19.6108	3.1500	16.0613	100
		500	18.0365	3.2149	17.8228	100
		700	18.5446	3.0000	16.1805	100

---

[1] TM stands for twist multiplier (Phrix type), expressed in tex$^{2/3}$cm^{-1}.

Count [tex]	TM [tex$^{2/3}$ cm^{-1}]	Gauge length [mm]	Mean [cN/tex]	Standard deviation [cN/tex]	Coefficient of variation [%]	Number of measurements
7.4	81	50	15.6189	3.3203	21.2607	900
		100	15.1432	2.5635	16.9326	100
		200	14.6986	2.5581	17.4040	100
		350	12.7838	1.9622	15.3522	100
		500	12.9284	1.9081	14.7568	100
		700	12.4689	1.6581	13.2925	100
10	38	50	14.9690	2.5200	16.8374	895
		500	12.9140	1.8110	14.0203	100
10	56	50	24.0620	2.6610	11.0600	900
		500	21.2190	2.2202	10.3795	100
10	81	50	18.4390	3.6670	19.8865	899
		500	14.3030	2.2200	15.5206	100
12.5	38	50	15.2096	2.6216	17.2359	898
		500	12.6216	1.9256	15.2568	100
12.5	56	50	25.2232	2.6520	10.5137	896
		500	22.4952	2.5384	11.2854	100
12.5	81	50	24.1752	4.2552	17.6002	898
		500	20.7248	4.1488	20.0191	100
16.5	38	50	12.2345	2.7915	22.8180	891
		500	11.4867	2.3127	20.1348	100
16.5	56	50	23.7285	2.1624	9.1131	900
		500	20.9091	1.5012	7.1810	100
16.5	81	50	25.8170	2.9436	11.4011	900
		500	23.6582	2.3745	10.0366	100

Count [tex]	TM [tex$^{2/3}$ cm^{-1}]	Gauge length [mm]	Mean [cN/tex]	Standard deviation [cN/tex]	Coefficient of variation [%]	Number of measurements
20	38	50	13.8640	2.3060	16.6333	899
		100	10.0190	2.0935	20.8954	100
		200	9.4920	1.6690	17.5807	100
		350	10.7435	1.7740	16.5138	100
		500	10.7100	1.7770	16.5926	100
		700	11.1990	1.8285	16.3269	100
20	56	50	24.2635	2.5215	10.3915	900
		100	21.8970	2.1635	9.8743	100
		200	22.0525	1.7185	7.7931	100
		350	22.3395	1.8955	8.4839	100
		500	22.1000	1.4830	6.7101	100
		700	20.9200	1.8240	8.7200	100
20	81	50	25.9525	3.0910	11.9105	899
		100	26.1465	2.5210	9.6415	100
		200	26.1090	2.3750	9.0962	100
		350	25.1120	1.9880	7.9163	100
		500	24.5135	2.2015	8.9805	100
		700	23.5575	2.0075	8.5220	100

APPENDIX D:
OUR RESULTS VERSUS
THE USTER STATISTICS 2001

Table D1

Yarn	Count [tex]	Mean Tenacity [cN/tex]				Coefficient of Variation of Tenacity [%]			
		Actual	Uster Statistics 2001			Actual	Uster Statistics 2001		
			5%	50%	95%		5%	50%	95%
Combed Ring Yarns	7.4	18.7	24.3	20.9	18.3	9.9	9.1	11.3	13.6
	10	20.1	25.5	21.3	17.5	8.2	7.5	9.5	11.9
	14.5	13.4	20.7	16.4	13.9	9.2	7.0	8.7	11.1
	16.5	13.1	21.1	16.7	14.6	8.9	6.7	8.2	10.4
	20	12.8	21.7	17.3	14.8	8.6	6.4	7.7	9.7
Carded Ring Yarns	20	16.5	21.3	16.4	14.1	5.8	6.1	7.5	9.6
	25	13.2	21.4	16.5	14.2	7.7	6.0	7.3	8.9
	29.5	15.7	21.5	16.6	14.3	8.3	6.0	7.2	8.3
Carded Rotor Yarns	20	9.6	14.4	12.9	9.8	9.6	8.0	9.2	11.3
	35.5	12.4	14.7	12.6	9.8	7.3	6.7	8.0	10.7
	42	11.4	14.5	12.4	9.6	6.4	6.3	7.7	10.4
Combed Compact Yarns	7.4	20.0	29.1	27.0	22.2	10.2	8.4	9.8	11.5
	10	18.4	27.4	25.2	21.1	7.4	7.9	9.0	10.4
	11.8	21.8	26.5	24.4	20.5	7.3	7.5	8.6	9.8

APPENDIX E: ACTUAL YARN STRENGTH HISTOGRAMS

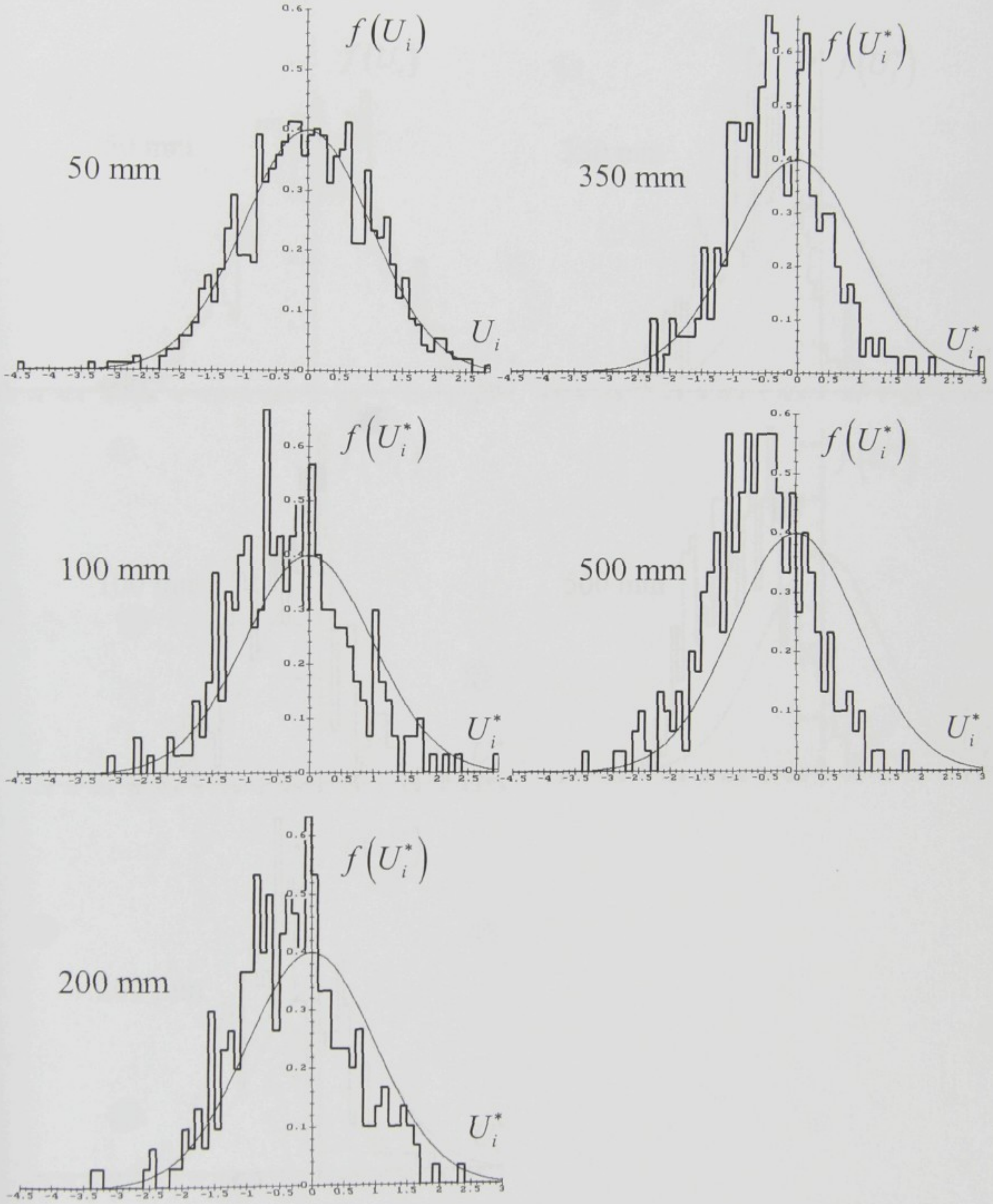
50 mm
$f(U_i)$
U_i
350 mm
$f(U_i^*)$
U_i^*
100 mm
$f(U_i^*)$
U_i^*
500 mm
$f(U_i^*)$
U_i^*
200 mm
$f(U_i^*)$
U_i^*
0.6
0.5
0.4
0.3
0.2
0.1
0
-4.5
-4
-3.5
-3
-2.5
-2
-1.5
-1
-0.5
0.5
1
1.5
2
2.5
3

Figure E1

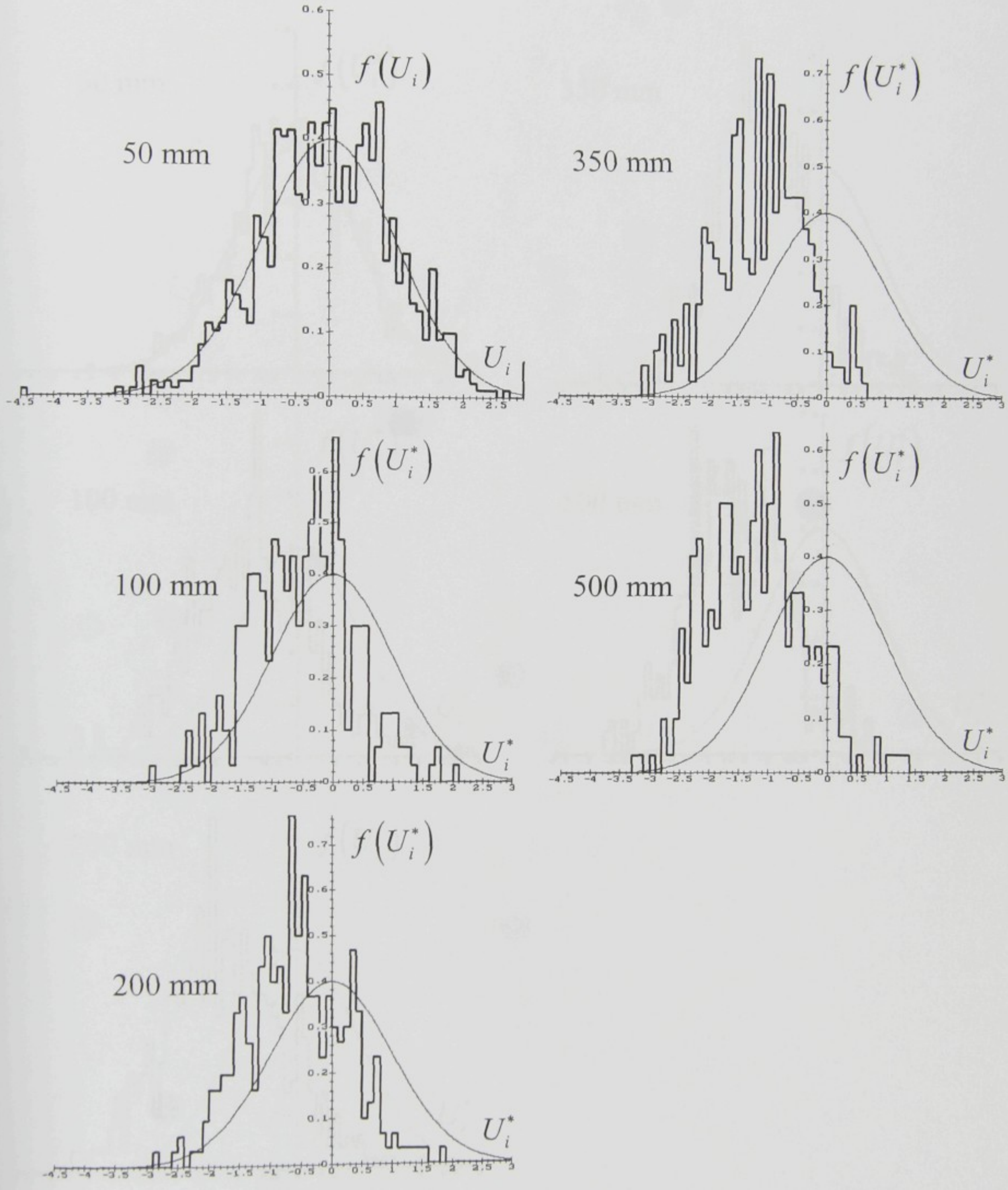
50 mm
$f(U_i)$
U_i
350 mm
$f(U_i^*)$
U_i^*
100 mm
$f(U_i^*)$
U_i^*
500 mm
$f(U_i^*)$
U_i^*
200 mm
$f(U_i^*)$
U_i^*
-4.5 -4 -3.5 -3 -2.5 -2 -1.5 -1 -0.5 0 0.5 1 1.5 2 2.5 3
0.1 0.2 0.3 0.4 0.5 0.6 0.7

Figure E2

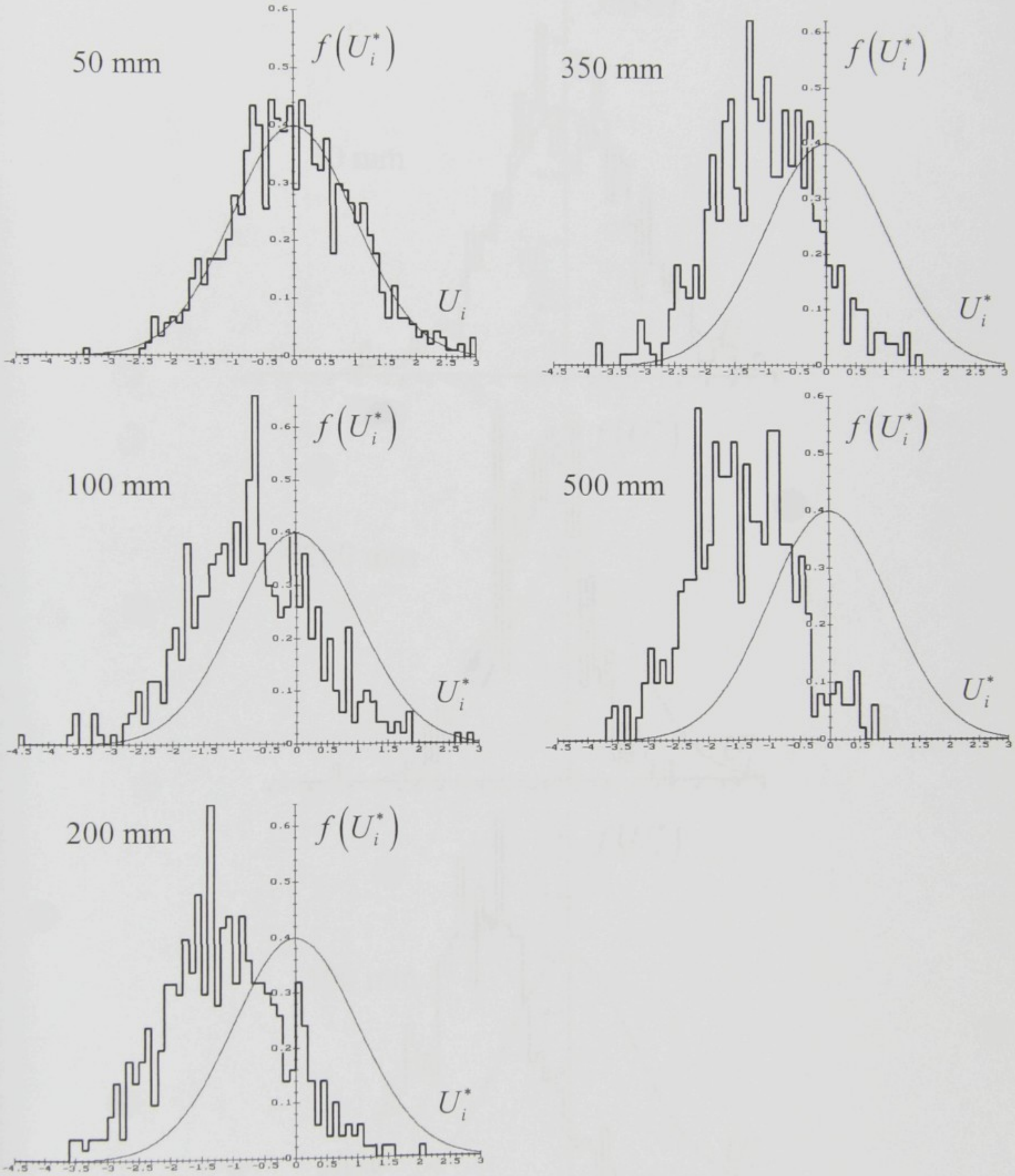
50 mm
$f(U_i^*)$
U_i
350 mm
$f(U_i^*)$
U_i^*
100 mm
$f(U_i^*)$
U_i^*
500 mm
$f(U_i^*)$
U_i^*
200 mm
$f(U_i^*)$
U_i^*
0.6
0.5
0.4
0.3
0.2
0.1
0
-4.5
-4
-3.5
-3
-2.5
-2
-1.5
-1
-0.5
0
0.5
1
1.5
2
2.5
3

Figure E3

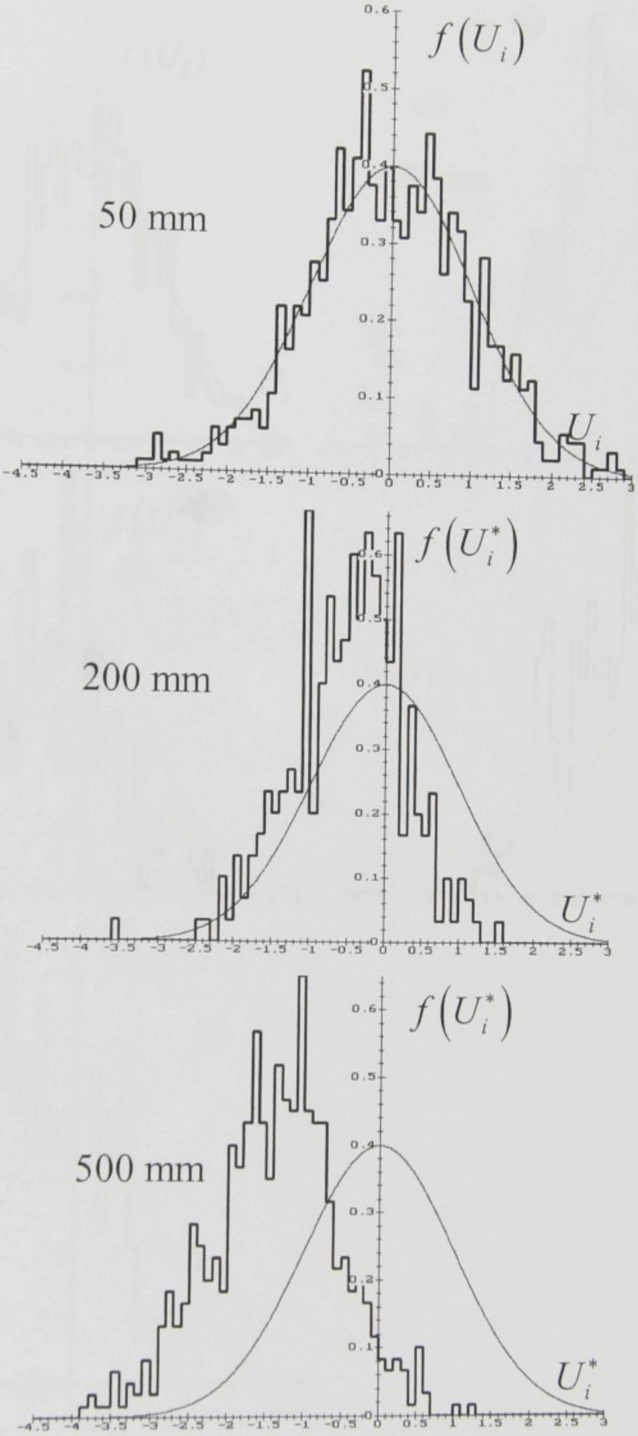
f(U_i)
50 mm
U_i
f(U_i^*)
200 mm
U_i^*
f(U_i^*)
500 mm
U_i^*
0.6
0.5
0.4
0.3
0.2
0.1
0
-4.5
-4
-3.5
-3
-2.5
-2
-1.5
-1
-0.5
0.5
1
1.5
2
2.5
3

Figure E4

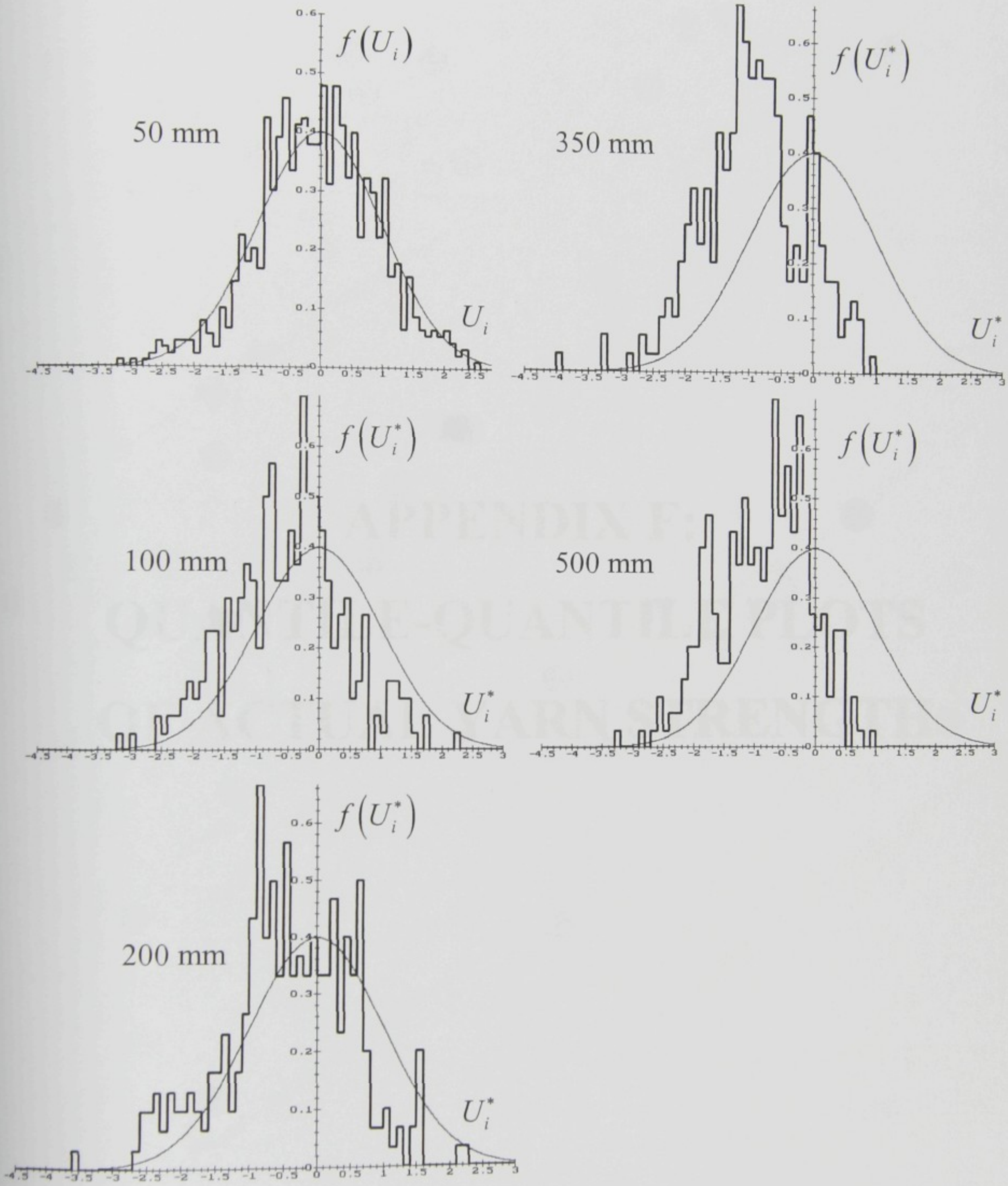
50 mm
f(U_i)
U_i
350 mm
f(U_i*)
U_i*
100 mm
f(U_i*)
U_i*
500 mm
f(U_i*)
U_i*
200 mm
f(U_i*)
U_i*
0.1
0.2
0.3
0.4
0.5
0.6
-4.5
-4
-3.5
-3
-2.5
-2
-1.5
-1
-0.5
0
0.5
1
1.5
2
2.5
3

Figure E5

APPENDIX F:
QUANTILE-QUANTILE PLOTS OF ACTUAL YARN STRENGTH

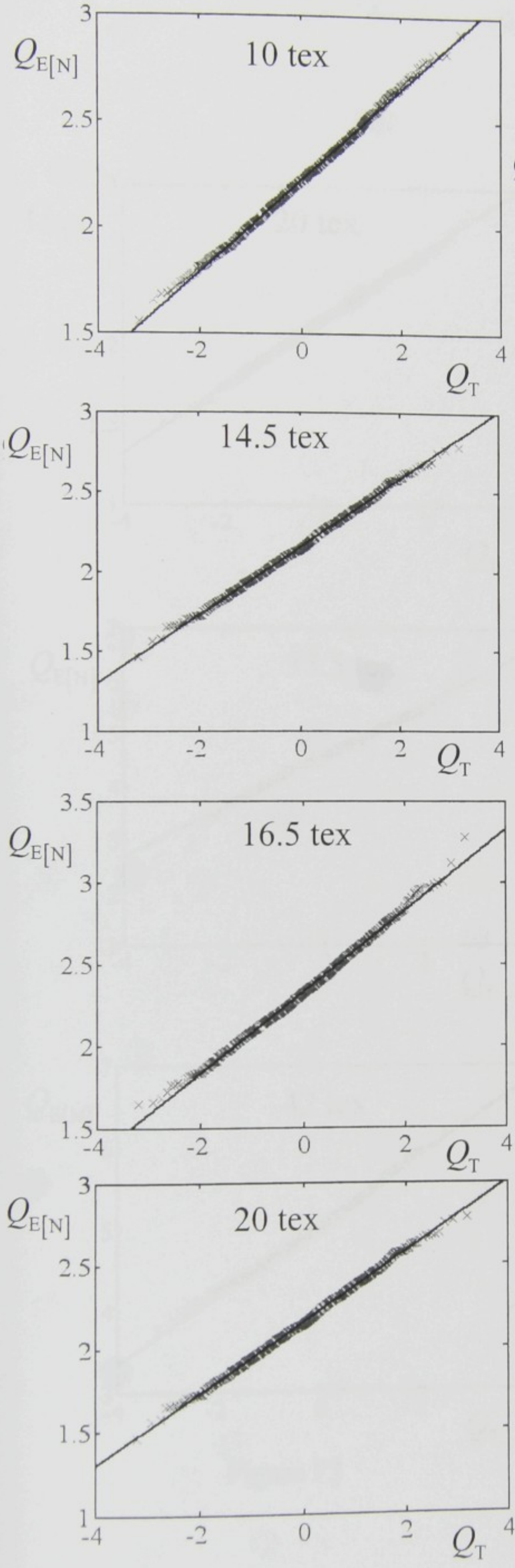

Figure F1

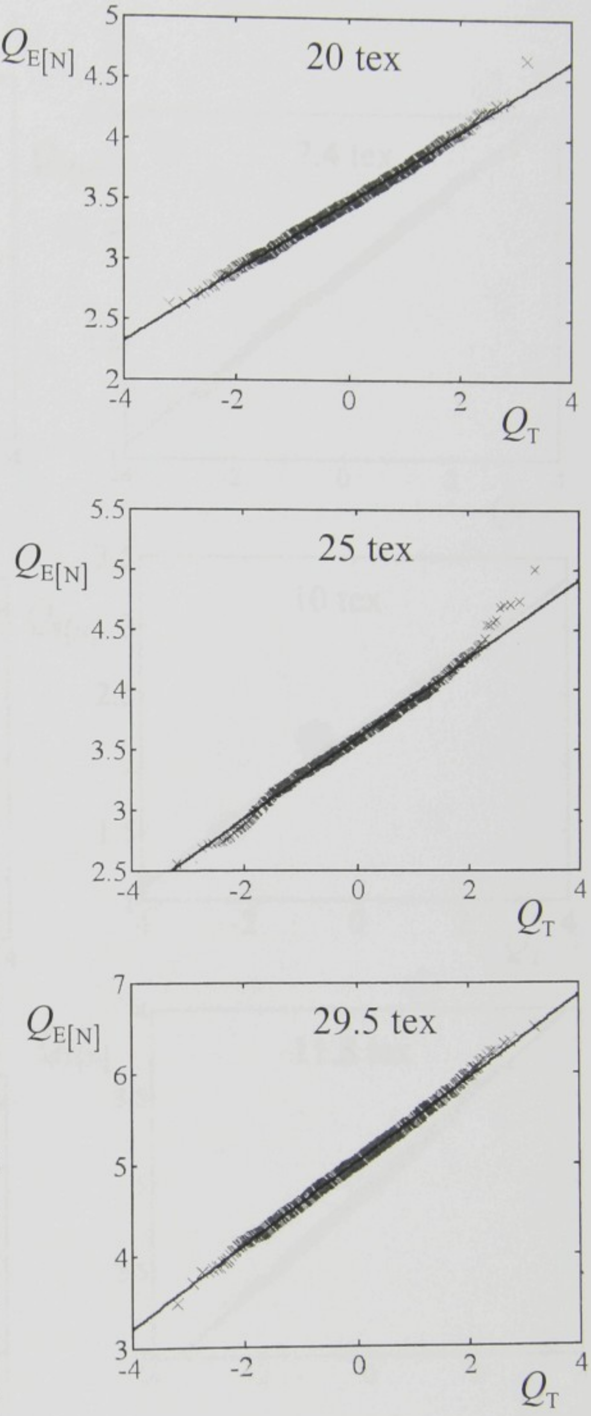

Figure F2

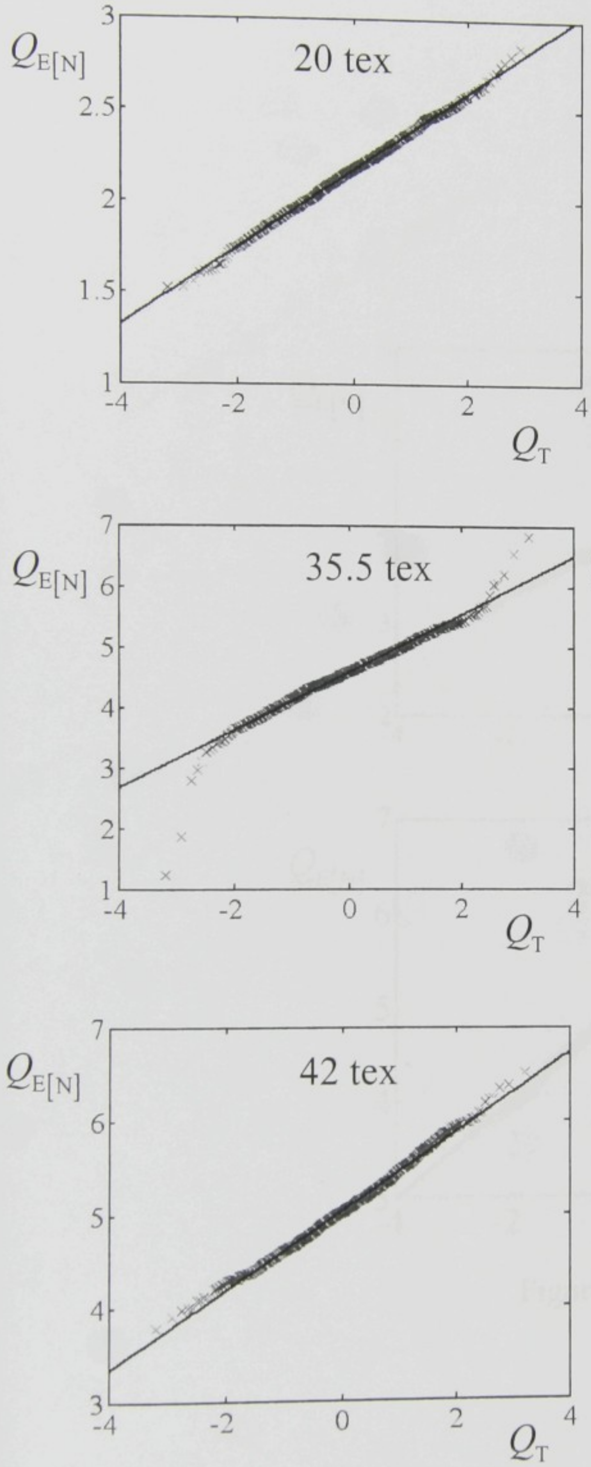

Figure F3

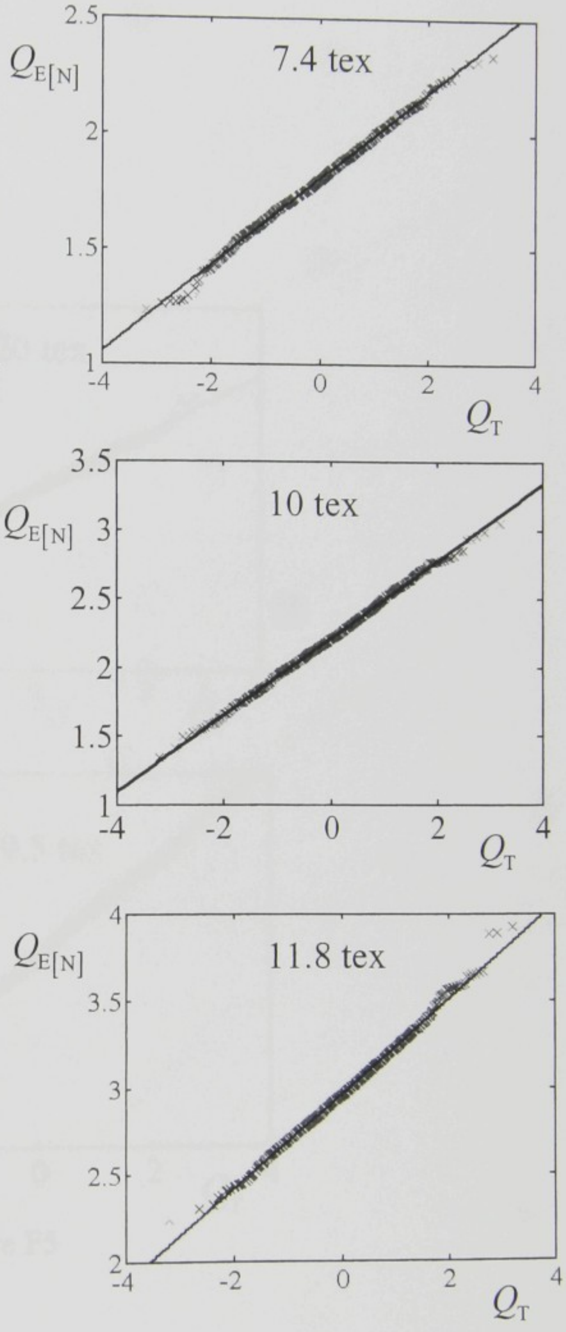

Figure F4

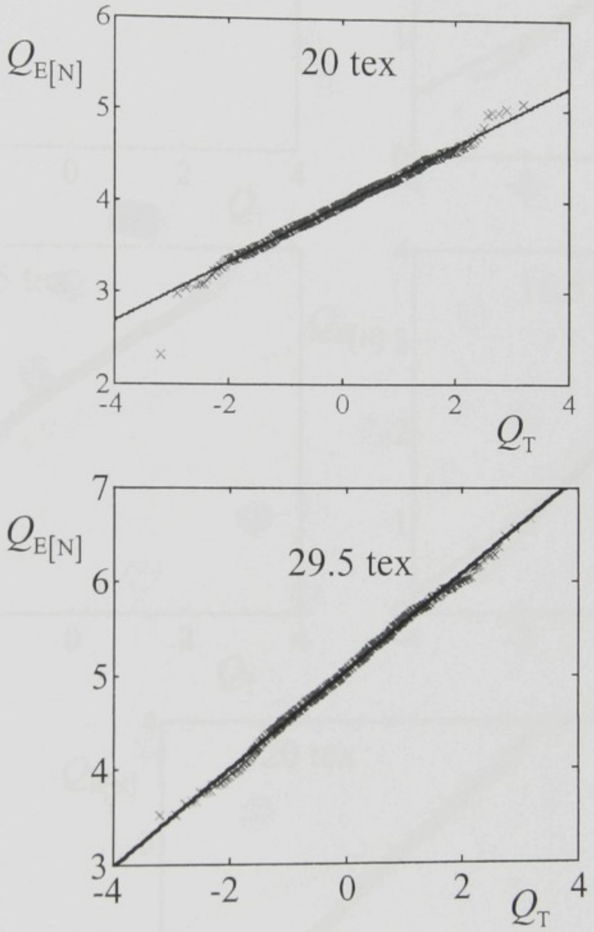

Figure F5

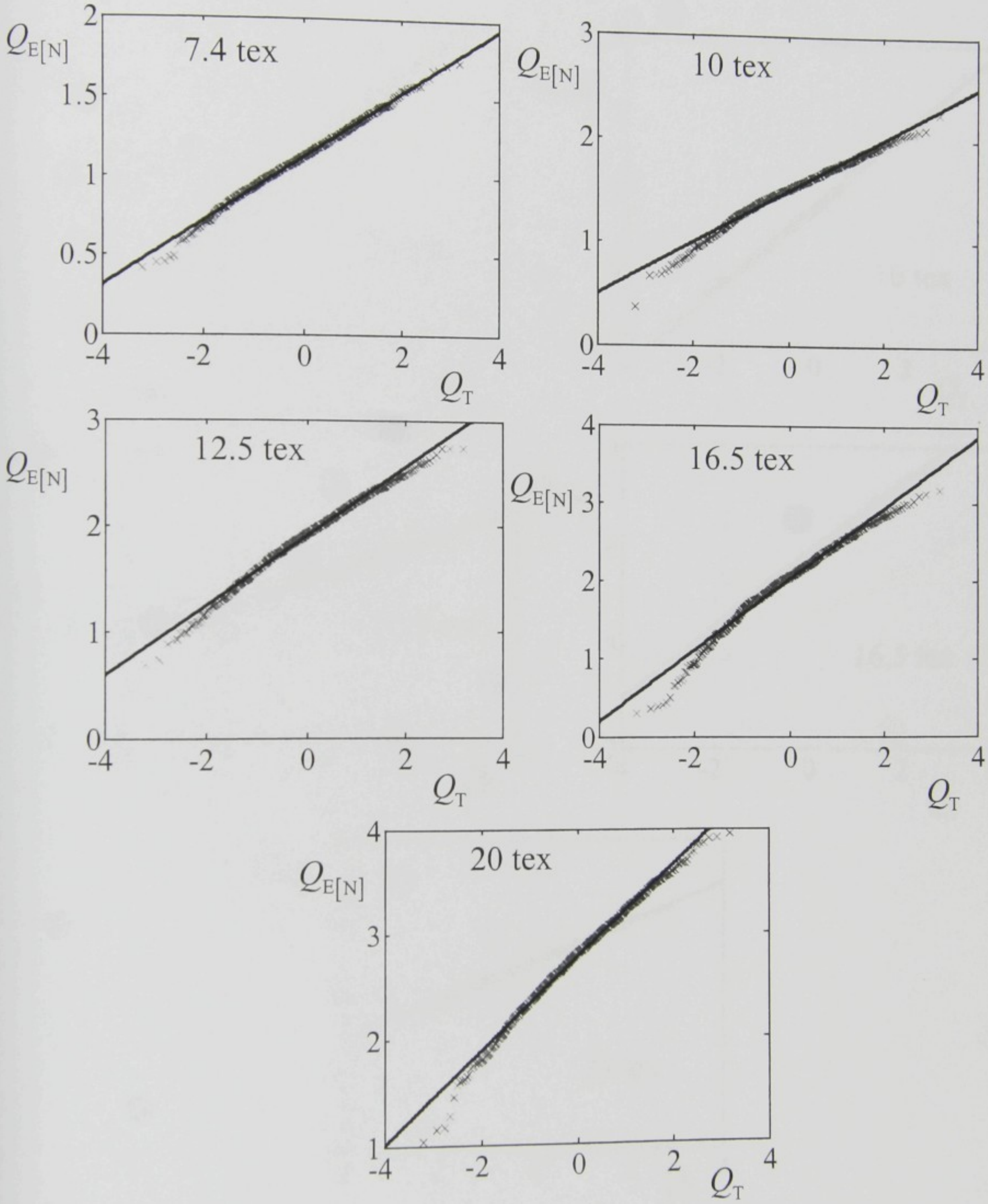
7.4 tex
$Q_{E[N]}$
2
1.5
1
0.5
0
-4
-2
0
2
4
Q_T
10 tex
$Q_{E[N]}$
3
2
1
0
-4
-2
0
2
4
Q_T
12.5 tex
$Q_{E[N]}$
3
2
1
0
-4
-2
0
2
4
Q_T
16.5 tex
$Q_{E[N]}$
4
3
2
1
0
-4
-2
0
2
4
Q_T
20 tex
$Q_{E[N]}$
4
3
2
1
-4
-2
0
2
4
Q_T

Figure F6

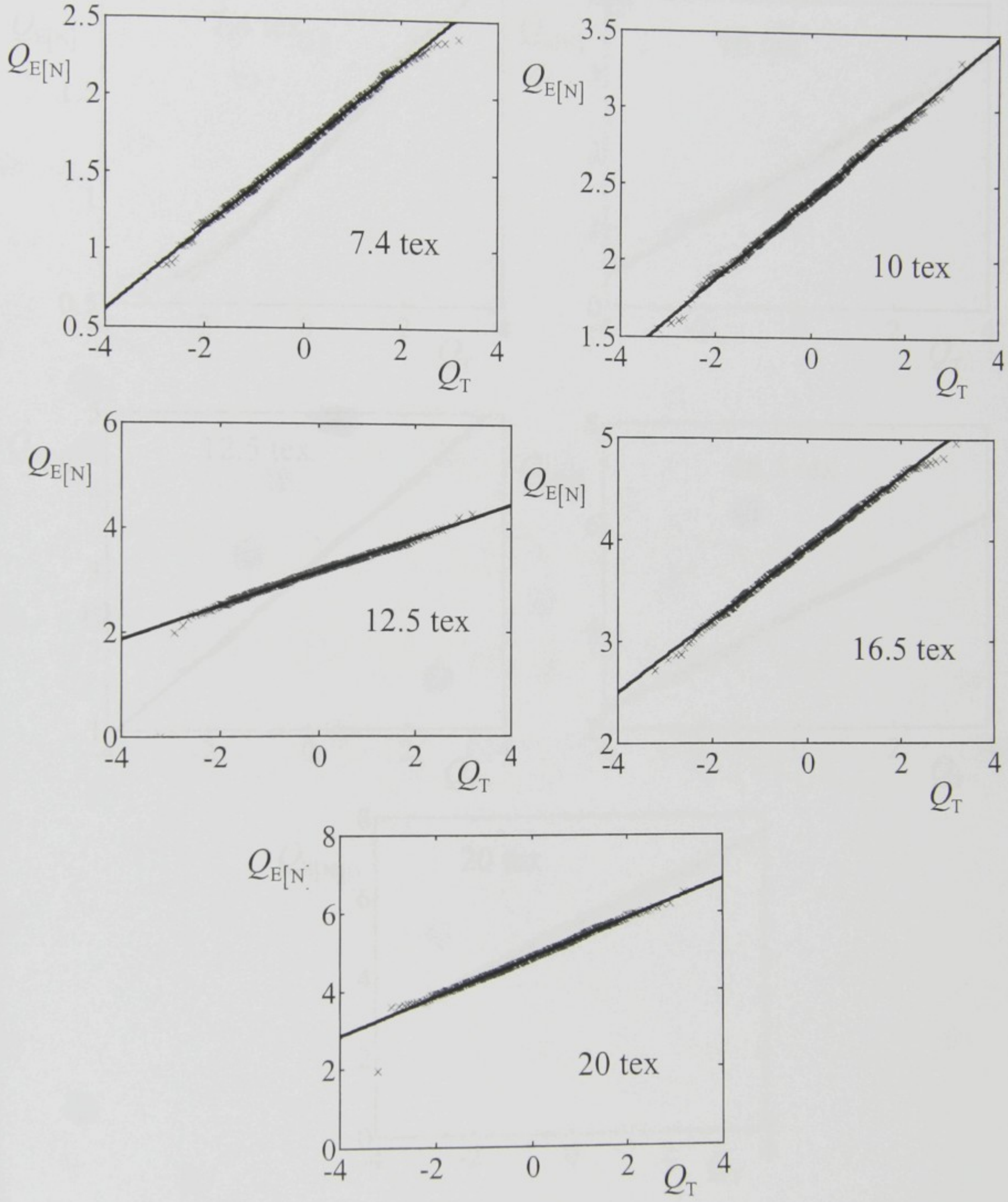
2.5
$Q_{E[N]}$
2
1.5
1
0.5
-4
-2
0
2
4
Q_T
7.4 tex
3.5
$Q_{E[N]}$
3
2.5
2
1.5
-4
-2
0
2
4
Q_T
10 tex
6
$Q_{E[N]}$
4
2
0
-4
-2
0
2
4
Q_T
12.5 tex
5
$Q_{E[N]}$
4
3
2
-4
-2
0
2
4
Q_T
16.5 tex
8
$Q_{E[N]}$
6
4
2
0
-4
-2
0
2
4
Q_T
20 tex

Figure F7

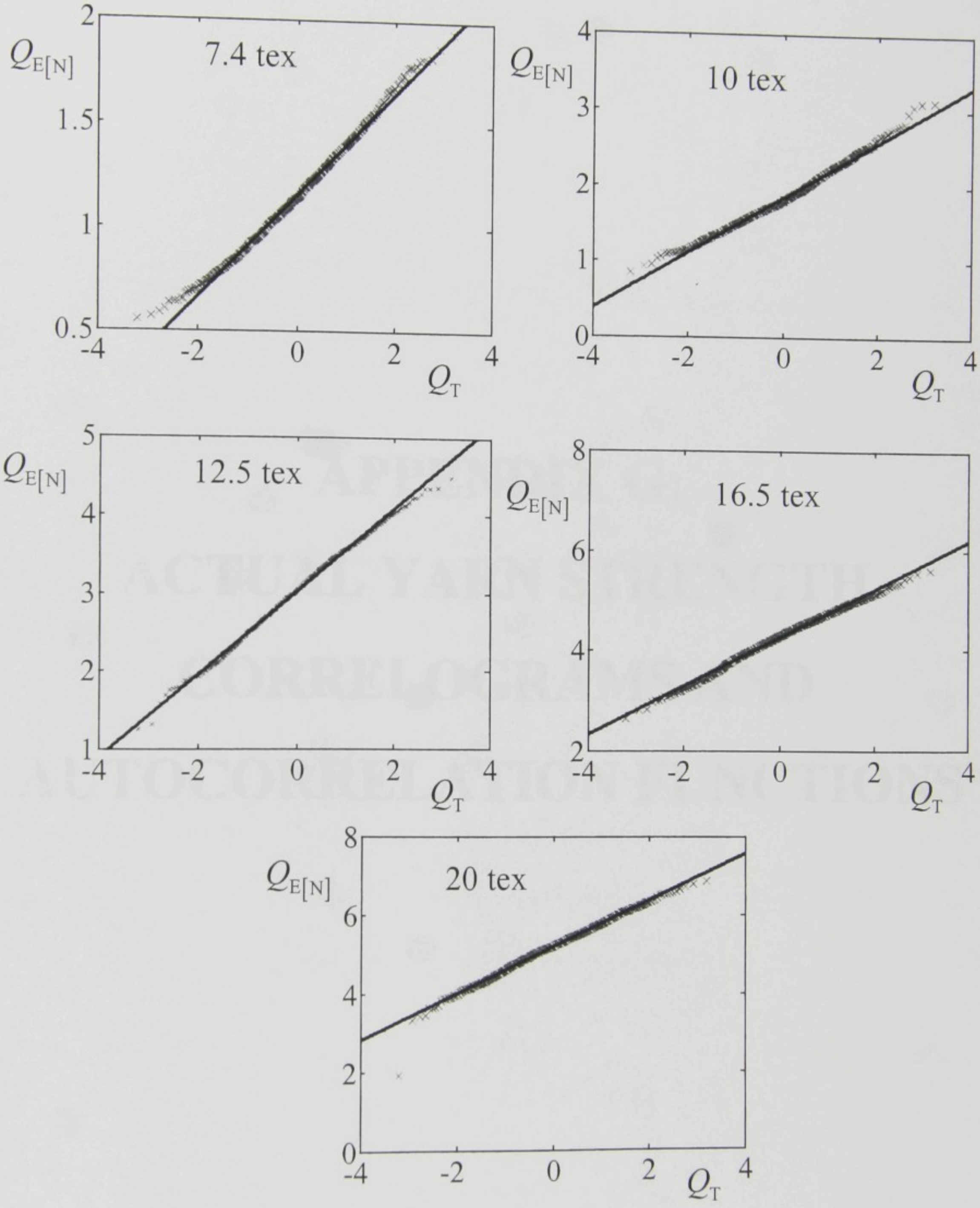

Figure F8

APPENDIX G:

ACTUAL YARN STRENGTH CORRELOGRAMS AND AUTOCORRELATION FUNCTIONS

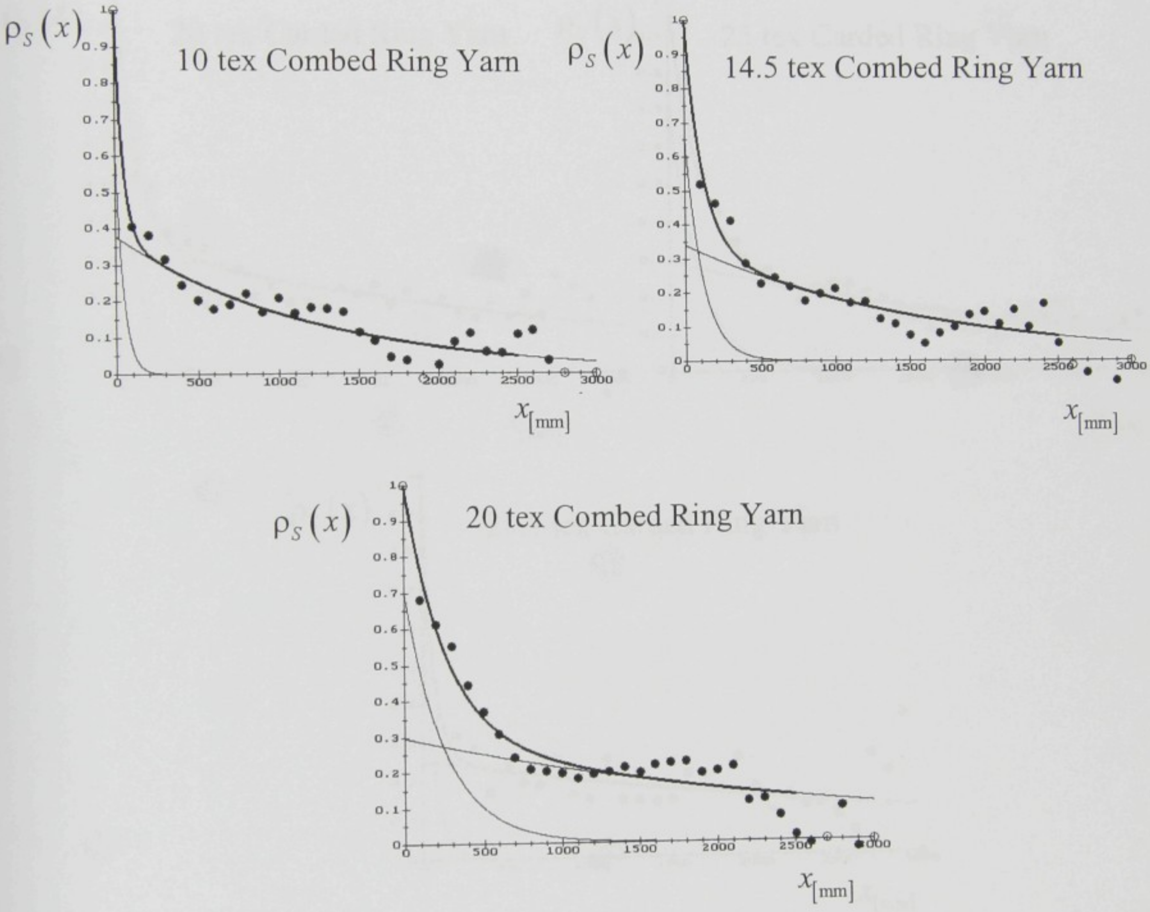
$\rho_S(x)$
10 tex Combed Ring Yarn
1
0.9
0.8
0.7
0.6
0.5
0.4
0.3
0.2
0.1
0
0
500
1000
1500
2000
2500
3000
$x_{[mm]}$
$\rho_S(x)$
14.5 tex Combed Ring Yarn
1
0.9
0.8
0.7
0.6
0.5
0.4
0.3
0.2
0.1
0
0
500
1000
1500
2000
2500
3000
$x_{[mm]}$
$\rho_S(x)$
20 tex Combed Ring Yarn
1
0.9
0.8
0.7
0.6
0.5
0.4
0.3
0.2
0.1
0
0
500
1000
1500
2000
2500
3000
$x_{[mm]}$

Figure G1

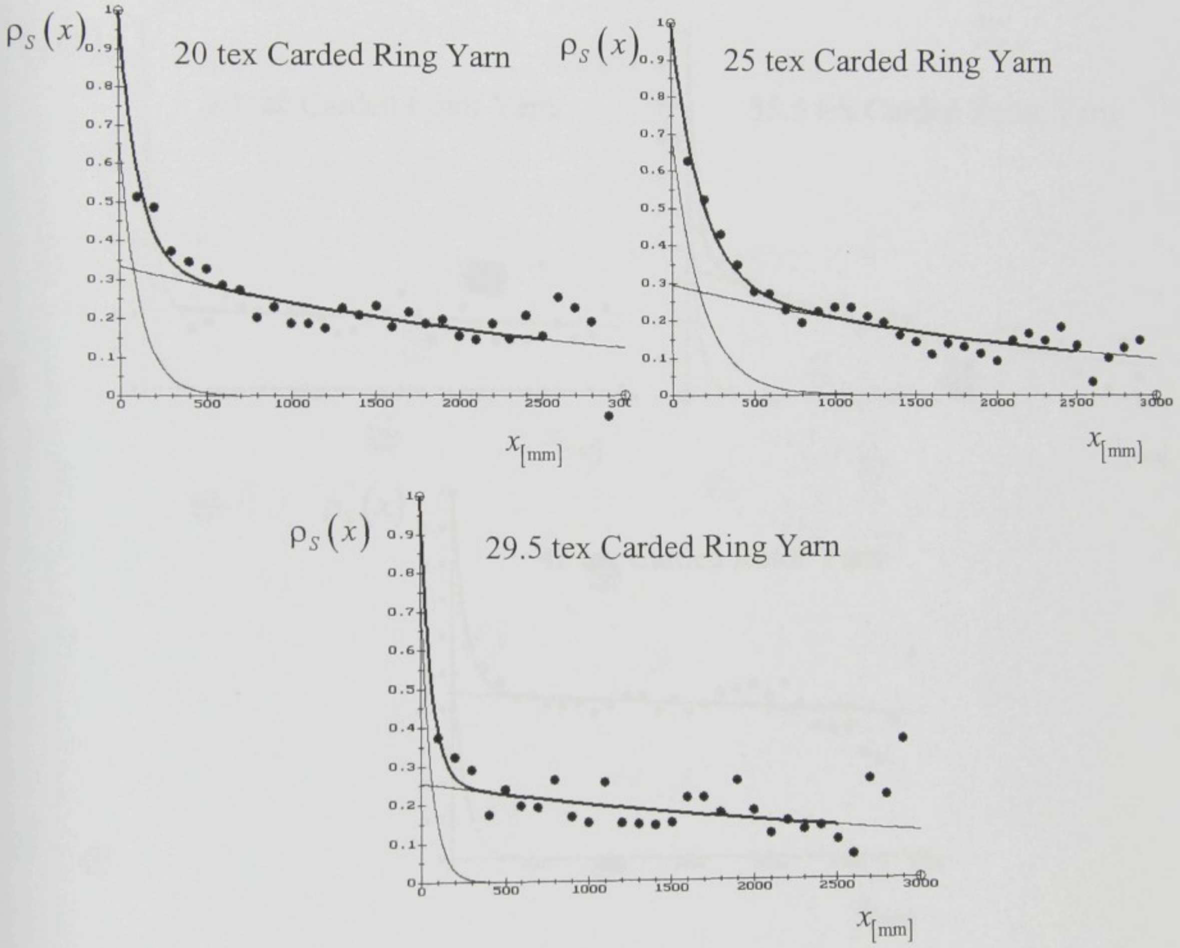
$\rho_S(x)$
20 tex Carded Ring Yarn
$\rho_S(x)$
25 tex Carded Ring Yarn
$\rho_S(x)$
29.5 tex Carded Ring Yarn
1
0.9
0.8
0.7
0.6
0.5
0.4
0.3
0.2
0.1
0
0
500
1000
1500
2000
2500
3000
$x_{[\mathrm{mm}]}$

Figure G2

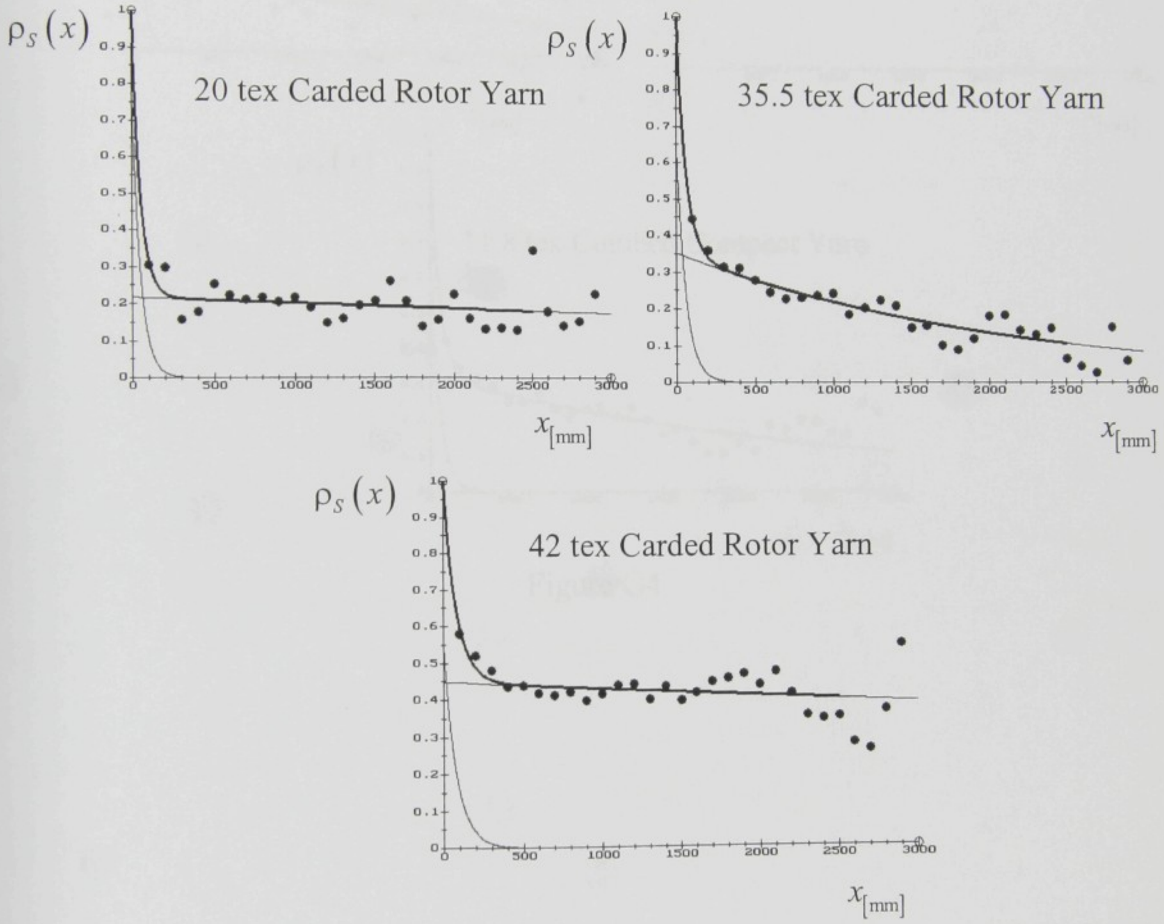
$\rho_S(x)$
20 tex Carded Rotor Yarn
0
0.1
0.2
0.3
0.4
0.5
0.6
0.7
0.8
0.9
1
0
500
1000
1500
2000
2500
3000
$x_{[\text{mm}]}$
$\rho_S(x)$
35.5 tex Carded Rotor Yarn
0
0.1
0.2
0.3
0.4
0.5
0.6
0.7
0.8
0.9
1
0
500
1000
1500
2000
2500
3000
$x_{[\text{mm}]}$
$\rho_S(x)$
42 tex Carded Rotor Yarn
0
0.1
0.2
0.3
0.4
0.5
0.6
0.7
0.8
0.9
1
0
500
1000
1500
2000
2500
3000
$x_{[\text{mm}]}$

Figure G3

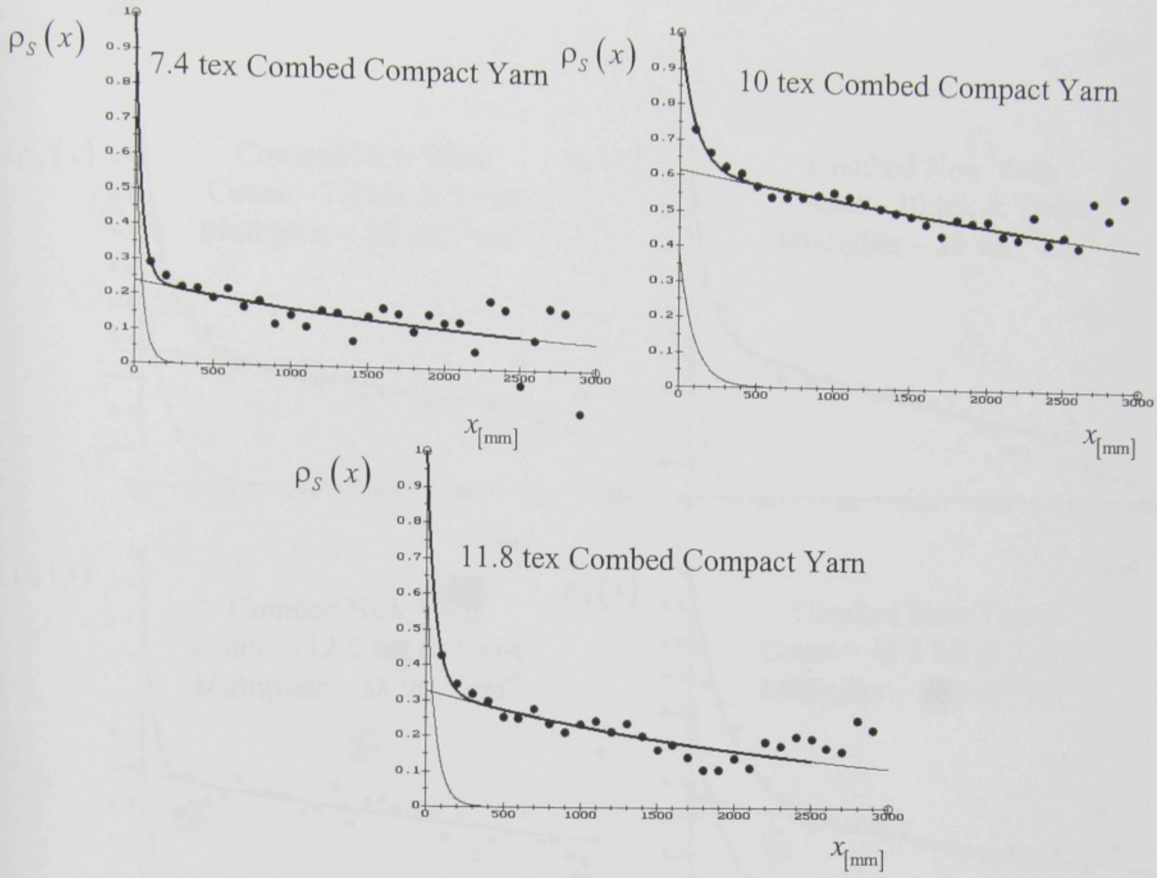

Figure G4

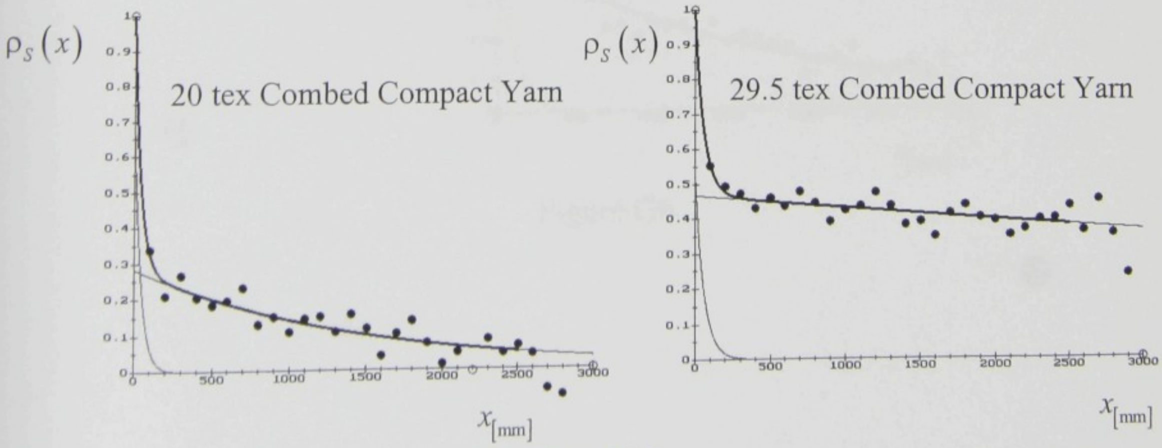

Figure G5

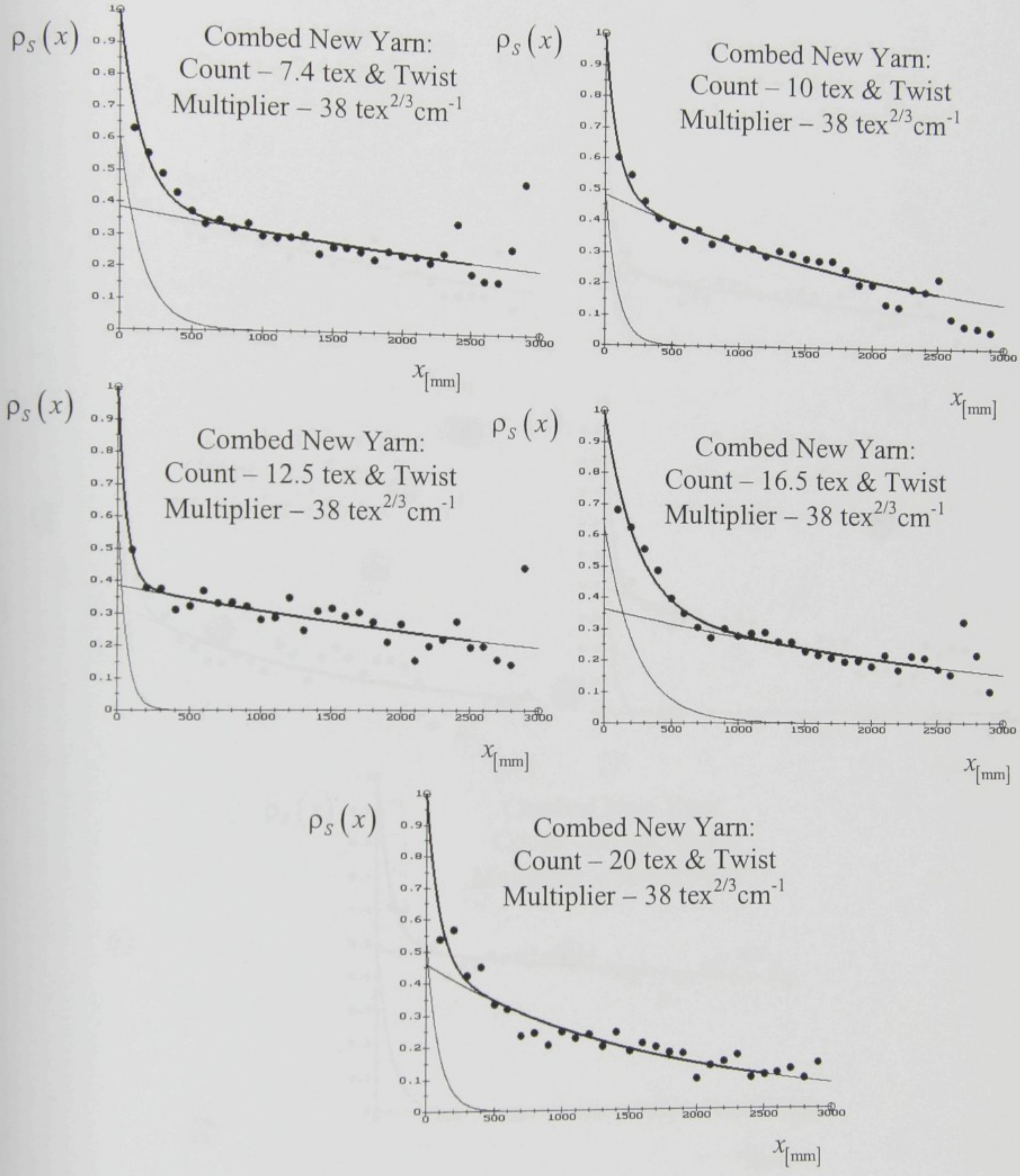

Combed New Yarn: Count – 7.4 tex & Twist Multiplier – 38 $tex^{2/3}cm^{-1}$

Combed New Yarn: Count – 10 tex & Twist Multiplier – 38 $tex^{2/3}cm^{-1}$

Combed New Yarn: Count – 12.5 tex & Twist Multiplier – 38 $tex^{2/3}cm^{-1}$

Combed New Yarn: Count – 16.5 tex & Twist Multiplier – 38 $tex^{2/3}cm^{-1}$

Combed New Yarn: Count – 20 tex & Twist Multiplier – 38 $tex^{2/3}cm^{-1}$

Figure G6

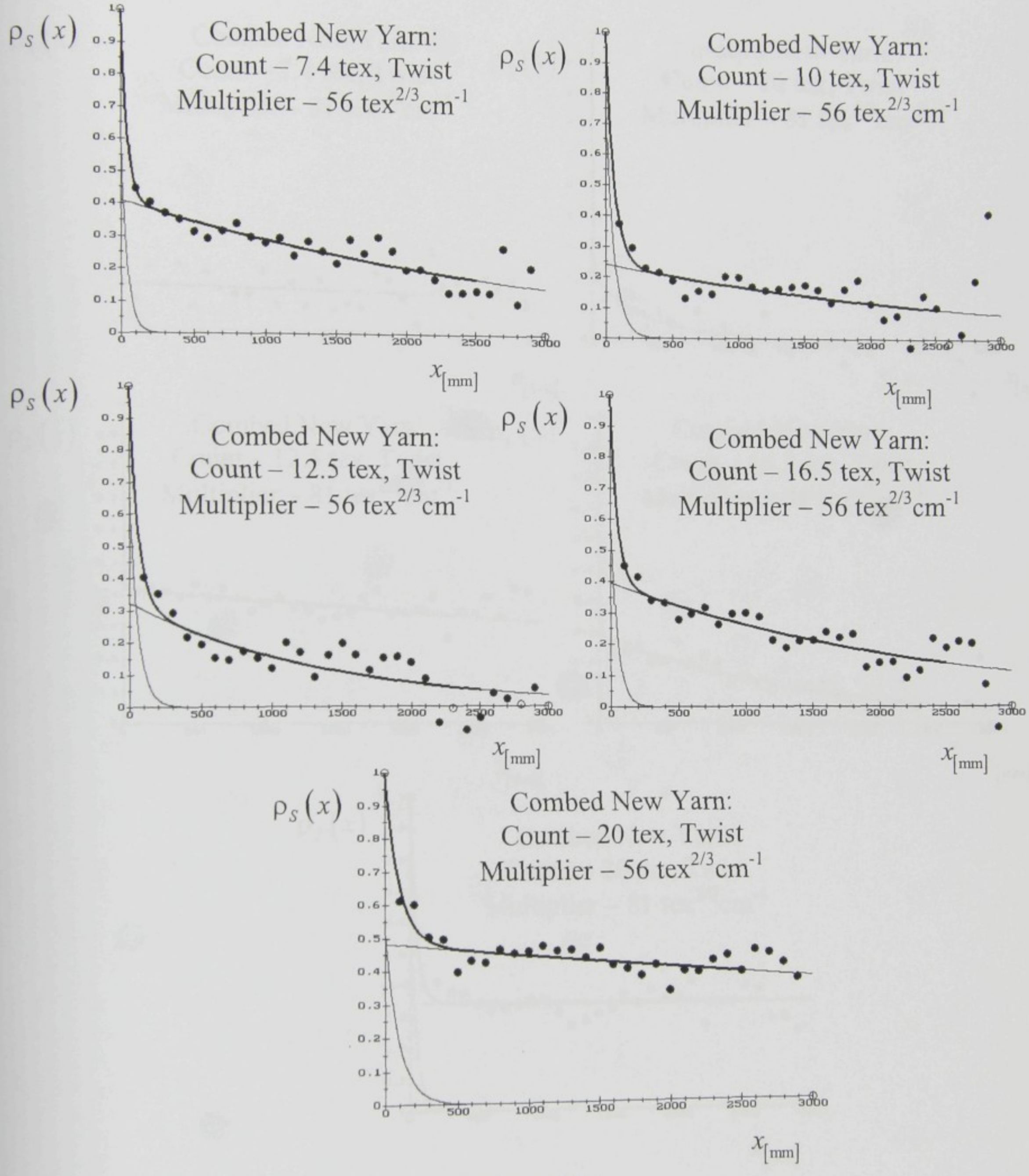
$\rho_S(x)$
Combed New Yarn:
Count – 7.4 tex, Twist
Multiplier – 56 tex$^{2/3}$cm^{-1}
$\rho_S(x)$
Combed New Yarn:
Count – 10 tex, Twist
Multiplier – 56 tex$^{2/3}$cm^{-1}
$\rho_S(x)$
Combed New Yarn:
Count – 12.5 tex, Twist
Multiplier – 56 tex$^{2/3}$cm^{-1}
$\rho_S(x)$
Combed New Yarn:
Count – 16.5 tex, Twist
Multiplier – 56 tex$^{2/3}$cm^{-1}
$\rho_S(x)$
Combed New Yarn:
Count – 20 tex, Twist
Multiplier – 56 tex$^{2/3}$cm^{-1}
0
0.1
0.2
0.3
0.4
0.5
0.6
0.7
0.8
0.9
1
0
500
1000
1500
2000
2500
3000
$x_{[mm]}$

Figure G7

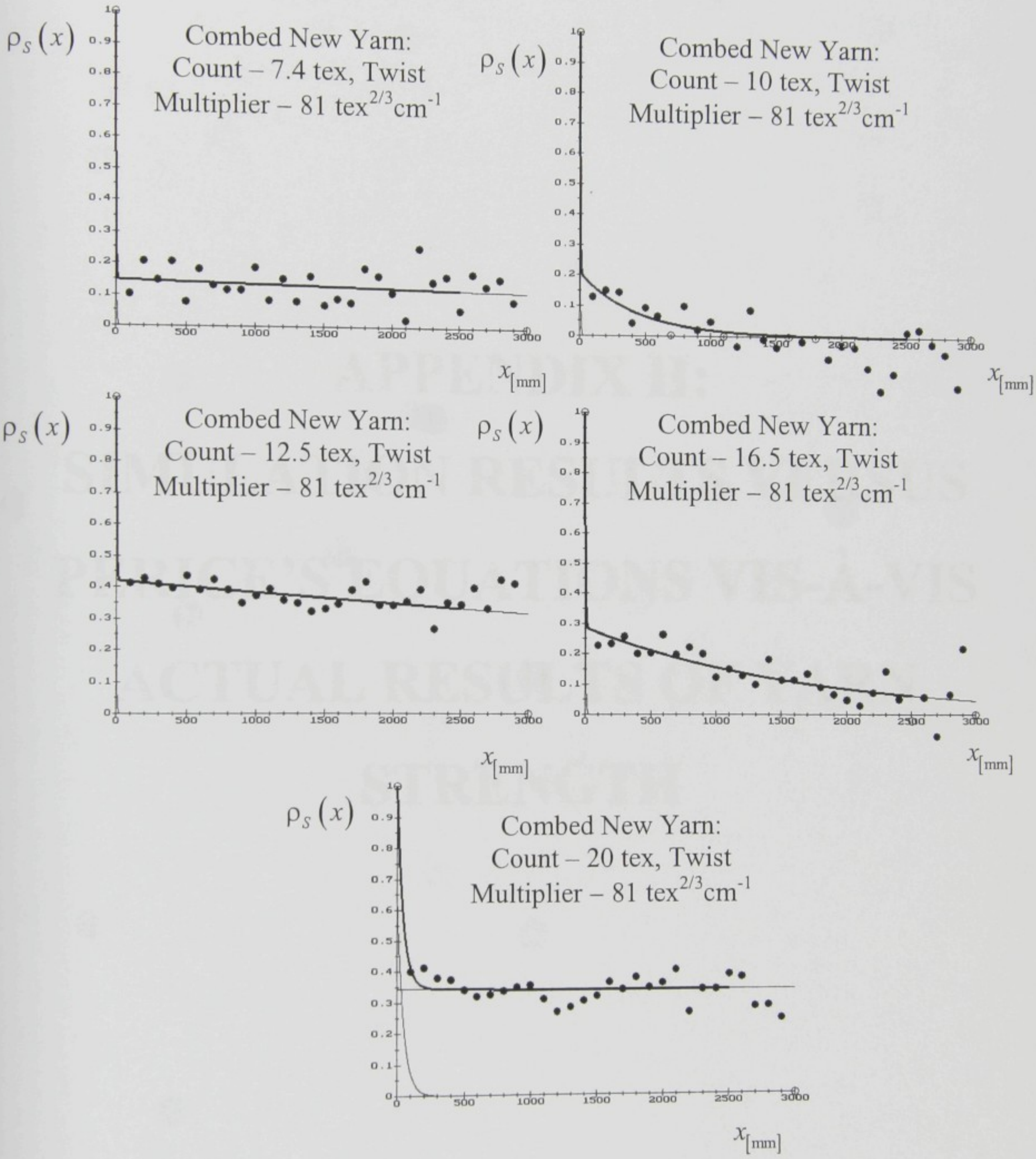
$\rho_S(x)$
Combed New Yarn:
Count – 7.4 tex, Twist
Multiplier – 81 tex$^{2/3}$cm^{-1}
$x_{[\mathrm{mm}]}$
$\rho_S(x)$
Combed New Yarn:
Count – 10 tex, Twist
Multiplier – 81 tex$^{2/3}$cm^{-1}
$x_{[\mathrm{mm}]}$
$\rho_S(x)$
Combed New Yarn:
Count – 12.5 tex, Twist
Multiplier – 81 tex$^{2/3}$cm^{-1}
$x_{[\mathrm{mm}]}$
$\rho_S(x)$
Combed New Yarn:
Count – 16.5 tex, Twist
Multiplier – 81 tex$^{2/3}$cm^{-1}
$x_{[\mathrm{mm}]}$
$\rho_S(x)$
Combed New Yarn:
Count – 20 tex, Twist
Multiplier – 81 tex$^{2/3}$cm^{-1}
$x_{[\mathrm{mm}]}$
0
0.1
0.2
0.3
0.4
0.5
0.6
0.7
0.8
0.9
1
0
500
1000
1500
2000
2500
3000

Figure G8

APPENDIX H: SIMULATION RESULTS VERSUS PERICE’S EQUATIONS VIS-À-VIS ACTUAL RESULTS OF YARN STRENGTH

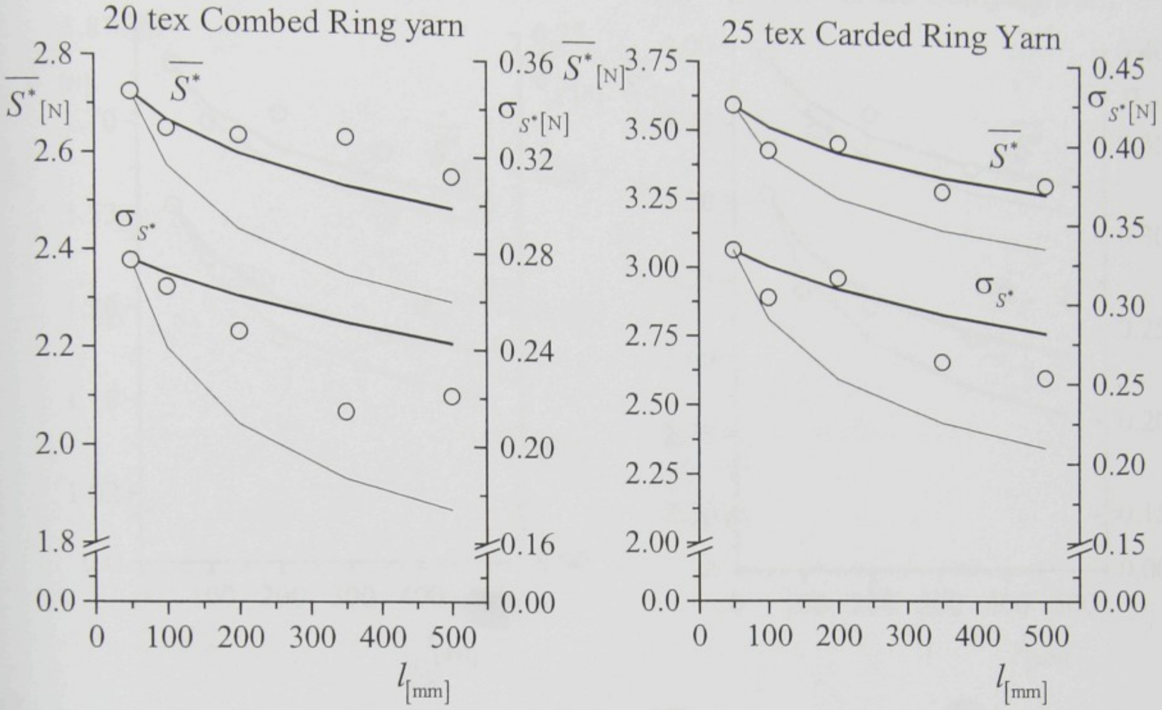

Figure H1

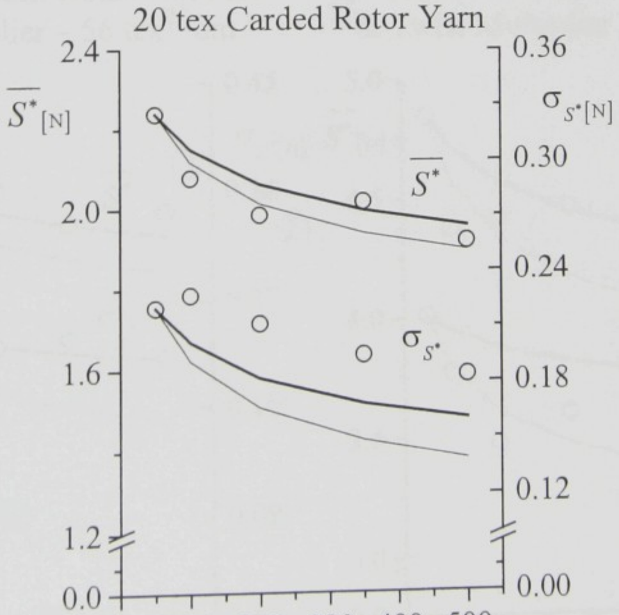

Figure H2

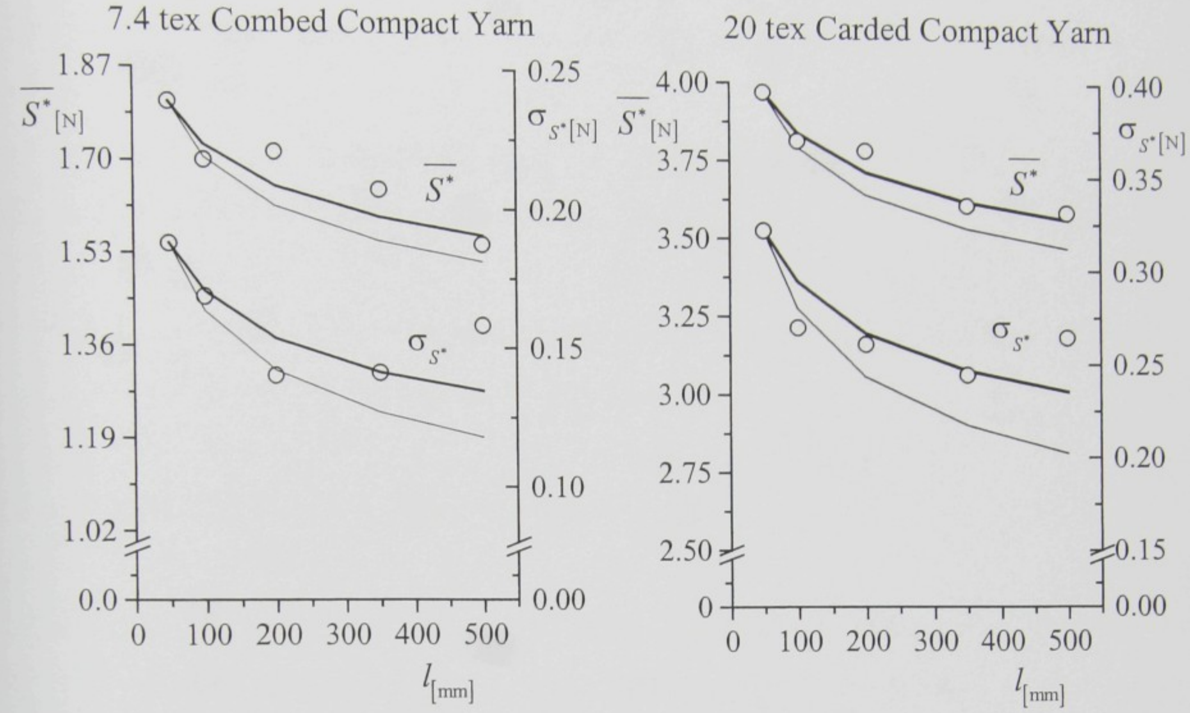
7.4 tex Combed Compact Yarn

20 tex Carded Compact Yarn

Figure H3

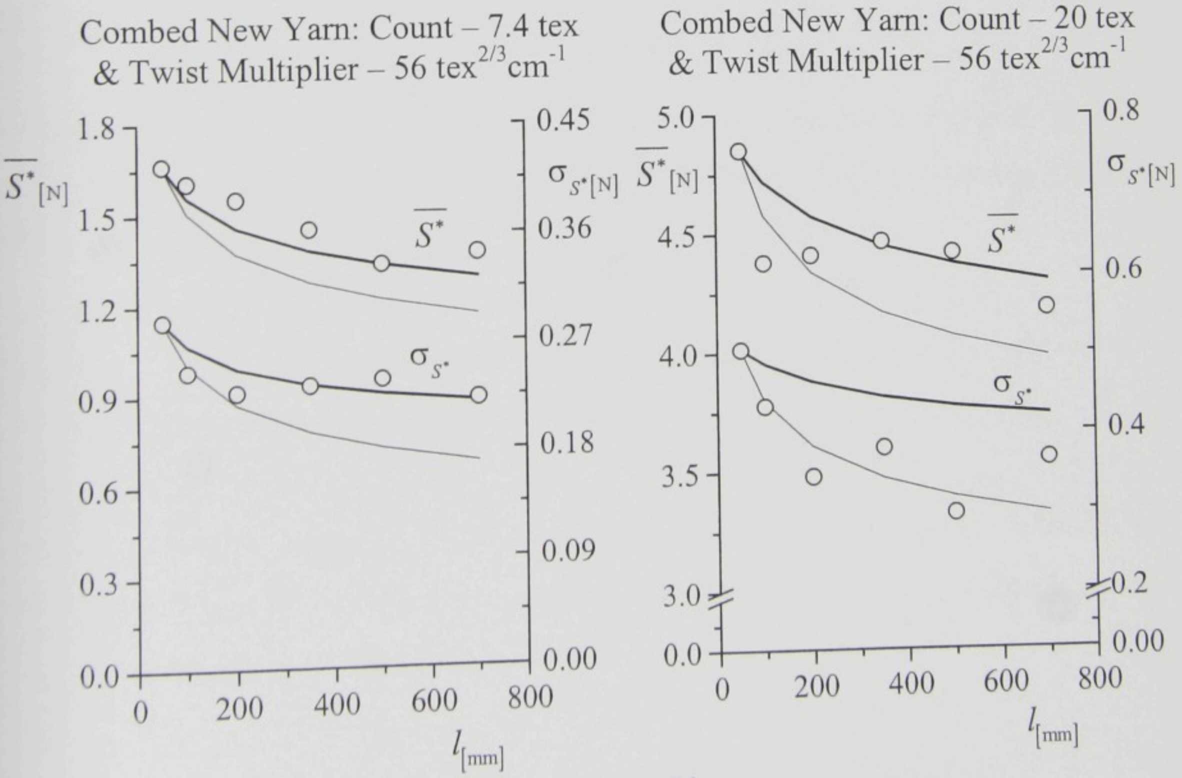
Combed New Yarn: Count – 7.4 tex & Twist Multiplier – 56 tex$^{2/3}$cm^{-1}

Combed New Yarn: Count – 20 tex & Twist Multiplier – 56 tex$^{2/3}$cm^{-1}

Figure H4

BIBLIOGRAPHY

Booth, J. E. 1968, *Principle of Textile Testing*, Heywood Books, London.

Bright, T. B. 1926, *Journal of Textile Institute*, vol. 17, p. T396.

El-Behery, H. M. & Mansour, S. A. 1970, 'Mass and Strength Variations in Yarns', *Textile Research Journal*, vol. 40, pp. 896-902.

Frydrych, I. 1992, 'A New Approach for Predicting Strength Properties of Yarn', *Textile Research Journal*, no. 62, pp. 340-348.

Gegauff, M. C. 1907, *Bull. Soc. Ind. Mulhouse*, vol. 77, p. 153.

Hamby, D. S., Stuckey, W. C., Gast, B. & Hader, R. J. 1960, 'The Analysis of Variations for Certain Physical Properties of Combed Cotton Yarns', *Textile Research Journal*, vol. 30, pp. 435-443.

Hansen, S. M., Rajamanickam, R. & Jayaraman, S., 1998, 'A Model for the Tensile Fracture Behavior of Air-jet Spun Yarns', *Textile Research Journal*, vol. 68, pp. 654-662.

Hearle, J. W. S. 1989, 'Mechanics of Yarns and Nonwoven Fabrics' in *Textile Structure Composites*, ed. T. W. Chou & F. K. Ko, Elsevier Science Publishers B. V., Amsterdam.

Hearle, J. W. S. & Thakur, V. M. 1961, 'The Breakage of Twisted Yarns', *Journal of Textile Institute*, vol. 52, pp. T149-T163.

Hussain, G. F. S., Nachane, R. P., Krishna Iyer, K. R. & Srinathan, B. 1990, 'Weak-link Effect on Tensile Properties of Cotton Yarns', *Textile Research Journal*, vol. 60, pp. 69-77.

Kapadia, D. F. 1935, 'Single-Thread Strength Testing of Yarns in Various Lengths of Test Specimen', *Journal of Textile Institute*, vol. 26, pp. T242-T260.

Kapadia, D. F. 1934, 'Studies in the Sample of Yarns for the Determination of Strength Property Part I-Frequency Curves of Strength Tests by Single Thread, Lea, and Ballistic Methods of Testing', *Journal of Textile Institute*, vol. 25, pp. T355-T370.

Kausik, R. C. D., Salhotra, K. R. & Tyagi, G. K. 1989, 'Influence of Extension Rate and Specimen Length on Tenacity and Breaking Extension of Acrylic/Viscose Rayon Rotor Spun Yarns', *Textile Research Journal*, vol. 59, pp. 97-100.

Knox, L. J., Jr. & Whitwell, J. C. 1971, 'Studies on Breaking Stress Distribution, Part I: The Weak-link Theory and Alternate Models', *Textile Research Journal*, vol. 41, pp. 510-517.

Koo, H., Suh, M. W. & Woo, J. L. 2001, 'Variance Tolerancing and Decomposition in Short-Staple Spinning Processes, Part I: Modeling Spun Yarn Strength Through Intrinsic Components', *Textile Research Journal*, vol. 71, pp. 1-7.

Mandl, G. 1981, *Melliand Textileberichte*, vol. 62, p. 33.

Mark, H. 1932, *The Physics and Chemistry of the Cellulose*, J. Springer, Berlin.

Meloun, M., Militky, J., and Forina, M. 1992, *Chemometrics for Analytical Chemistry, Volume 1: PC-Aided Statistical Data Analysis*, Ellis Horwood, New York.

Meredith, R. 1946, *Journal of Textile Institute*, vol. 37, p. T205.

Morton, W. E. & Hearle, J. W. S. 1992, *Physical Properties of Textile Fibers*, Buttorworths & Co. (Publishers) Ltd., The Textile Institute, Manchester.

Nanjundaya, C. 1966, 'Strength of Cotton Yarn with Particular Reference to the Structure at the Region of Break', *Textile Research Journal*, pp. 954-966.

Neckář, B. 2004, *Lectures on Structural Modeling of Fiber Assemblies and Yarns* (An Internal Publication), Technical University of Liberec, Liberec.

Neckář, B. 1998, *Morphology and Structural Mechanics of General Fibrous Assemblies* (Czech), Technical University of Liberec, Liberec.

Peirce, F. T. 1926, 'Tensile Tests for Cotton Yarns v. -The Weakest Link Theorems on The Strength of Long and of Composite Specimens', *Journal of Textile Institute*, vol. 17, pp. T 355-T368.

Perepelkin, K. E. 1991, 'Complex Evaluation of the Quality and Load-bearing Capacity of Yarns during Production and Processing', *Fibre Chem.*, vol. 23, pp. 115-133.

Perepelkin, K. E., Shkolyar, M. S., Dune, I., Rozhkov, N. N., & Karpuklin, L. N. 1987, 'Evaluating the Scale Effect During the Mechanical Testing of Industrial Filament Yarns', *Khim. Volok.*, vol. 29, pp. 47-48.

Platt, M. M. 1950, *Textile Research Journal*, vol. 20, p. 665.

Pozdniakov, B. P. 1978, *Methods of Statistical Control and Investigation of Textile Material*, Light Industry, Moscow.

Radhakrisnaiah, P. & Huang, G. 1997, 'The Tensile and Rupture Behavior of Spun Yarns Representing Different Spinning Systems', *Papers of the 10th EFS® System Research Forum*, North Carolina.

Realfe, M. L., Seo, M., Boyce, M. C., Schwartz, P. & Backer, S. 1991, 'Mechanical Properties of Fabrics Woven from Yarns Produced by Different Spinning Technologies: Yarn Failure as a Function of Gauge Length', *Textile Research Journal*, vol. 61, pp. 517-530.

Sippel, A. 1958, *Faserforschung und Textiletechnik*, vol. 9, p. 163.

Solovev, A. N. 1938, 'Yarn Strength and Its Dependence on the Count, Twist, Irregularity of Yarn and on Fiber Properties', A Report to SNTL-Press for Technical Literatures.

Spencer-Smith, J. L. 1947, 'The Estimation of Fiber Quality', *Journal of Textile Institute*, vol. 38, pp. P257-P271.

Suh, M. W., Koo, H., & Woo, J. L. 2001, 'Variance Tolerancing and Decomposition in Short-Staple Spinning Processes, Part II: Simulations and Applications to Ring and OE Spun Yarns', *Textile Research Journal*, vol. 71, pp. 105-111.

Tippet, L. H. C. 1925, *Biometrika*, vol. 17, p. 364.

Truevtsev, N. N., Grishanov, S. A. & Harwood, R. J. 1997, 'The Development of Criteria for the Prediction of Yarn Behavior under Tension', *J. Textile Inst.*, vol. 88, pp. 400-414.

Turner, A. J. 1928, *Journal of Textile Institute*, vol. 19, pp. T280-T314.

Vinter, Y. M. & Drokhanova, E. L. 1977, *Tekhnol. Tekstil. Prom.*, no. 1 (115), p. 20.

Yang, S. & Lamb, P. 1998, 'The Art of Spinning Prediction-Modeling Yarn Performance in Worsted Spinning', *The Second China International Wool Textile Conference*, China.

Zurek, W., Frydrych, I. & Zakrzewski, S. 1987, 'A Method of Predicting the Strength and Breaking Strain of Cotton Yarn', *Textile Research Journal*, vol. 57, pp. 439-444.

Zurek, W., Malinowski, L. & Plotka, E. 1976, 'Analytical Technological Method of Prediction of Strength and Breaking Strain of Cotton Yarn', *Papers of The Technical University of Lodz*, vol. 33, pp. 62-73.

Zurek, W. 1975, *The Structure of Yarn*, The National Center for Scientific, Technical, and Economic Information, Warsaw.

Date of Birth: 30th November 1976
Nationality: Indian
E-mail: dipayandas@yahoo.co.in

EDUCATIONAL QUALIFICATIONS

2000-2002: **Master of Technology in Textile Engineering**, Indian Institute of Technology Delhi

1995-1999: **Bachelor of Science (Technology) in Textile Technology**, Calcutta University, India

ACADEMIC ACHIEVEMENTS

- **Student Award** for the Best Research Paper Submitted at the Fiber Society 2004 Annual Meeting and Technical Conference, USA, 11th-13th October 2004
- **All India First** in Graduate Aptitude Test in Engineering (GATE) in Textile Engineering & Fiber Science with 99.76 percentile score, conducted by the Indian Institute of Technology Mumbai in 1999
- **University First** in Bachelor of Science (Technology) in Textile Technology in the Calcutta University in 1999
- **Precitex Award-1999** for the best student in Spinning in the College of Textile Technology Berhampore (India), given by the Precitex Rubber Industries Pvt. Ltd. (India)

PUBLICATIONS IN JOURNALS

- "Application of Artificial Neural Network for prediction of Rotor-Spun Yarn Properties," Das, D., Ishtiaque S. M., Mac, T., Veit, D., and Thomas, G., **Melliand International 10(3)**, pp. 183-185 (2004)
- "Evaluation of the Best Method of Fiber Blending on Uster MDTA 3," Das, D., Ishtiaque S. M., Mac, T., Veit, D., and Thomas, G., **Melliand International 10 (2)**, pp. 110-113 (2004)
- "Raw Material Characteristics Vis-À-Vis Rotor Spinning Technology: A Review," Das, D., **Vlákna a Textil (Fiber and Textile) 11 (3)**, pp. 94-98 (2004)

- "Influence of Drawing Parameters on the Quality of Single Worsted Yarn," Banerjee, S., Das, D., Bodhak, T. K., and Chandra, A., **Man Made Textiles in India 43 (4)**, pp. 170-173 (2003)
- "Yarn Strength as a Stochastic Process," Neckář, B., and Das, D., **Textile Research Journal** (Accepted for Publication)
- "Modeling of Radial Fiber Migration in Yarns," Neckář, B., and Das, D., **Textile Research Journal** (Accepted for Publication)
- "Mechanics of Parallel Fiber Bundles," **Fibers & Textile in Eastern Europe** (Accepted for Publication)
- "Yarn Strength Behavior at Different Gauge Lengths," Das, D., and Neckář, B., **Indian Journal of Fiber and Textile Research** (Accepted for Publication)
- "Autocorrelation Function of Yarn Unevenness," Neckář, B., and Das, D., **Indian Journal of Fiber and Textile Research** (Accepted for Publication)
- "Yarn Strength as a Function of Gauge Length – A Critical Review," Das, D., **Vlákna a Textil** (Communicated for Publication)

PRESENTATIONS AT CONFERENCES

- "Mathematical Modeling and Experimental Investigation of Yarn Strength as a Stochastic Process," Das, D., **The Fiber Society 2004 Annual Meeting and Technical Conference** (Oral), Ithaca (USA), 2004
- "A Stochastic Approach to Yarn Strength," Das, D., and Neckář, B., **7th Asian Textile Conference** (Oral), New Delhi (India), 2003
- "Investigation of a Suitable Blending Technique on Uster MDTA 3," Das, D., and Ishtiaque, S. M., **5th International Conference TEXSCI** (Oral), Liberec (Czech Republic), 2003
- "Classification of Models of Internal Yarn Structure," Das, D., and Neckář, B, (Communicated for Poster Presentation at **The Fiber Society Spring 2005 Conference**)

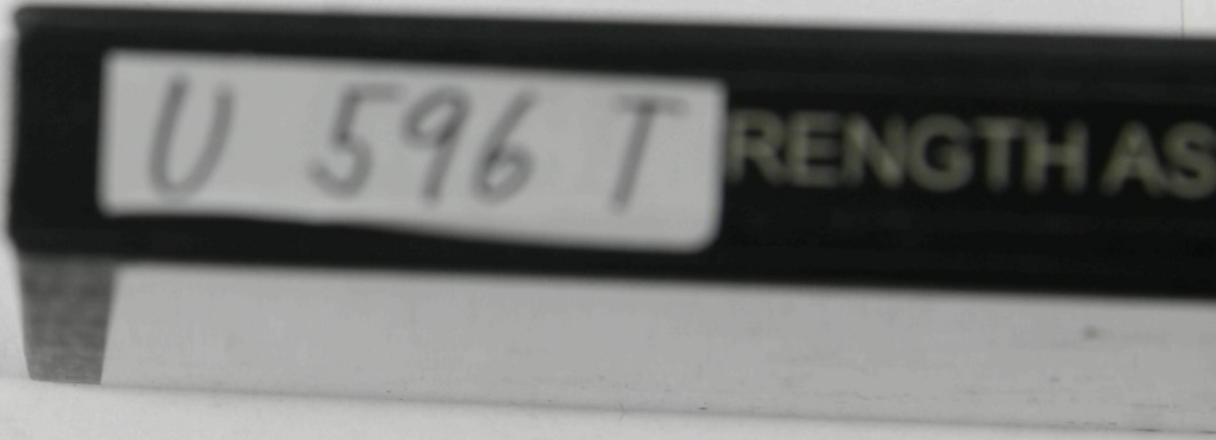
RENGTH AS